Università degli Studi di Milano
Dottorato in Scienze Farmacologiche Sperimentali e Cliniche
Dipartimento di Scienze Farmacologiche e Biomolecolari

Clinical and experimental evidences of the direct vascular effect of Proprotein Convertase Subtilisin/Kexin type 9

SUPERVISORE: Chia.mo Prof. Alberto Corsini
COORDINATORE: Chia.mo Prof. Alberico L. Catapano

Silvia MARCHIANÓ
Matricola: R11227
XXXI° ciclo

Anno Accademico 2017 / 2018

Now this is not the end.

It is not even the beginning of the end.

But it is, perhaps, the end of the beginning.

Winston Churchill

Index

List of Figures

Abstract

English version

Proprotein Convertase Subtilisin Kexin type 9 (PCSK9), together with *LDLR* and *APOB* genes, had been identified as the third gene associated with Familial Hypercholesterolemia (FH). Secreted PCSK9 in fact, targets the hepatic LDL receptor (LDLR) for degradation thus preventing its recycling on the cell surface. The decreased expression of LDLR determines an increase in the circulating LDL particles, leading to increased cholesterol levels. Secreted PCSK9 is mainly derived from the liver, but it is also expressed in other tissues such as the brain, the kidney, the pancreas as well as the cells that composed the arterial wall. It is therefore possible that it could exert multiple paracrine effects. Our research group found that PCSK9 is expressed and secreted by smooth muscles cells (SMCs) which constitute the atherosclerotic plaque. The aim of my project was to determine the paracrine role of PCSK9 on the neointima formation through preclinical and clinical approaches. The immunohistochemical analysis of *Pcsk9*$^{-/-}$ and *Pcsk9*$^{+/+}$ mice revealed that, after vascular manipulation, the PCSK9-null mice were protected from the formation of neointima with lower intima area (28100 ± 4901 μm^2 and 14350 ± 2990 μm^2 for *Pcsk9*$^{+/+}$ and *Pcsk9*$^{-/-}$ mice respectively, $p<0.05$), associated with decreased intima/media ratio of 1.48 ± 0.34 and 0.60 ± 0.18 for *Pcsk9*$^{+/+}$ and *Pcsk9*$^{-/-}$ mice respectively, ($p<0.05$). The *in vitro* studies on isolated SMCs from *Pcsk9*$^{-/-}$ and *Pcsk9*$^{+/+}$ mice showed that the absence of PCSK9 induced a more contractile phenotype, associated with a reduced proliferation rate (doubling time were 57.3 ± 2.1h and 106.3 ± 4.5h, respectively [$p<0.001$]). The response to the chemotactic agent PDGF-BB (Platelet-derived growth factor), measured with Boyden's chamber assay, was also impaired in the absence of PCSK9. These were rescued after the reconstitution of PCSK9 in the *Pcsk9*$^{-/-}$ cell line, which led to a more synthetic phenotype associated with a doubling time of 32.2± 3.1h and 41.2 ± 1.9h [$p< 0.001$], for *Pcsk9*$^{-/-}$ and *Pcsk9*$^{-/-}{}_{REC}$ SMCs, respectively. The difference in proliferation between *Pcsk9*$^{-/-}$ and *Pcsk9*$^{-/-}{}_{REC}$ SMCs was maintained also after the incubation with 40μM of simvastatin, suggesting that PCSK9 could improve SMCs proliferation through mechanism independently from cholesterol levels. The cell cycle analyses of the *Pcsk9*$^{-/-}$ and *Pcsk9*$^{-/-}{}_{REC}$ SMCs showed a decreased activation of p21 and p27, associated with an increased expression of cyclin E and cyclin D1; presumably due to a different activation of the PDGF receptor pathway mediated by LRP1. Finally, the observational study, carried out in

collaboration with the Brisighella Heart Study research group, demonstrated that serum levels of PCSK9, together with aging, is positively correlated to the pulse wave velocity. This is an indirect parameter used to evaluate the arterial stiffness and hence the presence of atherosclerotic plaques. Taken together, these results demonstrated that aside from its function on in regulating cholesterol homeostasis, PCSK9 plays a direct pro-atherogenic role in the arterial wall by sustaining SMC synthetic phenotype, proliferation, and migration.

Versione Italiana

La proproteina convertase subtilisina/kexina di tipo 9 (PCSK9) rappresenta, insieme al recettore delle LDL e all'apolipoproteina B, il terzo gene associato all'ipercolesterolemia familiare. PCSK9 è prevalentemente secreta dal fegato, una volta in circolazione, ha come bersaglio il recettore delle LDL, mediandone la degradazione per via lisosomiale e impedendone perciò il riciclo sulla superfice degli epatociti. La ridotta espressione del recettore porta così all'aumento delle LDL circolanti e un conseguente aumento della colesterolemia. Oltre al fegato, PCSK9 è espressa anche in altri tessuti, come il cervello, i reni, il pancreas e anche le cellule che compongono la parete dei vasi, suggerendo che, oltre all'effetto sistemico, potrebbe esercitare anche numerosi effetti paracrini. Studi precedenti del nostro gruppo di ricerca hanno dimostrato che PCSK9 è espressa a livello delle cellule muscolari lisce (CML) presenti all'interno della placca aterosclerotica. Lo scopo del mio progetto di ricerca è stato quello di determinare il ruolo di PCSK9 nello sviluppo della neointima attraverso modelli preclinici e clinici. L'analisi morfometrica delle carotidi di topi *Pcsk9*$^{-/-}$ and *Pcsk9*$^{+/+}$ dopo il posizionamento di un collarino non occlusivo sulla carotide destra, ha evidenziato che l'assenza di PCSK9 è associata ad una ridotta formazione dell'inspessimento neointimale con un'area della tonaca intima pari a 28100 ± 4901 μm^2 e 14350 ± 2990 μm^2 (p<0.05) ed un rapporto intima/media di 1.48 ± 0.34 e 0.60 ± 0.18, rispettivamente per i topi *Pcsk9*$^{+/+}$ and *Pcsk9*$^{-/-}$ (p<0.05). L'assenza di PCSK9 nelle CML isolate dall'aorta di topi *Pcsk9*$^{-/-}$ ha comportato una ridotta capacità proliferativa (tempo di duplicazione pari a 57.3 ± 2.1 ore per le CML *Pcsk9*$^{+/+}$ e 106.3 ± 4.5 ore per le CML *Pcsk9*$^{-/-}$, p<0.001) associata ad un fenotipo prevalentemente contrattile. La risposta al fattore chemiotattico di derivazione piastrinica (PDGF-BB) è stata valutata attraverso la camera di Boyden e, anche in questo caso, l'assenza di PCSK9 ha portata ad una ridotta migrazione cellulare. Per confermare l'effetto di PCSK9 sulle CML, abbiamo ricostituito l'espressione della proteina nella linea knock-out. Le CML *Pcsk9*$^{-/-}_{REC}$ hanno mostrato un fenotipo prettamente sintetico, associato ad un aumento del tempo di duplicazione (32.2± 3.1 ore e 41.2 ± 1.9 ore, per le CML *Pcsk9*$^{-/-}$ e *Pcsk9*$^{-/-}_{REC}$ rispettivamente, p>0.001). Queste differenze in termini di proliferazione erano mantenute anche dopo incubazione con simvastatina 40μM, suggerendo che l'effetto di PCSK9 sulla proliferazione cellulare sia indipendente dai livelli di colesterolo. L'analisi delle proteine del ciclo cellulare ha mostrato una ridotta espressione di p21 e p27, associata ad un aumento dell'attivazione delle cicline E e D1; presumibilmente per una diversa

attivazione del recettore del PDGF mediata da LRP1. Infine, lo studio osservazionale condotto in collaborazione con il gruppo di ricerca Brisighella Heart Study ha dimostrato che i livelli di PCSK9 circolante, insieme all'età del paziente, siano i due fattori positivamente correlati alla pulse wave velocity, ovvero alla rigidità arteriosa. Questo risultato, insieme ai dati dello studio in vivo e dello studio in vitro, ha portato alla conclusione che PCSK9 agisca direttamente a livello della placca aterosclerotica, modificando il fenotipo la proliferazione e la migrazione delle cellule muscolari lisce.

Introduction

Cholesterol homeostasis: the good, the bad and the ugly.

Atherogenic lipoproteins

Lipids are a class of molecules characterized by different chemical structure and biological function; they can be divided in three major classes: 1) ***fatty acids***, that are the main source of energy for our organism and they are stored as triglycerides in the adipose tissues; 2) ***cholesterol and phospholipids***, essential to maintain membrane structural integrity and fluidity; 3) ***lipid-derived bioactive molecules***, like steroid hormones and the arachidonic acid derivatives.

Since lipids are insoluble in water, they require the association with proteins, named apolipoproteins, which are responsible for the structure and the catabolism of the lipoproteins per se [1]. Lipoproteins are therefore molecular complexes of lipids and proteins that can be divided in different groups, according to the density, the lipid composition and the type of apolipoproteins, as shown in **Table 1**.

Lipoprotein	Density	Diameter (nm)	Particle composition (weight %)				Major apolipoproteins
			Triglycerides	Cholesterol	Phospholipids	Protein	
Chylomicron	0.93	80-1200	85-95	2-5	3-8	1-2	B-48, A-I, A-II, A-IV, (C, E)
VLDL	0.93-1.006	30-80	50	22	19	8	B-100, A-I, C, E
IDL	1.006-1.019	23-35	20	38	23	19	B-100, C, E
LDL	1.019-1.063	18-25	11	47	22	21	B-100
HDL_2	1.063-1.125	9-12	6	22	30	41	A-I, A-II, C, E
HDL_3	1.125-1.21	5-9	6	15	23	55	A-I, A-II, C, E

Table 1. Lipoprotein classes. *Modify from "Introduction to lipids and lipoproteins" and "The composition and metabolism of large and small LDL" [1, 2]. Sd-LDL: small-dense LDL; Lb-LDL: large buoyant-LDL.*

The Framingham study was the first epidemiological study that demonstrated the association between serum cholesterol and the risk of atherosclerotic cardiovascular diseases (ASCVDs); decades after, serum cholesterol levels, especially cholesterol contained in the LDL particles, still represent one of the major risk factors for CVDs (**Figure 1**) [3-7].

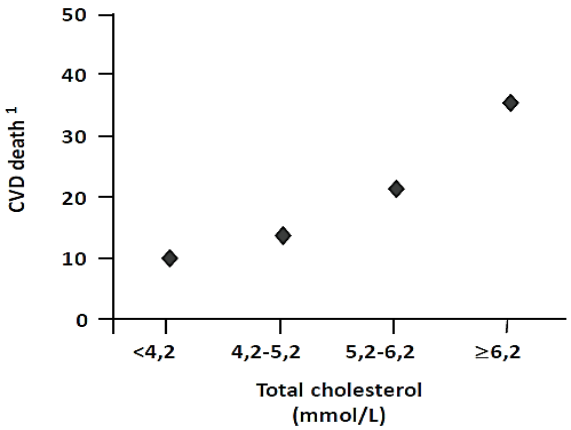

Figure 1. Crude date rate for cardiovascular diseases (per 10,000/year)[1]. *These data suggest that there is a direct relationship between the serum total cholesterol (TC) concentration and the rate of death from CVD and, further, that death due to CVD is very uncommon in individuals with a plasma TC concentration < 4.2 mmol/L. Adapted from Neaton JD et al. [7].*

Atherosclerosis per se, is a progressive inflammatory disease initiated by the accumulation of lipid within the artery wall [8]. The pathologist Rudolf Virchow (1821-1902) was the first one who describes "atherosclerosis" – term invented in 1829 by the surgeon Jean-Fréderic Lobstein – as "*endoarteritis deformans*", literally chronic and degenerative inflammation of the artery. Atherosclerotic lesions occur principally in large and medium-sized elastic and muscular arteries, they are initially manifested as asymptomatic lesions, named fatty streaks, common in infants and young children. The progression of the disease leads to the formation of complicated lesions which may cause vascular events like: ischemic stroke, myocardial infarction, peripheral diseases/thrombosis and cerebrovascular events. Even if the etiology of atherosclerosis is still controversial [9-11], the lipid accumulation within the artery wall is a critical steps for the manifestation of the symptoms. Besides hypercholesterolemia (intended as elevation in total serum cholesterol levels and LDL-cholesterol), also hypertriglyceridemia has been recently considered as causal factor for ASCVD [12]. The role of triglycerides (TGs) in atherogenesis is matter of debate not only because the postprandial metabolism of TGs but also because abnormal triglyceride levels are featured of other metabolic disorders, like diabetes mellitus type 2 or metabolic syndrome, generally known to be associated to an increased risk of CVDs [13].

The plasmatic concentration of lipids is modulated by both exogenous (dietary intake) and endogenous (biosynthesis) pathways; the former occurs in the intestine, which is responsible for the absorption (800mg dietary cholesterol/day) and the latter in the liver, which is responsible for the metabolism (900mg synthetized cholesterol/day); extrahepatic organs, such as muscles and adipose tissue also contributes to net balance of serum total cholesterol levels [14]. The lipids absorbed by the diet are mainly fatty acids esterified with glycerol (TGs) and cholesterol; within the intestinal lumen, TGs are digested into monoacylglycerols and free fatty acids by the action of pancreatic lipase, whereas cholesterol and vitamins are emulsified in micelles with are transported inside the enterocytes through the sterol transporter called Niemann-Pick C1- like 1 (NPC1L1) and the Scavenger Receptor Class B Type I (SR-BI) [15]. Inside the enterocytes, free fatty acids are resynthesized into triglycerides and bound to a molecule of apolipoprotein B48 (apoB-48) by the action of the Microsomal Triglyceride Transfer Protein (MTTP), leading to the formation of chylomicrons; dietary cholesterol instead is esterified into cholesterol esters by the action of acyl-CoA Cholesterol Acyl Transferase (ACAT). Before secretion in the lymph, cholesterol esters and TGs are packaged into chylomicron [1]. This class of lipoproteins is mostly composed by TGs (85-95% w/w) and therefore, they are the largest and the least dense particles (**Table 1**). The lymphatic circulation distributes the chylomicron to the extrahepatic organs, like muscles and adipose tissue, where the free fatty acids are hydrolysed after the action of the Lipoprotein Lipase (LPL). This is mediated by apolipoprotein C (apoC), which is another apolipoprotein carried by chylomicrons, co-factor of LPL. The resulting particles are called chylomicron remnants, those lipoproteins are enriched in cholesterol esters, and, compared with chylomicrons, they loss apolipoprotein A-I and apolipoprotein C, whereas they acquire apolipoprotein E [16]. The formation of chylomicrons occurs during the fasting state; size and composition of those particles are closely dependent on the amount and type of fat absorbed by the intestine [17, 18]. The acquisition of apo-E from the systemic circulation is fundamental for the hepatic clearance of chylomicron remnants. As mentioned before, apoB-48 is the structural apolipoprotein present in the chylomicron but it is not recognized by the low dense lipoprotein receptor (LDLR), the main player of lipids metabolism; thus, the hepatic clearance of chylomicron remnants occurs upon the binding of apoE to the LDLR expressed on the surface of hepatocytes. Once in the liver, cholesterol becomes a substrate of different enzyme/transporters ad thus, channelled to different pathways: the action of cholesterol-7-α-hydroxylase directs cholesterol to bile

acids synthesis, the action of ATP-Binding- Cassette A1 (ABCA1) exports free cholesterol into high-density lipoproteins and finally, the action of Acyl CoA-cholesteryl Acyl Transferase 2 (ACAT2) esterified cholesterol into cholesteryl esters that are incorporated into the very-low-dense lipoproteins (VLDLs). Liver is the starting point of the endogenous pathway of lipoprotein metabolism, the esterified cholesterol and triglycerides are incorporated onto a molecule of apoB-100 inside the endoplasmic reticulum (ER); the nascent VLDL is large and enriched in triglycerides. The biogenesis of VLDL is closely dependent on the hepatic triglycerides content, in fact, without lipidation, a significant amount of nascent apoB gets degraded [19]; moreover, the amount of triglycerides available in the liver, that mostly derives from the exogenous pathway, regulates the production rate of VLDLs[20, 21]. Once in the circulation, just like chylomicrons, VLDLs are substrate of LPL expressed in peripheral tissues, and the resulting particles is called intermediate density lipoproteins (IDL), smaller and enriched in cholesterol. Both VLDLs and IDLs are cleared from the circulation by the action of the LDLR, preferentially via apoE, rather than apoB-100 [22]. In both the endogenous and the endogenous pathway, the lipoprotein lipase metabolizes triglycerides rich lipoproteins (chylomicrons and VLDLs) in remnant lipoproteins (chylomicron remnants and IDL). The formation of those particles occurs during the postprandial state [23] and it is considered a causal factor of ASCVD as well as LDL-cholesterol, mainly due to their size. In fact, they can be directly absorbed into the arterial wall: the endothelium of blood vessels is permeable only to small lipoproteins (<70nm of diameter) whereas large lipoproteins like chylomicrons and nascent VLDL can be absorbed only in the presence of fenestrated endothelium (like in the liver) [24]. Once those particles infiltrate the sub-endothelial space, they can accelerate macrophage foam cell formation. Moreover, lipoproteins remnants can promote atherosclerotic lesion formation by increasing the expression of adhesion molecules and chemoattractant agents (such as VCAM-1, ICAM-1 and MCP-1), thereby enhancing the inflammatory response, and by promoting smooth muscles cells proliferation [22].

After the action of hepatic lipase, IDL particles depleted of the TG content, form the low-density lipoproteins (LDL); those particles contain apoB-100 and represent a major fraction of circulating cholesterol, due to their long half-life (2-3 days compared to minutes for CMs, VLDLs and IDLs) and therefore they are considered the primary target for the prevention and the treatment of ASCVDs. LDL particles, as well as lipoprotein remnants are able to infiltrate the arterial wall but their retention is strongly dependent on the serum concentration: within

the physiological range of LDL cholesterol (1.0mmol/L or 20-40 mg/dL [25]), the probability of LDL particle retention inside the arterial wall is low [26], but a raise in the concentration leads to a dose-dependent increase in retention time and consequently in the risk of ASCVDs [27]. The production and the clearance of LDL particles depends on the action of LDLR, an increased clearance of IDL by LDLR leads to a decrease in LDL production, vice versa, an increased expression of LDLR enhances LDL clearance [28]. LDL particles, in the presence of molecules like free radicals and reactive nitrogen intermediates, can undergo oxidation and therefore cleared from the bloodstream by the interaction with scavenger receptors expressed on the membrane of macrophages, like scavenger receptor class A (SR-A) and CD-36 [29, 30], this process contributes to enhance the atherogenicity of LDL particles.

The lipoproteins described so far embody apoB as the main structural apolipoprotein and their main role is to deliver triglycerides and cholesterol to the cells; the high-density lipoproteins (HDLs) instead contains apoA-I and they are involved in what it is called “reverse cholesterol transport”. This process is necessary for most of the cells that cannot process cholesterol (like the cells present in the gonads and adrenal glads) and therefore, the only way to decrease intracellular cholesterol content is to secrete it via the transporter ABCA1. The biogenesis of HDLs begins with the synthesis of apoA-I by liver and intestine; once in the circulation, apoA-I acquires cholesterol and phospholipids via the action of the transporter ABCA1, as mentioned above. The nascent HDLs are called preβ-HDL, the cholesterol is localized on the surface of the particles in the form of free cholesterol; in order to form mature HDL, those particles undergo the action of lecithin-cholesteryl acyltransferase (LCAT), that esterifies free cholesterol with a molecule of fatty acid, derived from phospholipids. The mature and large HDLs can be either cleared from the circulation by the binding of apoA-I with the scavenger receptor SR-BI expressed in the liver, or they can receive triglycerides from the apoB containing lipoproteins in exchange for cholesteryl esters. This process is mediated by the action of cholesteryl ester transfer protein (CETP) and the resulting HDLs, enriched in TGs, are then substrate of different lipases [1]. Because of their role in reverse cholesterol transport, HDL particles are inversely correlated with the risk of ASCVDs [31]; in particular the presence of low HDL-cholesterol, combined with high LDL-cholesterol levels and elevated triglyceridemia is a common pattern called atherogenic lipid triad that predispose to premature ASCVDs [32]. Recently, the Copenhagen City Heart Study demonstrated that the correlation between the risk of ASCVDs and the concentration of circulating HDL was a U-

shape, with both extreme high and low HDL cholesterol concentrations being associated with high mortality. The paradoxically association between extreme high HDL cholesterol and higher mortality could be explained by genetic mutations in genes like CETP, ABCA1, LIPC, and SCARB1, which are associated with both high risk of coronary heart disease and high concentrations of HDL cholesterol [Eur Heart J. 2017 Aug 21;38(32):2478-2486].

The current guidelines for prevention and treatment of cardiovascular diseases are indeed based on the lipid profile of the patient: the primary target therapy is LDL-cholesterol, which has to be below 70mg/dl or reduced by a 50%. For high-risk patients, the evaluation of HDL-cholesterol and triglycerides levels are used in the stratification of the population[33-36]. The reduction of ASCVDs risk based on reduction of cholesterol levels accordingly to European Society of Cardiology (ESC) and the European Atherosclerosis Society (EAS) guidelines [37, 38] and to the American Heart Association (AHA) and the American College of Cardiology (ACC) guidelines [39] are summarized in Table 2.

	ESC/EAS guidelines	**AHA/ACC guidelines**
Secondary prevention of ASCVDs	LDL-C < 70 mg/dl (1.8 mmol/l) or a decrease of LDL-C by ≥ 50 %. If such a reduction is not achieved with statin monotherapy, consider combination therapy.	"High-intensity" statin therapy (atorvastatin (40)–80 mg, rosuvastatin 20 (40) mg). If a reduction of LDL-C of ≥ 50 % is not achieved, consider combination therapy.
Statin intolerance in secondary prevention	Decrease statin dose, consider combination therapy.	Moderate- and low-Intensity statin therapy, consider combination therapy.
Primary prevention when LDL-C is >190mg/dl (4.9 mmol/L)	Goal: LDL-C < 100 mg/dl (2.5 mmol/l). If target value not achieved, consider combination therapy.	"High-intensity" statin therapy with the goal to decrease LDL-C by ≥ 50 %.
Diabetes mellitus without ASCVD	Diabetes mellitus with other risk factors or end-organ damage—goal: LDL-C < 70 mg/dl (1.8 mmol/l) or a decrease of LDL-C by ≥ 50 %. Diabetes mellitus without complications: LDL-C < 100 mg/dl (< 2.5 mmol/l).	Diabetes with high cardiovascular risk (≥ 7.5 % in 10 years): high-intensity statin therapy. Diabetes with low cardiovascular risk: statin treatment with moderate intensity.
Primary prevention	SCORE for fatal cardiovascular events ≥ 5 %: LDL-C target < 100 mg/dl (2.5 mmol/l).	Risk for cardiovascular events ≥ 7.5 %: moderate to high-intensity statin therapy. Risk between 5 and 7.5%: moderate-intensity statin therapy.
Primary dyslipidemia and atherogenic secondary dyslipidemia, Lp(a)	Recommendations based on observational studies or on pathophysiologic plausibility.	No position taken, as it is beyond the scope of the guideline objectives.

Table 2. Prevention and management of atherosclerotic cardiovascular diseases accordingly to the European and American guidelines [39]. *Lp(a) or lipoprotein (a) share some features with LDL particles, except for the presence of the apolipoprotein apo(a). It has been found in several studies to be an additional risk marker for ASCVDs, serum levels Lp(a) are not recommended for risk screening in the general population; however, Lp(a) measurement should be considered in people with high CVD risk or a strong family history of premature atherothrombotic disease [40, 41].*

Hypercholesterolemia and atherosclerotic cardiovascular diseases: from genetics to pharmacology.

Genetic studies, prospective epidemiologic cohort studies, Mendelian randomization studies, and randomized trials of LDL-lowering therapies, throughout the decades, strongly demonstrated that LDL cholesterol is a causal factor for atherosclerotic cardiovascular diseases (**Figure 2**) [36, 42].

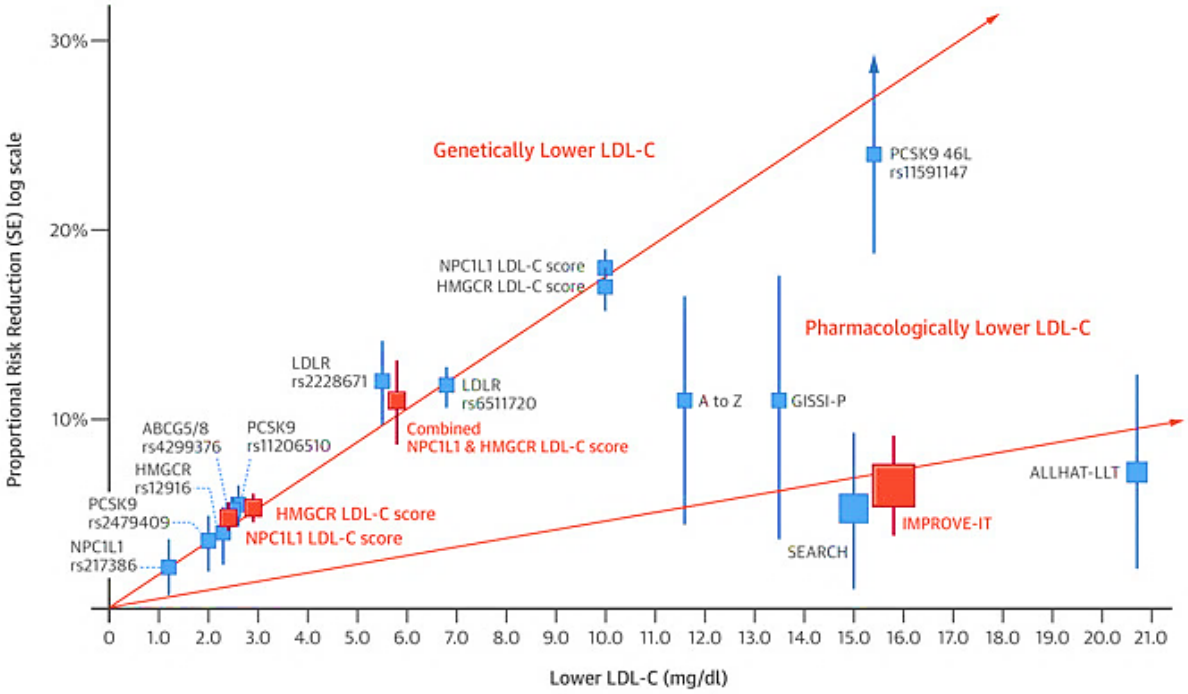

Figure 2. Log-linear association per unit change in low-density lipoprotein cholesterol (LDL-C) and the risk of cardiovascular disease. *The reduction in cardiovascular events is directly proportional to the absolute reduction of LDL-cholesterol, intended as reduction in LDL particles, and the cumulative duration of exposure to lower LDL-cholesterol [42, 43].*

In this contest, inherited disorders of lipid metabolism, like familial hypercholesterolemia (FH), could provide the first evidences of the direct relationship between LDL-cholesterol and atherosclerotic cardiovascular diseases (ASCVD). FH patients are characterized by severely elevated LDL particles from birth that lead to atherosclerotic plaque formation and cardiovascular events very early in life. In most of the cases, FH is presented as an autosomal dominant mutations in genes like the LDL receptor (*LDLR*), accounting for the majority of the cases, the apolipoprotein B100 (*APOB*) and Proprotein convertase subtilisin/kexin type 9 (*PCSK9*) [44, 45]. Because the risk of ASCVD is dose-dependent, the heterozygosity/homozygosity of one or more of the genes (compound heterozygosity/homozygosity) is associated with a different degree of severity in the

phenotype. The mutations on the *LDLR* gene are described as loss-of-function, which means that the LDL receptor is unable to clear LDL particles from the bloodstream; this leads to an increase retention of those inside the arterial wall. The mutation in the *APOB* gene, is also a loss-of-function mutation that results in a reduction in the clearance of LDL particles due to a reduce affinity of apoB-100 for LDLR.

Those mutations were known to be the most common leading causes of FH until 2003, when Abifadel et al. discovered a mutation in the *PCSK9* gene, previously known as NARC-1 (or neural apoptosis regulated convertase), in 23 French families affected by FH not related to mutations in *LDLR* or *APOB* [46, 47]. The protein PCSK9 belongs to a family of nine secretory serine proteases that are related to bacterial subtilisin and yeast kexin: the proprotein convertase 1 (PC1), PC2, furin, PC4, PC5, paired basic amino acid cleaving enzyme 4 (PACE4) and PC7, subtilisin kexin isozyme 1 (SKI-1) and PCSK9. The first seven members activate cellular and pathogenic precursor proteins by cleavage at basic residues, whereas SKI-1 and PCSK9 regulate cholesterol and/or lipid homeostasis via cleavage at non-basic residues and through induced degradation of receptors, respectively [48]. PCSK9 is mainly expressed in the liver and it is synthetized as a pro-protein; within the endoplasmic reticulum (ER), it undergoes an autocatalytic cleavage that removes the pro-domain and allows the secretion of the protein. The crystal structure of secrete PSCK9 revealed that the pro-domain is bound to the catalytic domain, probably inactivating the protein as an enzyme. Once in the circulation, PCSK9 binds the LDLR onto its extracellular EGF-A domain, as shown in Figure 3

[49], this binding mediates the internalization of the receptor into lysosome for degradation, thereby the recycling of the receptor to the surface of the hepatocytes is prevented.

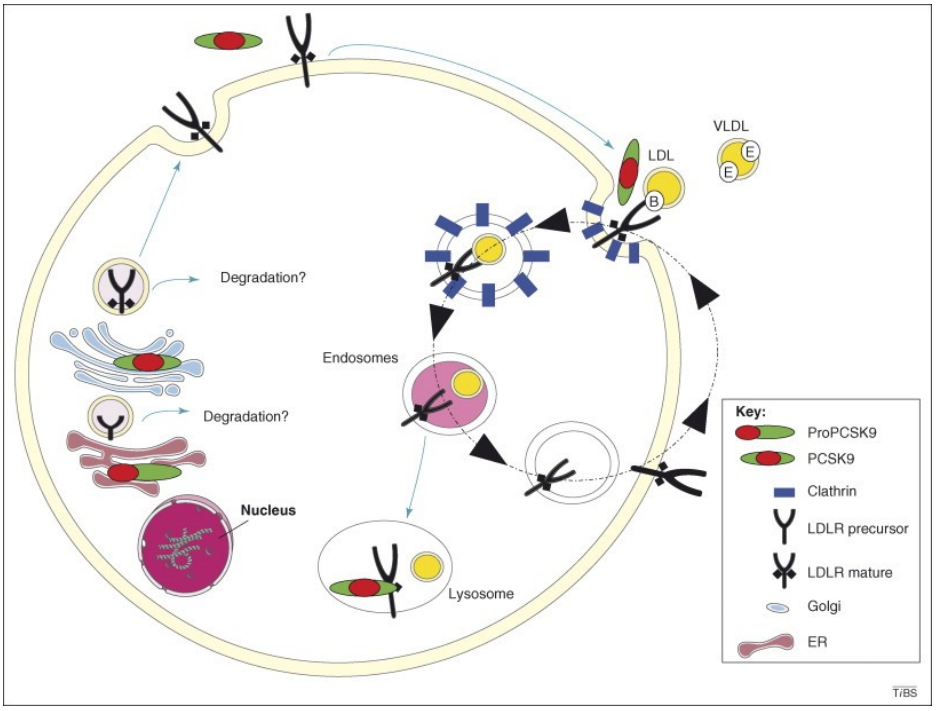

Figure 3. The effect of PCSK9 on LDLR expression in hepatocytes*. At the cell surface the complex formed by the LDLR and apoB- or apoE-rich lipoproteins (yellow) is endocytosed in clathrin (blue) coated pits. Within endosomes the acidic pH (pink) probably triggers the release of the lipoprotein and its degradation in lysosomes, whereas the receptor is recycled at the cell surface, PCSK9 prevents this process upon the bind on the EGF-A domain of the receptor [49]. PCSK9 could also mediates the degradation of LDLR during its maturation.*

Mutations on *PCSK9* gene hence leads to an impaired cholesterol homeostasis (**Figure 4**), loss-of-function mutations are associated with very low LDL cholesterol, whereas gain-of-function mutations determine an extremely severe FH phenotype, characterized by total cholesterol levels above 10 mmol/L (more than 300mg/dl) and manifestations of ASCVDs symptoms very early in life [50].

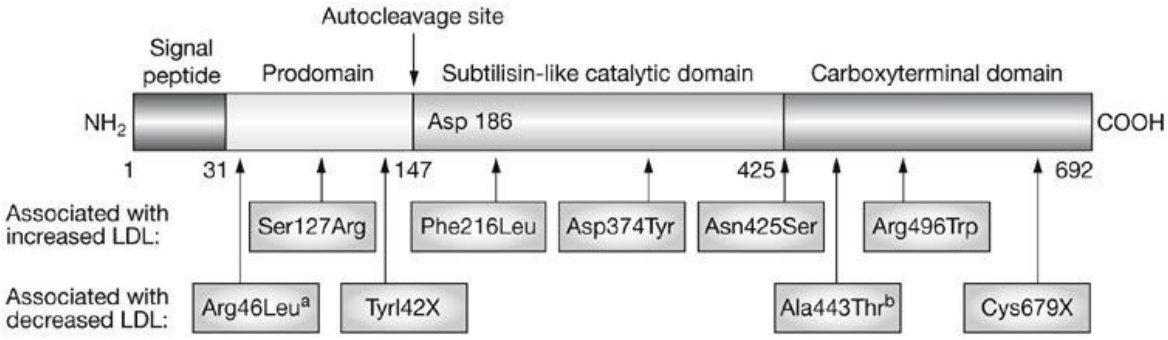

Figure 4. Schematic structure of PCSK9 showing the different domains and the mutations associated with hypercholesterolemia or hypocholesterolemia. *[a]Only associated with low cholesterol in whites. [b]Only associated with low cholesterol in American blacks homozygous for the variant [45].*

Besides LDLR, APOB and PCSK9, mutations in other genes that encode for proteins involved in cholesterol homeostasis could be associated with the risk of ASCVDs like NPC1L1 or MTTP. Accordingly, pharmacological treatments that impact cholesterol homeostasis could be beneficial in the prevention and treatment of dyslipidemia and thereby reducing the risk of ASCVD. The relationship between LDL-C and ASCVD is so strong that, independently from the mechanism used to reduce LDL-C, the odd ratio between the pharmacological treatment and the respective mutations in the related gene are comparable with each other (Figure 5). It is important to mention that the pharmacological treatments for primary prevention are started usually in adults, thereby the association between the reduced risk of ASCVDs per mmol/L of cholesterol is less strong compared to that of genetic mutations, present since birth as shown by the different steepness in the log-linear curves in **Figure 2**.

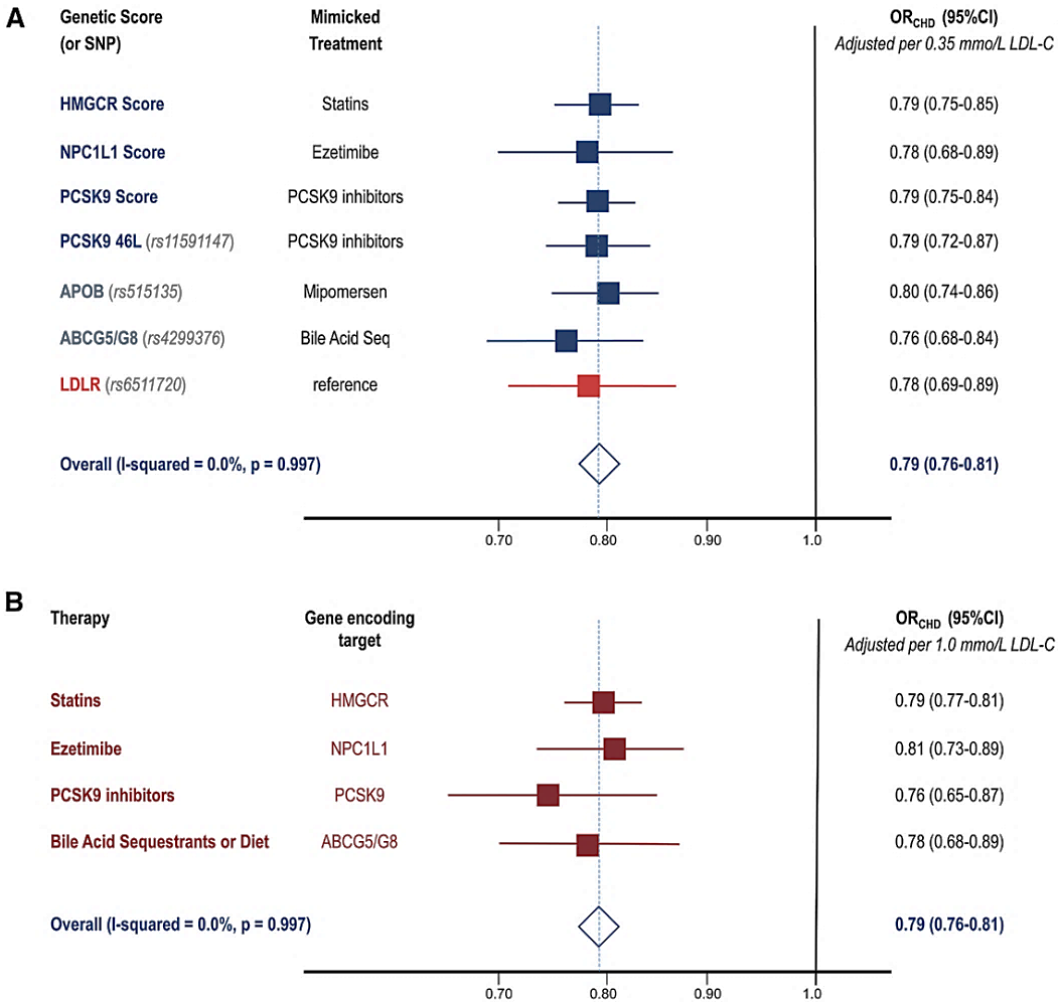

Figure 5 Effect of exposure to lower low-density lipoprotein cholesterol (LDL-C) by mechanism of LDL-C lowering*. A) Genetic variants or genetic scores combining multiple variants in the genes involving the targets of currently available LDL-C-lowering therapies, compared to mutations in LDL receptor gene, odd ratio adjusted for a standard decrement of 0.35 mmol/L lower LDL-C. B) Lipid lowering therapy involved in the LDLR pathway, adjusted per millimole per litre lower LDL-C [42].*

PCSK9 inhibition: the era of intensive LDL-cholesterol reduction.

The strong association between PCSK9 and cardiovascular diseases is well documented by Mendelian randomized studies and randomized trials. As shown in Figure 6, the presence of high levels of circulating PCSK9 is associated with increased risk of cardiovascular diseases. Blocking PCSK9 thus represents a valid approach to lower LDL-cholesterol by increasing the recycling of LDL receptors on the surface of hepatocytes.

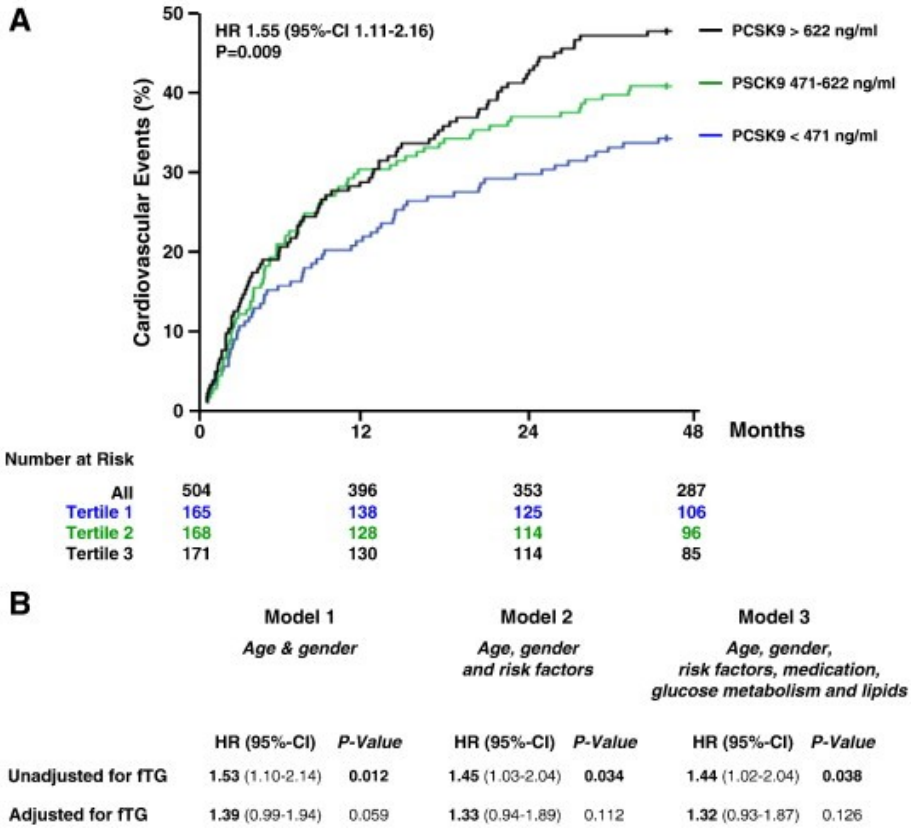

Figure 6. Risk prediction associated with PCSK9 levels in patients with stable coronary artery diseases on statin treatment*. A) Kaplan–Meier plots of primary outcomes stratified by tertiles of PCSK9 concentrations. B) Adjusted hazard ratio (HR) with 95% confidence intervals (95%-CI) for the time to the first primary outcome event of the study cohort, stratified by tertiles of the PCSK9 concentration [51].*

Statins are the gold standard for the prevention and treatment of ASCVDs; these drugs inhibit the Hydroxy Metil co enzyme A reductase (HMGCR) expressed in the liver (due to the tropism of statin), which is the rate-limiting step in cholesterol biosynthesis. This inhibition causes a decrease in intracellular levels of cholesterol, thereby activating the Sterol Responsive Element Binding Protein (SREBP) which in turn activate the expression of LDLR, in order to restore the intracellular levels of cholesterol [52]. The increased expression of LDLR on the surface of the hepatocytes mediates the uptake of LDL particles in the bloodstream, resulting in a reduction in circulating LDL particles and hence serum cholesterol [53]. The HMGCR

inhibitors reduce ASCVDs of approximately 30-35%, intended as the risk for a new fatal or non-fatal cardiac event, providing that LDL is decreased by 25-35% [54]. A large meta-analysis of statin trials demonstrated that for each 1 mmol/L reduction in LDL-C there is a proportional reduction of 22% in the risk of major vascular events [55]. However, many patients do not achieve the recommended levels of LDL-C [56] and thereby experience cardiovascular events despite maximum statin therapy. This could be explained by either the variability in the pharmacodynamic response to statins and by a reduced compliance of the patient to the treatment due to the present of statin-associated muscle symptoms (SAMS) or idiosyncratic drug-induced liver injury [57]. SAMS and statin-induced liver toxicity have been reported only in less than 5% of treated patients and the majority of patients with liver injury or myalgia have recovered after cessation of therapy. Inadequate LDL-C reduction and presence of high residual risk suggests that additional therapies will be required to reach an effective cardiovascular prevention. The IMPROVE-IT trial (Improved Reduction of Outcomes: Vytorin Efficacy International Trial) demonstrated that a combinational therapy with two lipid lowering drugs (statin and ezetimibe, an inhibitor of NPC1L1, as described in Atherogenic lipoproteins) was able to significantly decrease the risk for ASCVDs for an additional 20%. This is due to the additive effect of the two lipid lowering mechanisms: decrease absorption (ezetimibe) and increase hepatic uptake (statin) [32.7% vs. 34.7% in the ezetimibe/simvastatin and simvastatin arms, respectively; hazard ratio [HR] 0.94, 95% confidence interval [CI] 0.89-0.99; p = 0.016] [58]. The serum LDL cholesterol reached after one year of ezetimibe/simvastatin combinational therapy was 53.7 mg/dl, compared to 69.5 mg/dl in the simvastatin monotherapy group and accordingly, the reduction of LDL-C was correlated with a reduction in ASCVD risk. Only with the discovery of PCSK9 as a new therapeutic target, the levels of serum cholesterol that can be reached, on top of statin therapy, are extremely low, similar to or even lower than those seen in nonhuman species or newborn (21 mg/dl) [59].

The first PCSK9 inhibitors approved were monoclonal antibodies, alirocumab (Praluent from Regeneron/Sanofi) and evolocumab (Repatha from Amgen). They bind PCSK9 in the circulation thereby preventing its binding with LDLR, the enhanced recycling of the receptor on the hepatocyte surface results in a significant decrease of LDL-cholesterol (Figure 7) [60]. Those antibodies are produced in Chinese Hamsters Ovary cells by recombinant DNA technology. Depending on the dose of the agent, the reduction in all the apoB containing

lipoproteins ranges from 50% to 60%. In addition, PCSK9 inhibitors also lower lipoprotein(a) by 25%, mainly due to the LDLR-mediated clearance of the those particles [61].

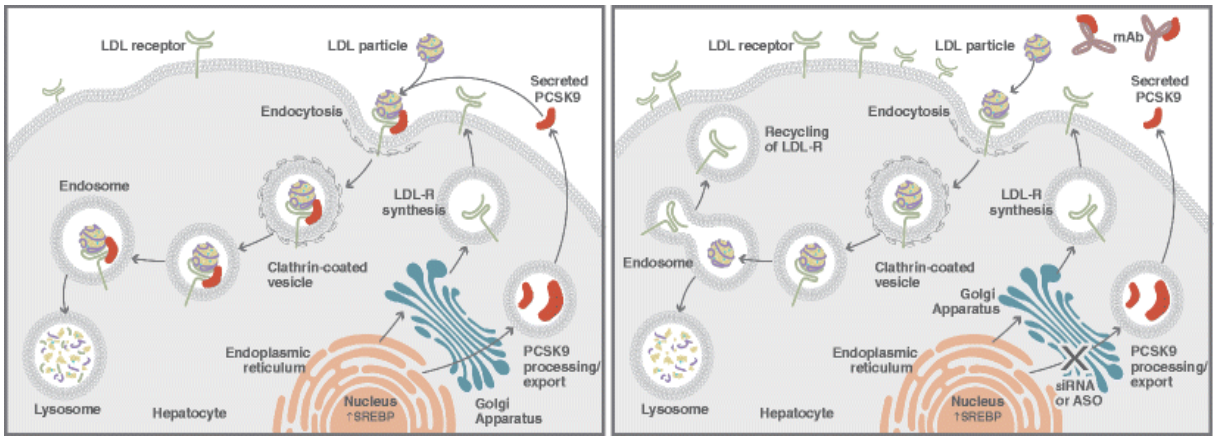

Figure 7. Effect of PCSK9 inhibition on LDLR cycle*. The monoclonal antibody (mAb), due to their size, cannot diffuse inside the cells or cross the blood-brain barrier; therefore, they can bind only secreted PCSK9 [60].*

In both the clinical trials involving the monoclonal antibodies (FOURIER and ODISSEY) the reduction on LDL-C compared to placebo was 60% on average, accompanied by a reduction on the total events of 15%, after a median follow-up of 2.2 years. Moreover, cardiovascular death, myocardial infarction or stroke were reduced by 20% [62].

In the GLAGOV (Global Assessment of Plaque Regression with a PCSK9 Antibody as Measured by Intravascular Ultrasound), the effect of evolocumab on coronary atheroma was assessed by intravascular ultrasound and the arm treated with the monoclonal antibody showed a reduction in the atheroma volume of about 1% ($P < .001$). Notably, an induced plaque regression was reported in a group of patients with LDL-C below 20 mg/dL (**Figure 8**).

These findings further demonstrated that reaching very low levels of LDL cholesterol not only decreases the progression but also may lead to regression of atherosclerosis, even when applied during a limited time period (GLAGOV primary endpoint 76weeks) [63, 64].

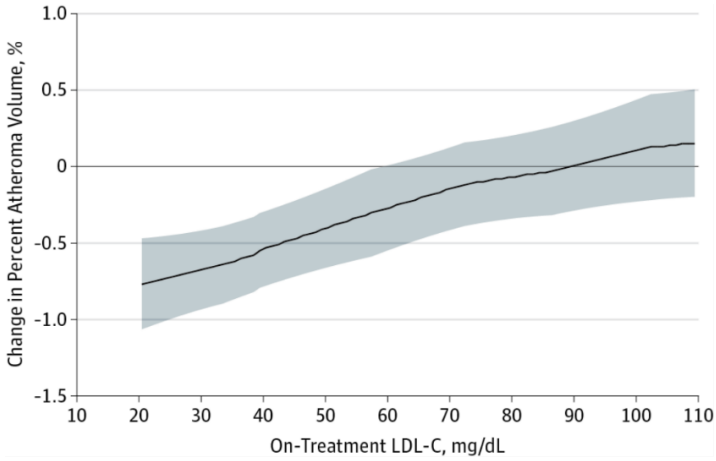

***Figure 8. Change in percent atheroma volume associated with reduction of LDL-C**. Local regression (LOESS) curve illustrating the post hoc analysis of the association between achieved low-density lipoprotein cholesterol (LDL-C) levels and the change in percent atheroma volume in all patient assessed with IVUS (Intra-Vascular Ultrasound) [63].*

Besides monoclonal antibodies, other strategies to inhibit PCSK9 comprise: inhibition of PCSK9 synthesis in the endoplasmic reticulum (antisense oligonucleotides, siRNAs) and inhibition of the binding with the EGF-A domain of LDLR (small molecules) [65]. The main differences with the monoclonal antibodies are the size of the molecule, which allows those inhibitors to enter inside the cells and counteract PCSK9 effects both on the intracellular and extracellular sides and, naturally, the pharmacokinetics. The antisense nucleotide (inclisiran) is now in phase III, it inhibits PCSK9 synthesis by binding of PCSK9 mRNA and inducing its degradation [66]. To direct the effect of inclisiran through the liver, the antisense oligonucleotide is conjugated to triantennary N-acetylgalactosamine (GalNAc) which is a ligand for hepatocyte expressed asialoglycoprotein receptors (ASGPR); this increased hepatic tropism allows a reduction in the dose and volume of drug injected and extrahepatic side effects [67]. The reduction in intracellular PCSK9 levels mediates the increase in the intracellular cholesterol pool, which leads to a decrease in the activity of both SREBP and non-SREBP pathways involved in lipogenesis, lipidation of apoB, and the uptake and degradation of VLDL particles [68, 69], resulting in a more sustained lipid lowering effect. It is reasonable to expect that the phase III trial with the siRNA would provide additional benefit in the reduction of cardiovascular mortality [70]. In summary, inhibiting PCSK9 broaden the possibilities of clinicians to reduce significantly LDL-C in high-risk patients or in patients intolerant to statins.

As mentioned above, the levels of LDL-C reached with PCSK9 inhibition are comparable to LDL-C levels present in the newborns (21±0.8 mg/dL) [71]. It is important to investigate whether those extremely low LDL-C levels may provoke adverse effects in humans, since, indeed, cholesterol is essential for maintenance of cells' membranes and it's the precursor of steroid hormone and bile acids. In this contest, there are some clinical conditions that can provide some evidences about the safety of this extreme low LDL-C: in heterozygous familial hypobetalipoproteinemia patients, for example, there is a reduction in the production of LDL so the lifetime LDL cholesterol is <0.78 mmol/L. Patients with nonsense or missense mutations in angiopoietin-like protein 3 (*ANGPLT3)* gene, which inhibits the LPL activity, have LDL-C of 0.56- 1.03 mmol/L; moreover, patients with loss-of-function mutations in the *PCSK9* gene exhibit extremely low levels of LDL-C. In those clinic conditions, the adverse events are mainly related to the target, rather than to the levels of LDL-C [72]. It is important to consider in fact that the saturation kinetics of the binding of LDL to its receptor has a KD_{50} of 0.064 mmol/L (2 mg/dL) [27], even for the cells that are surrounded by interstitial fluid, where the concentration of LDL is five times less of that in plasma, LDL-C of 20 mg/dL would still be more than sufficient for the uptake [59]. Therefore, also in the presence of extremely low levels of LDL-C, steroid hormone production and bile acids synthesis are preserved, the long term clinical trials with PCSK9 inhibitors (OSLER-1 [73] and ODISSEY LONG TERM [74]) will provide additional evidences not only regarding the potential of sustained extreme low LDL-C levels to further reduce complications of atherosclerosis but also they will be of great interest to evaluate the safety.

Extrahepatic effect of PCSK9

The amount of PCSK9 present in the bloodstream is mainly derived from the liver as demonstrated by the total and the liver-specific knock out mice for PCSK9. They exhibited a 42% and 27% decrease in cholesterol levels respectively, showing that hepatic PCSK9 is responsible for two third of the phenotype [75]. However, PCSK9 is expressed also in other tissues and organs, like the intestine, the kidney, the vascular wall and the brain, in which it exerts different functions (Figure 9).

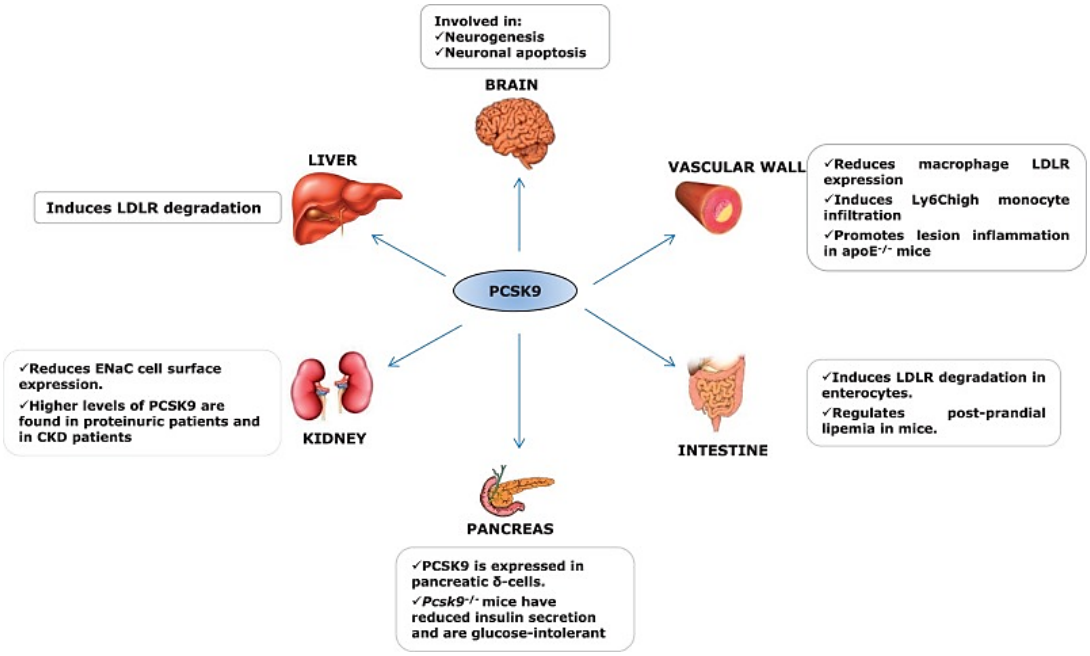

Figure 9. PCSK9 expression in human tissues with relative reported functions [68].

As mentioned above, PCSK9 mediates the degradation of LDLR in the hepatocytes, leading to an increase in the LDL particles in the circulation; intracellularly, PCSK9 could affect the lipid metabolism by interacting with transcriptional (like SREBP) or post-transcriptional (like MTTP) factors. It has been demonstrated that in the presence of high concentration of lipids, especially cholesteryl esters, the liver responds by increasing the secretion of apo B-100 containing lipoproteins, which can explain the increased levels of VLDL and remnants in patients carrying gain-of-function (GOF) mutations in the *PCSK9* gene. It has been hypothesized in fact, that in patients carrying the GOF S127R mutation, PCSK9 is able to bind apo B-100 and preventing its autophagosomal degradation, and enhances its secretion [76]. The effect of PCSK9 on triglycerides-rich lipoproteins is also been reported in the intestine, in fact mice lacking PCSK9 are protected from post-prandial hypertriglyceridemia which could be either explained by the increased clearance of particles via apo E/LDLR/VLDLR and CD36

pathways or decrease production of apo B-48 via SREBP-2 pathways. The clinical studies with PCSK9 inhibitors, however, showed that the reduction in TRL was modest and mainly related to the action of PCSK9 on the LDLR pathway: the monoclonal antibodies, that inhibit only the circulating PCSK9, were able to reduce plasma TG levels of less than 20%, compared to placebo control and this effect was principally due to enhanced hepatic clearance of remnants. The ASO inclisiran, which acts both extracellular and intracellular ways, exerted the same effect on TG levels in the Phase II clinical trial, although data on lipoprotein kinetics are still to be determined [77].

PCSK9 was previously known as NARC-1, expressed in the brain where the role of this protein is still not completely understood. PCSK9 is found in brain areas with high proliferative index, such as the embryonic brain telencephalon neurons and peri-ischemic regions, where neurogenesis takes place; the induction of neuroectoderm in pluripotent mouse P19 embryonal carcinoma cells with retinoic acid is associated with increased expression of PCSK9, suggesting that PCSK9 could have a role in the development and differentiation of neural cells [47, 78]. Moreover, PCSK9 could be also associated with neurodegenerative diseases, such as Alzheimer's and Parkinson's: it has been shown that PCSK9 induced the non-acetylated form of BACE1 [ß-site amyloid precursor protein (APP)-cleaving enzyme 1] and thus, decreasing neuronal apoptosis; although another work reported no effects on either BACE-1 or Aβ, the final product of BACE-1 [79, 80]. Recently, our research group, in collaboration with the research group of Dr. Franco Bernini, reported that PCSK9 levels is increased in the cerebrospinal fluid (CSF) of Alzheimer's patients. Moreover, it positively correlates with the levels of apo E4 (ε4 isoform), which is usually found increased in AD patients, probably due to the effect of PCSK9 on Apo E receptor [81].

PCSK9 is also expressed in the kidneys, where it has been reported an increased in PCSK9 levels in patients with chronic kidney disease (CKD) and proteinuria; PCSK9 is also expressed in the pancreatic δ-cells: PCSK9-null mice showed a reduction in insulin secretion and glucose-intolerance [68].

Recently, different research groups independently reported that PCSK9 is expressed also in the cells that compose the artery wall: endothelial cells, macrophages and smooth muscles cells [82, 83], suggesting that PCSK9 could exert an atherogenic phenotype by both a systemic and a paracrine effect.

The atherogenic-prone areas within the vascular wall are associated with disturbed blood flow. In fact, the shear stress induced by the hemodynamics could activate the endothelial cells by altered expression of pro-inflammatory Nuclear Factor kappa B (NFκB) and oxidant/antioxidant pathways [84]. Ding et al. demonstrated that low shear stress increased the formation of reactive oxygen species that in turn promotes the activation of NFκB and thus PCSK9 expression, possibly via the activation of the scavenger receptor LOX-1 (lectin-like oxidized low-density lipoprotein receptor-1) [85]. The role of PCSK9 in the macrophages is still debated: murine J774A macrophages did not express PCSK9, whereas murine peritoneal macrophages have been reported to secrete functional PCSK9. Another group reported that peritoneal macrophages did not express PCSK9, but they were able to respond to PCSK9 expressed by nearby tissues [68]. Our research group found that the PCSK9 expressed by the smooth muscles cells was able to reduce the expression of macrophage LDLR in a paracrine way [82]. Moreover, the incubation with increasing dose of recombinant PCSK9 promoted an inflammatory phenotype in THP-1-derived macrophages and human primary macrophages via LDLR-pathway [86], supporting that PCSK9 could have a local proatherogenic role.

Due to those extrahepatic functions exerted by PCSK9, it is of great interest to evaluate the possible target-related adverse effects of the different PCSK9 inhibitors in the various tissues. The use of monoclonal antibodies offered a stronger safety profile, compared to the antisense oligonucleotide or the small molecules, mainly because they target only the secreted PCSK9 and they cannot enter the blood-brain barrier. On the other hand, targeting both the extracellular and the intracellular PCSK9 could provide additional benefit in tissues, such as intestine and the vasculature, where PCSK9 is actively involved in the development of additional ASCVD risk factors, such as hypertriglyceridemia and subendothelial inflammation.

Coronary Artery Diseases

Pathophysiology of coronary artery diseases

The formation of atherosclerotic plaques occurs principally in large and medium-sized elastic and muscular arteries, displayed initially as a subendothelial inflammation, progressively degenerates in complicated lesions by accumulation of lipids and inflammation [8]. Those events gradually modify the lumen of the arteries and consequently the oxygen supply to the tissues, leading to ischemic lesions. Patients with coronary artery diseases (CADs) generally present either chronic and acute symptoms which imply different pathophysiology, clinical manifestations and therapeutic treatments.

The chronic CAD are generally manifested as chest pain (angina pectoris) and shortness of breath, indicating either a defect in myocardial oxygen supply or a reduced myocardial blood flow. The underlying cause of the chronic CAD is the presence of stenotic plaques, with partial or complete occlusion of the vessel. The formation of those plaques starts with endothelial dysfunction caused by several risk factors, such as dyslipidaemia, hypertension or hyperglycaemia. The activation of endothelial cells starts the inflammatory response by increasing the expression of adhesion molecules which attracts circulating leukocytes to the inner surface of the artery wall[87]. Those cells initiate the plaque formation by secreting prostanoids, leukotrienes, cytokines, complement components and other mediators of inflammation and immunity leading to SMCs migration and proliferation within the subendothelial space. The extracellular matrix produced by migrated SMCs is able to bind lipoproteins, prolong their residence in the intima and render them more susceptible to oxidative modification and glycation, resulting in enhanced activation of macrophages [87]. Degradation of extracellular matrix by metalloproteinases, calcification and cell death are factors that can modify the physiology of the plaque leading to the formation of a lipid-rich necrotic core, surrounded by a fibrous cap [88]. Generally, stenotic lesions are characterized by a small lipid core enclosed in a thick fibrous cap, with different degrees of calcification, usually without compensatory remodelling (or enlargement) of the vessel [89]. This type of lesion becomes manifested especially when the oxygen demand increases, during exercise for example, and patients experience extreme fatigue or chest pain. However, in most of the cases, this condition remains subclinical. In fact, for much of its course, the atherosclerotic lesion grows outward, or abluminally, rather than inward. Thus, a substantial burden of

atherosclerosis can exist without producing stenosis [90]. On the electrocardiogram (ECG), chronic CADs are often seen as an ischemic event that requires therapies aimed to either increase the blood flow by revascularization (percutaneous transluminal coronary angioplasty, coronary artery bypass graft or stent placement) or decrease the oxygen demand by slowing down the heart rate and strength (negative inotropic effect) with nitrates, β-blockers and calcium antagonist. Usually, those types of medication require the association with a radical change in life style. Aggressive management of modifiable risk factors are proven to reduce death rates, myocardial infarction, stroke and other cardiovascular events, including re-hospitalization [91].

Acute CADs, also named acute coronary syndromes (ACSs) are the clinical manifestation of the so-called "complicated plaques". Generally, ACSs could either derive from atherothrombotic events, defined as the complete occlusion of the vessel, or thrombotic events, largely caused by plaque rupture. Myocardial infarction, stroke and peripheral diseases are the general clinical manifestation of ACSs. On the ECG, myocardial infarction is classified based on the elevation or non-elevation of the S-T segment. The former is caused by a complete occlusion of the coronaries and require urgent treatment, the latter by a transitory or partial occlusion and could be managed by drug therapy. The main features of a vulnerable or complicated high-risk plaque are a large central lipid core, an abundance of inflammatory cells, a paucity of SMCs and a thin fibrous cap. This weak structure is susceptible to fissuring by different mechanisms that leads to vascular event. As mentioned in the paragraph "Atherogenic lipoproteins", atherosclerosis is defined as a progressive inflammatory disease. Inflammation in fact is one of the factors involved in the evolution of lesion to a more complicated one [8, 87]. With the development of new and more advanced techniques, such as optical coherence tomography (OCT) and intravascular ultrasound (IVUS), it is possible to evaluate the evolution of a plaque during the progression of the disease [92]. Thus, the plaque rupture mediated by inflammatory cells is now defined as one out of four potential mechanisms that leads to ACSs. In fact, plaque rupture could occur in individuals without symptomatic ACSs and in absence of systemic inflammation [93, 94]. Moreover, plaque erosion and plaque without thrombus are other sign of ACSs that are not mediated directly by inflammation. This diversification is important in the stratification of the patients aimed to a more personalized and targeted therapy.

Nonetheless, the most common mechanism through which a complicated plaque results in a vascular event involves inflammation. Systemic inflammation is generally diagnosticated by evaluating the levels of C-reactive protein (CRP) in patients' blood. Macrophages are responsible for the degradation of the thin fibrous cap by increasing the number of active proteinases and reducing the levels of the corresponding inhibitors, like cystatins [95]. Moreover, an imbalance in adaptive immune pathways could modulate atherosclerotic plaque activity. Although the mechanisms responsible for T-cell dysregulation in ACSs remains unknown, it has been observed that the subset of T-lymphocytes $CD4^+/CD28^-$ was particularly elevated in patients with ACSs. They promote inflammation by secretion of interferon-γ and tumor necrosis factor [96]; vice versa, the number of $CD4^+/CD25^+$ (regulatory T cells), which secrete interleuchin-10 and interleuchin-4 (anti-inflammatory action) were generally reduced [97]. Thus, it is convincible to think that therapy aimed to decrease inflammation could ameliorate the stability of the plaque and potentially prevent the rupture of the plaque itself. Recently, a large phase III trial (CANTOS: Canakinumab Anti-Inflammatory Thrombosis Outcomes Study) tested the efficacy of a fully humanized monoclonal antibody anti IL-1β (an inflammatory cytokine) in reducing major cardiovascular events. In this study, patients with previous myocardial infarction and CRP levels >2mg/L that received canakinumab 150mg, subcutaneously every three months showed a decrease of about 15% in myocardial infarction, stroke or death as primary endpoints and of 17% in secondary endpoint, including urgent revascularization [98, 99]. Plaque rupture, however, could occur also in absence of systemic inflammation. Intense physical exertion, local mechanical stress but also psychological stress could provoke plaque rupture. It has been hypothesized that the activation of sympathetic nervous system with the release of catecholamine induce the plaque rupture by increasing heart rate, blood pressure and vasoconstriction, those mechanism favour plaque disruption with consequent platelet activation [100]. Moreover, the presence of free cholesterol within the lipid core could induce the rupture and activate the inflammasome, an intracellular complex that generate IL-1β and IL-18 [101]. In this contest, the most effective therapy consists in reduce cholesterol crystal formation by an intensive lipid-lowering treatment.

Plaque erosion is a superficial event characterized by the activation of neutrophil and the loss of endothelial cells. Recent study demonstrated that hyaluronan and its receptor, CD44, colocalize along the erosion-prone plaques promoting the apoptosis of endothelial cells and activation of platelet and the subsequent thrombus formation. This mechanism seems to

involve the toll-like receptor 2 in modifying endothelial monolayer [102]. Therefore, therapies aimed to decrease neutrophil activation and limitation of thrombus formation could result in a more beneficial effect rather than the common revascularization. Jia et al have recently observed that patients with OCT-defined erosion and treated with anti-coagulant/antiplatelet therapy showed more than 50% reduction of thrombus volume after 1 month [103].

Finally, ACS could derive from a functional alteration of coronary circulation likely due to a hyperreactivity of the SMCs. Epicardial coronary vasospasm and microvascular spasm could cause myocardial ischemia even in the absence of obstructive atherosclerosis; this may result from an impaired vasodilatation/vasoconstriction of the SMCs potentially due to an increase of Rho kinase activity [104, 105]. On this matter, therapies that reduce Rho kinase activity [106] or the vasospasm (long-acting nitrates and calcium channel blockers [107]) should be taken into account.

Epidemiology of coronary artery diseases in Europe

Coronary artery diseases are the leading cause of mortality in Europe. They are responsible for over 3.9 million deaths a year, which consists of 45% of all deaths. In men, CVD accounts for 1.8 million deaths (40% of all deaths), while in women it is responsible for 2.1 million deaths (49% of all deaths). By comparison, cancer, the next most common cause of death, accounts for just under 1.1 million deaths (24%) in men and just under 900,000 deaths (20%) in women respectively (Figure 10).

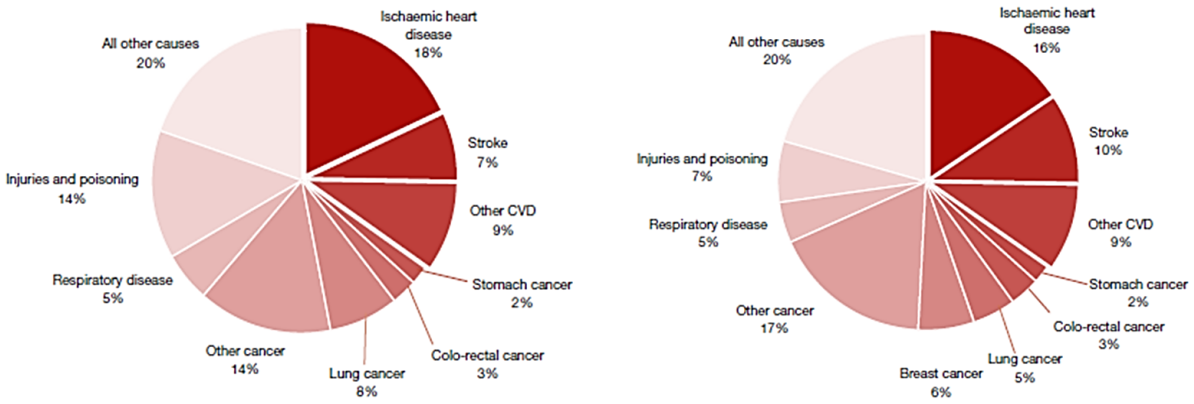

Figure 10. Overall deaths under 75 years by cause in Europe. *Left panel represent death by cause in males, the right panel represent death by cause in females. Data collection form the World Health Organization, the Institute for Health Metrics and Evaluation, and the World Bank of 56 European countries, analysed by the European Society of Cardiology [108].*

Ischemic heart diseases like myocardial infarction remain the leading single cause of mortality in Europe, responsible for 862,000 deaths a year (19% of all deaths) among men and 877,000 deaths (20%) among women each year. Within the ACS, also stroke represent the second most common single cause of death in Europe, accounting for 405,000 deaths (9%) in men and 583,000 (13%) deaths in women each year. It has been estimated that the total cost for cardiovascular diseases is near 210€ billion per year. This cost not only comprises the actual treatment for primary and secondary prevention, but also the estimated cost of patients undergoing heart failure due to myocardial infarction [108]. Nonetheless, the overall mortality rates over the past 30 year is decreasing as well as the rate of hospitalization for acute myocardial infarction. This have been attributed, at least in part, to risk factor modification at population level. Besides the non-modifiable risk factors (age, sex and genetic mutations), modifiable risk factors represent a huge component in establish the total risk of cardiovascular events. The Framingham study and the case-control study INTERHEART conducted in 52 country established the importance of evaluating the major risk factor in the primary and secondary prevention of CVDs. Among all, dyslipidaemia, hypertension, alcohol consumption,

diabetes, obesity, sedentary lifestyle, and smoking account for >90% of the population attributable risk of acute myocardial infarction in all regions of the world. [4, 109]. The National Cholesterol Education Program Adult Treatment Panel III and European guidelines strongly underline the controlling of modifiable risk factor as an important component of primary and secondary prevention, as mentioned in Atherogenic lipoproteins.

The major risk factors historically associated with the risk of CVD, particularly ACS, besides dyslipidemia, are hypertension, metabolic disorders and unhealthy habits (smoking, sedentary life style). Generally, those factors are strongly associated with each other, and little changes determine a huge impact on the risk of CVD. Hypertension is a highly prevalent condition in the population, especially during aging. Hypertension could be due to a progressive, age-related hardening of the artery walls as well as the loss of elasticity mediated by the diffusion of atherosclerotic lesions. Moreover, hypertension could be caused by a functional changes of the artery wall per se, with an increase in sympathetic system activity probably due to decreased sensitivity of beta-receptors. This leads to an inefficient distension of the artery wall during the systole with a consequent increase in both systolic and pulse blood pressure. From epidemiological and randomized-controlled studies, it has been demonstrated that a reduction of 1mmHg in blood pressure lowers the long-term risk of MI by 2% to 3% [110]. Obesity is another world-wide condition that affect both adults and children [108], especially in high-income countries. This condition is associated with vascular defects, endothelial dysfunctions, arterial stiffening and dysregulated adipose tissue signalling; overall contributing to defining obesity as an important risk factors for CVD. Obesity leads to an increase in adipocytes number and size, resulting in adipose tissue expansion and macrophages infiltration, generating a low-grade chronic subclinical inflammatory state [111]. This persistent release of proinflammatory cytokines interacts with inflammatory and immune pathways and directly contributes to vascular dysfunction, through the activation of endothelium. Moreover, the adipose tissue per se is able to directly induce cardiovascular events by actively secreting the so-called adipokines [112]. Leptin, adiponectin, retinol binding protein 4 (RBP4) and resistin could interact with both central and peripheral tissues and therefore affecting carbohydrate and lipid metabolism, inflammation, coagulation and blood pressure [113, 114]. Another important metabolic condition is diabetes mellitus. The risk of CVD mortality in type 2 diabetic patients is more than double compared with that in age-matched subjects. Stroke events and all manifestations of CVD, myocardial infarction (MI),

sudden death, and angina pectoris are at least twofold more common in patients with type 2 diabetes (DMT2) than in nondiabetic individuals [115]. The presence of high glucose levels in the blood due to DMT2 and poor glycemic control, determined glycation of lipoproteins, especially in the protein portion. Glycosylation is a non-enzymatic reaction in which a reducing sugar (such as glucose with its α-oxoaldehyde metabolites and fructose), via formation of a Schiff's base, links with exposed lysine residues of a protein, like the apolipoproteins. Glycate lipoproteins have higher affinity for scavenger receptors expressed on the surface of inflammatory cells, like macrophages. This could contribute to increase foam-cell formation within the sub-endothelial space [116]. Besides glycosylation, diabetes is often associated with other pathological conditions like obesity or hypertension, therefore enhancing the risk in developing CVD.

It is therefore interesting how epidemiological data regarding cardiovascular mortality and the management of risk factor are robustly associated with each other. Although a significant part of the total risk of a vascular event is non-modifiable, changing in lifestyle and pharmacological intervention are able to considerably modify the trajectory of the disease (Figure 11).

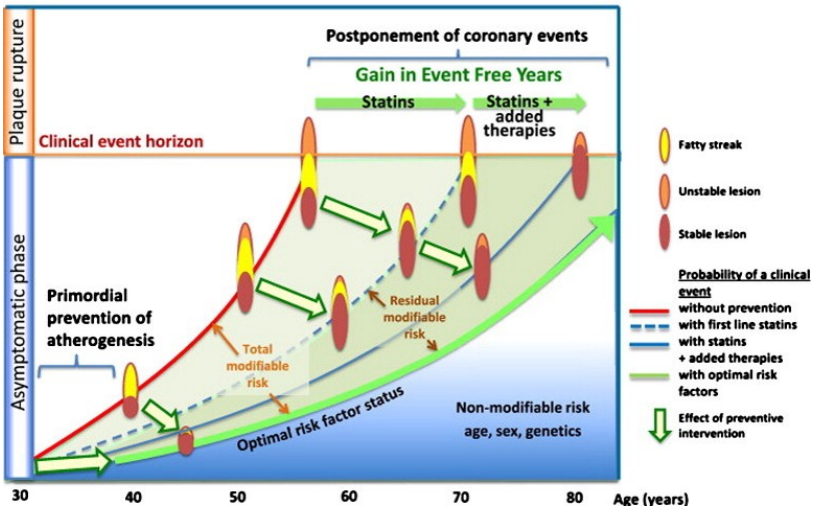

Figure 11. Disease trajectories in cardiovascular disease prevention. *The optimal risk factor status (defined by the green line) represents the baseline risk status determined by non-modifiable risk like age, sex and genetics. Pharmacological and surgical interventions shift the trajectory of the disease (red line) closer to the optimal risk. However, there is still a significant percentage of residual risk even after interventions. The new therapies are therefore aimed to reduce this residual modifiable risk status; stratification of patients based on concomitant diseases (metabolic disorders and hypertension) and defining the pathophysiology of CAD represent an important component for this final goal [117].*

Reducing the number of rehospitalization and revascularization (secondary prevention) are considered crucial endpoints in the treatment of ACSs. On this matter, restenosis is the major adverse event that occur after revascularization. The techniques for mechanical reperfusion of the vessel have been improved through the decades. The prevalence of acute and chronic vessel occlusion following balloon angioplasty was 30% to 60%, mostly due to acute and chronic recoil and constrictive remodelling. The advent of bare-metal stents (BMS) appeared to eliminate the issue of acute and chronic recoil but introduced a new entity, neointimal hyperplasia (Figure 12). This process is mediated by the migration and proliferation of the SMCs from the media inside and around the stent, causing the re-occlusion of the vessel. The extent of restenosis with BMS is around 16% to 44% within all the cases, with the highest percentile with long lesion length and small vessel caliber [118]. The advent of the drug-eluting stent (DES) with antiproliferative drugs furthermore reduced the prevalence of this ADE of about 16% [119]. Nonetheless, the residual risk of vessel re-occlusion is still a current problem [120].

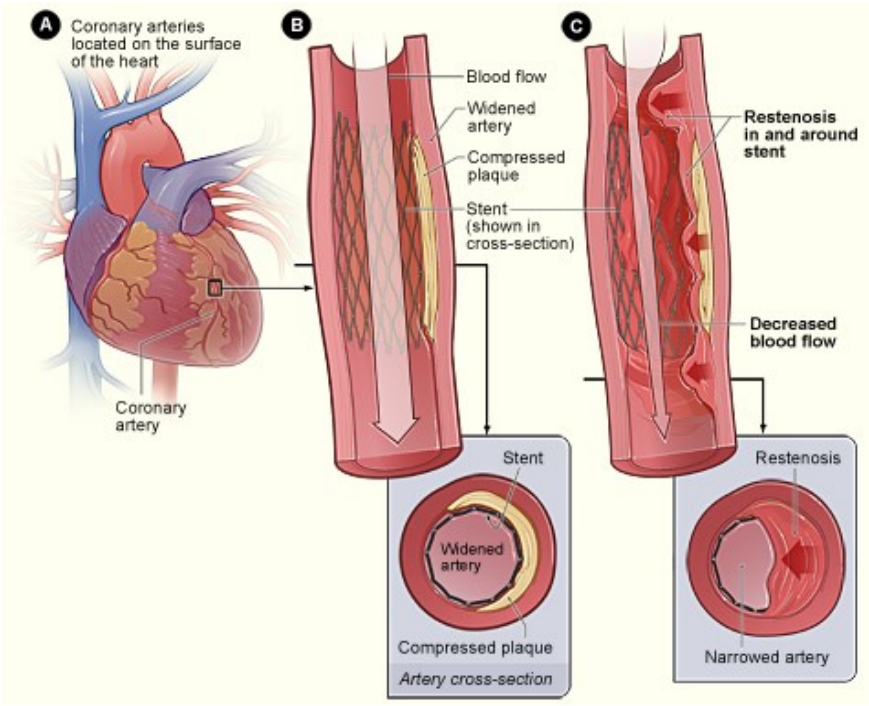

***Figure 12. Mechanism of restenosis following revascularization by stent placement**. A) The angiography guides the position of the stent trough the occluded artery. B) The stent-widened artery re-acquires normal blood flow. C) neointima hyperplasia starts to occur leading to narrowing of the vessel [121].*

The role of smooth muscle cells during neointima hyperplasia

The main feature of SMCs is represented by the extreme plasticity of these cells. Even in adult organisms, these cells are not terminally differentiated. Indeed, their phenotype can undergo profound changes in response to local environmental cues including growth factors or growth inhibitors, mechanical influences, cell-cell and cell-matrix interactions, and various inflammatory mediators. In the presence of vascular injury or atherosclerotic lesion, a strong reorganization of the structure of the vessel occurs; determining profound changes in the environment that surround vascular SMCs [122]. Those cells are actively involved in the formation of atherosclerotic plaques; the secretion of pro-inflammatory factors by the resident macrophages in fact induced the migration and proliferation of the SMCs within the sub-endothelial space, gradually narrowing the lumen of the vessel. Moreover, SMCs can secrete a conspicuous amount of extracellular matrix which traps lipoproteins and makes them susceptible to oxidative modification, worsening the progression of lesion [123].

Regulation of smooth muscle cells phenotype

One of the major challenges in describing the phenotypic modulation of SMCs and their involvement in neointima hyperplasia is the heterogeneity of vascular SMCs. This could derive either from a different clonal expansion from stem cell population or from environmental cues that surround the SMCs. It is well accepted that SMCs could space from a contractile phenotype to a synthetic one, with different degree of differentiation. Within the same vessel, even within the same lesion, it is possible to distinguish different subset of SMCs.

The more contractile phenotype is associated with increased expression of markers such as α-smooth muscle actin, which is also an early marker of SMCs differentiation, myosin heavy chain and transgelin or SM22α, which are expressed in adult smooth muscle cells. The ultrastructure studies of contractile SMCs revealed a paucity of endoplasmic reticulum and Golgi's apparatus, but a relative abundance of contractile structures like myofilaments. This determines an elongated and spindle-shaped morphology. In contrast, synthetic SMCs exhibit cobblestone morphology which is referred to as epithelioid or rhomboid. On an ultrastructure level, the synthetic SMCs contain a high number of organelles involved in protein synthesis as well as extracellular matrix production, with a disorganized contractile apparatus (Figure 13).

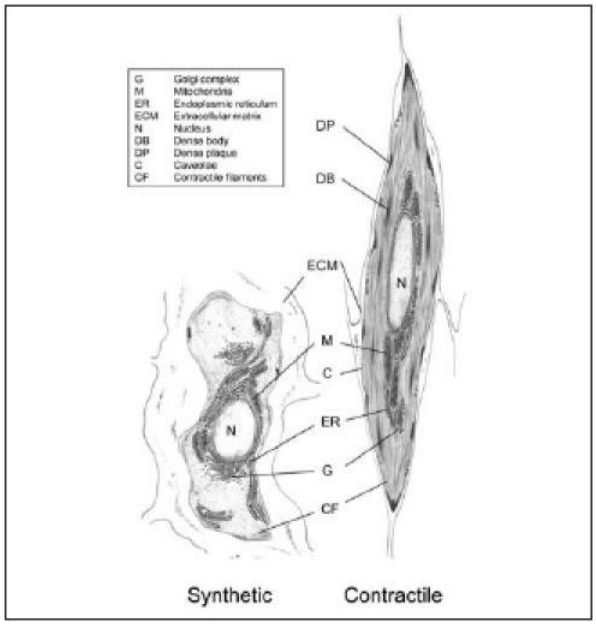

Figure 13. Structural difference between synthetic and contractile SMCs*. N: nucleus, ECM: extracellular matrix, C: caveolae, M: mitochondria, G: Golgi's apparatus, ER: endoplasmic reticulum, DP: dense plaque, DB: dense body, CF: contractile filament [124].*

The difference in morphology is also reflected in the expression markers of the synthetic SMCs. The expression of extracellular matrix-related proteins is the major discrepancy. Even those markers are not specific to SMCs, higher expression of collagen I, nonmuscle myosin heavy chain II-B (SMemb) and I-caldesmon characterize the synthetic phenotype. The cellular retinol binding protein (CRBP)-1 is seen to be upregulated in SMCs after vascular injury and in SMCs that localized in atherosclerotic lesion therefore it could be considered as a synthetic marker. Generally, synthetic SMCs are characterized by increased proliferation and migration rates.

SMCs can switch their phenotype based on genetic and epigenetic factors; which component has the major influence, is still an open question. The genetic component has been hypothesized based on the observation that after vascular injury, the overall expression of contractile markers goes down but in a very heterogeneous way. Furthermore, the re-expression of contractile markers at later time point does not occur uniformly but, first, in clusters of cells. The genetic variance between SMCs could be explain by the different SMCs progenitors. The vascular SMCs could either derive from various mesodermal lineages such as the splanchnic mesoderm, lateral plate mesoderm, somatic or paraxial mesoderm [125] or neural crest [126]. It is convincible to think that heterogeneous SMCs could derive from multipotent vascular stem cells that differentiated into specific subpopulations with different functions [127, 128]. Moreover, Bochaton-Piallat et al. transplanted arterial SMCs with distinct phenotypic features into the intima of denuded rat carotid artery and confirmed that SMC heterogeneity may be controlled genetically and not influenced by local stimuli [129]. However, changes in the local environment due to blood pressure adjustment or atherosclerotic lesion formation have been documented to profoundly influence SMCs phenotype.

During vascular development, the platelet-derived growth factor (PDGF) plays an essential role in the initial stages of SMC differentiation by recruiting mesenchymal cells and by inducing their proliferation [130]. In adult SMCs, PDGF secreted by endothelial cells, monocytes and SMCs themselves, is able to downregulate the expression of α-SMA in rat aortic SMCs [131] and to increase proliferation and migration in pig coronary artery SMCs [132]. Moreover, in vivo studies showed that inhibition of PDGF pathway after arterial injury leads to reduced neointima formation [133].Transforming growth factor β (TGF-β) on the other hand seems to promote a more contractile phenotype. Cultured neural crest cells treated with TGF-β differentiates towards a spindle-shaped SMCs and the activation of TGF-β signalling is required for SMCs gene expression in embryoid bodies [134, 135]. When added to adult SMCs, TGF-β promotes the contractile phenotype by upregulation of phenotypic marker like α-SMA, myosin heavy chain and calponin and by inducing cell cycle proteins such as p21, leading to cell cycle arrest and cell division suppression [136, 137]. Besides those factors, activin A, retinoids, angiotensin II, and tumour necrosis factor-α (TNF- α), FGF, insulin-growth factor (IGF)-I and -II, endothelin-1, nitric oxide (NO), reactive oxygen species,

peroxisome proliferator activated receptor-gamma ligands and complement 3 protein have been shown to affect SMC phenotype as well [124].

Mechanical components such as extracellular matrix composition and endothelial-mediated shear stress response are able to directly affect SMCs phenotype. It has been demonstrated that the presence of fibrillar collagen type I in the ECM promotes the contractile phenotype of SMCs, whereas monomeric collagen type I activates SMC proliferation. When comparing SMCs cultured on either monomeric or polymerised collagen, completely different gene expression profiles are observed [138]. Endothelial cells can respond to blood pressure or difference in blood flow by activation of nitric oxide pathway and cell-cell interaction. Both of these components directly affect SMCs behaviour [139].

Intima-media thickness as an indirect biomarker of atherosclerosis

The elastic nature of large- and medium-sized arteries is a critical factor in determining flow pulsatility and generate a steady flow of blood at the capillary level by reflecting the pulsed waves of blood from the heart [140]. A decrease in elasticity is associated with aging, atherosclerosis, diabetes, hypertension and obesity and it is generally refereed as arterial stiffness. There is a reciprocal interaction between arterial stiffness and atherosclerosis; atherosclerotic lesion indeed modifies the functional and the mechanics of the vessel due to the formation of a fibrous cap. It has also been proposed that the changes in carotid elasticity further promote both plaque development and rupture [141]. Moreover, computational models of plaque within an elastic artery emphasize that hemodynamic stress occurs in regions of mismatched elasticity: for example, where the fibrous cap meets a normal vessel wall [142]. The loss of elasticity or the increase of arterial stiffness derived from the proliferation and migration of the SMCs within the intima, resulting in a decreased lumen area corresponding to an increased intima-media thickness. Overall, the thickening of the intima-media layers is considered to represent development of vascular wall hypertrophy, intimal hyperplasia, and atherosclerotic plaque burden, which may have been caused by the effect of multiple risk factors, such as blood pressure and total cholesterol, on the carotid arterial wall over time [143]. For this reason, intima-media thickness has been associated with the risk of coronary artery disease, stroke, and myocardial infarction, and it predicts the progression of coronary artery disease [144]. The available epidemiological data indeed indicate that increased IMT (at or above 1 mm) represents a risk of myocardial infarction and/or

cerebrovascular disease; moreover, increased IMT is a powerful predictor of coronary and cerebrovascular complications with a higher predictive value when IMT is measured at multiple extracranial carotid sites than solely in the distal common carotid artery [143].

Since atherosclerosis is a progressive disease, the evaluation of intima-media thickness could be useful in stratification of patients with stable or non-symptomatic atherosclerosis, mainly because coronary artery angiography cannot detect little changes in vessel morphology. Other techniques, such as intravascular ultrasound or MRI are more accurate and precise in determining plaque progression; however, those are invasive technique: for example, patients undergo MRI scanning have to take bradycardic agents in order to allow the detection of atherosclerotic plaque. Intravascular ultrasound on the other hand, is a real surgical procedure that requires the sedation of the patient in order to place the catheter inside the vessel.

B-mode ultrasound is used to monitor the carotid intima-media thickness (carotid IMT) and it is characterized by a higher resolution without being invasive. It is therefore one of the best methods for the detection of the early stages of atherosclerotic disease. As shown in Figure 14, ultrasounds could provide a direct visualization of the thickening of the vessel.

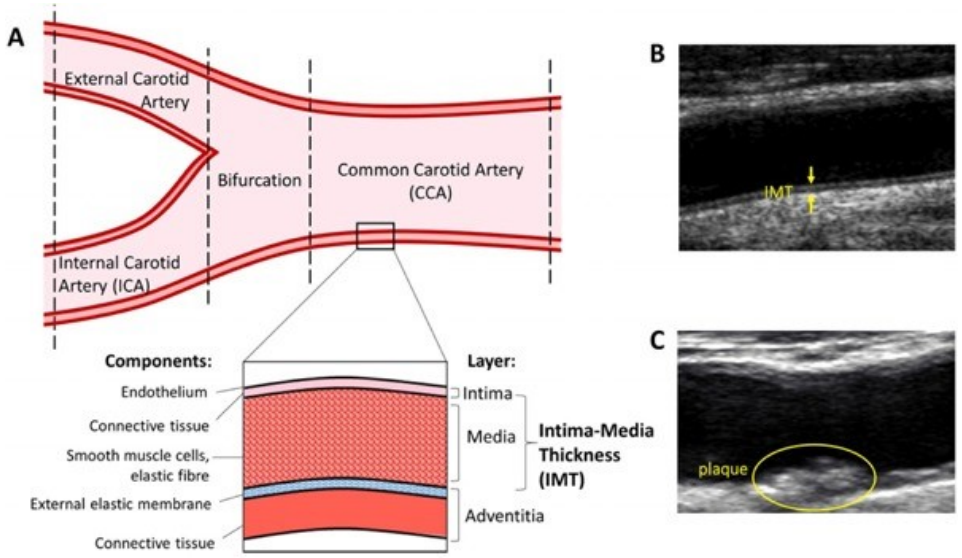

***Figure 14. General visualization of carotid artery**. A) Schematic representation of the common carotid artery (CCA) and each element is depicted in the enlargement. B) Ultrasound image of the CCA, yellow arrow indicates the intima-media thickness. C) Ultrasound image of atherosclerotic plaques [145].*

Another non-invasive technique that could be helpful in assessing the risk in asymptomatic patients is the evaluation of the aortic pulse wave velocity. This measure is inversely correlated with the arterial stiffness. PWV consists of the measurement of the pulse wave

transmission through the arteries and it is calculated as the length between 2 measurement sites divided by the time the pulse wave needs to cover that distance (m/s) [146]. Distensibility of muscular arteries, as mentioned above, is determined by structural components of the artery wall, changes in composition or function of those directly impact the elasticity of the vessel. It has been demonstrated that the PWV is acutely regulated by endothelium-related changes in vascular tone and constitutively released NO; moreover, flow-mediated reduction of PWV could be indicative of endothelial dysfunction [147]. A recent prospective study compared B-mode ultrasound and pulse wave velocity in patient with and without coronary artery diseases and demonstrated that patients with CAD had increased values of aortic PWV compared with patients without CAD (12.5±0.7 vs 10.9±0.6, p<0.001) and carotid IMT significantly correlated with aortic PWV (r=0.787, p<0.001); furthermore validating the use of PWV as a non-invasive methods for atherosclerosis detection in patients with known cardiovascular risk factors [144].

Aim of the study

Since the discovery of PCSK9 as a novel regulator of cholesterol homeostasis, a huge body of literature established PCSK9 as an independent risk factor for atherosclerotic cardiovascular diseases [51]. Although the main connection between PCSK9 and ASCVDs is due to its action on hepatic LDLR, the presence of PCSK9 in extrahepatic tissue suggests potential paracrine effects which could impact the progression and the development of ASCVDs [68]. Previous studies from our research laboratory demonstrated that PCSK9 was expressed in human atherosclerotic plaque and its expression co-localized with the staining of α-smooth muscle actin. In vitro experiments demonstrated that SMCs not only secrete a discreet amount of PCSK9 but also this could directly affect the expression of LDLR on macrophages [82].

Vascular SMCs are undoubtedly active players in the formation of atherosclerotic lesion and vascular remodeling, mainly due to their plasticity in response to various stimuli. The migration and proliferation of SMCs determine the neointima formation, not only in the early phase of the atherosclerotic disease but also during restenosis.

The aim of this study is to investigate the possible direct role of PCSK9 on artery wall through in vivo, in vitro and clinical observations.

Material and Methods

In vivo experiments

Male C57BL/6 mice with *Pcsk9*$^{+/-}$ genotypes (10-week-oldkindly provide by Dr. Philippe Costet (INSERM, Nantes, France [148]) were used in accordance with the Guide for the Care and Use of Laboratory Animals published by the US National Institutes of Health (NIH Publication No. 85-23, revised 1996). *Pcsk9*$^{-/-}$ and *Pcsk9*$^{+/+}$ homozygous mice were generated by intercrossing heterozygous mutant mice. The colonies were fed with normal chow diet.

Perivascular carotid collar placement

Sixteen-weeks-old mice (n = 14 per group) were anaesthetized by intraperitoneal injection of Avertin and subjected to carotid collar placement (12 µl/gr body weight of 2.5% solution). Collars (length: 3 mm, internal diameter: 0.38 mm, external diameter: 2.2 mm) were made from Tygon® tubing and were positioned around the right carotid artery. The contralateral left carotid artery was sham-operated to serve as intra-animal control. Following surgical manipulation, mice were fed a normal chow diet and sacrificed after 9 weeks.

Histochemical and morphometric analysis

At sacrifice, both right and left carotids were collected and fixed overnight in 4% PFA (paraformaldehyde). Tissues embedded in paraffin were cut in serial transversal sections (thickness 5 µm). Every 200 µm ≈, along the entire length of the tissue specimen (not including portions outside – proximal or distal – of the collar), a cross-section was stained with hematoxylin and eosin (H and E). Images were taken under a Zeiss Microscope and morphometrically determinations performed by OPTIMAS 6.2 image software (Media Cybernetics, Silverspring, MD). The perimeters of the lumen and the external elastic lamina were recorded and used to derive the lumen area and the area surrounded by the external elastic lamina (EEL), respectively, using the formula perimeter^2 $(4\pi)^{-1}$, to normalize for artefacts due to fixation or other steps of sample processing, including occasional deformation and potential tissue shrinkage.

Immunostaining

Picrosirius red stain was performed on adjacent sections (one every five sections per animal) and analysed under polarized light after treatment with ImmPRESS Reagent kit (Vector,

Burlingame, CA, USA) according to manufacturer's instructions. The following antibodies were used for immunostaining: α-smooth muscle actin (α-SMA), rabbit polyclonal anti F4/80 (Biovision; Milpitas, CA, USA) and rabbit polyclonal anti PCSK9 kindly provided by Costet et al. [148]

Plasma cholesterol evaluation

Plasma samples were collected from mice by retro-orbital puncture at sacrifice. Fast protein liquid chromatography (FPLC) analysis was conducted to determine the lipoprotein fraction whereas serum total cholesterol levels were measured by an enzymatic colorimetric assay (DASIT, Milan, Italy).

In vitro experiments

Cell cultured reagents were from Euroclone (Milan, ITALY). Complete growth media is composed by Dulbecco's Modified Eagle's Medium High Glucose with sodium pyruvate media, 10% Fetal Bovine Serum, 10mg/mL of penicillim/streptomycin, 2mM L-glutamine and 100µM of non-essential aminoacids.

Isolation of *Pcsk9*$^{+/+}$ and *Pcsk9*$^{-/-}$ SMCs.

Four aortas of each *Pcsk9*$^{+/+}$ ad *Pcsk9*$^{-/-}$ mice were collected after lethal intraperitoneal injection of Avertin. Aortas were then cleared from adventia layer and fat and digested for 15min at 37°C in DMEM containing collagenase IV 100U/mL (Thermo Fisher Scientific, Cat. N. 17104019). Media was replaced with normal growth media and SMCs were collected after three days after trypsinization (Euroclone, Cat. N. ECB3052D). The experiments were done using at least two different cell trains for each genotype.

RNA preparation and quantitative real-time PCR

Total RNA was extracted with the iScript Sample Preparation Buffer cDNA synthesis preparation reagents (BIO-RAD laboratories) and reverse transcription performed with the Maxima 1st strand DNA RT-qPCR (Thermo Fisher Scientific, Waltham, MA, USA), accordingly to manufacture's instruction. Quantitative real time PCR (qPCR) was performed with Kit Thermo SYBR Green/ROX qPCR Master Mix (Thermo Fisher Scientific, Waltham, MA, USA) and the ABI Prism®7000 Sequence Detection System (Applied Biosystems; Life Technologies Europe BV, Milan, ITALY) using the following thermal condition: 95°C for 10 minutes; 95°C for 15second, 60°C for 1minute repeated for 40 cycles.

Primer sequence:

Gene	FWD	RVS
mPcsk9	TTGCCCCATGTGGAGTACATT	GGGAGCGGTCTTCCTCTGT
m α-SMA	CCCAGACATCAGGGAGTAATGG	TCTATCGGATACTTCAGCGTCA
mMyosin heavy chain	ATGAGGTGGTCGTGGAGTTG	GCCTGAGAAGTATCGCTCCC
mCalponin	TTGAGAGAAGGCAGGAACATC	GTACCCAGTTTGGGATCATAGAG
mCaldesom	CCACACTCTCTCAAATTGCCT	GCTGGCTTAGACTCTTCATCGG
mKLF4	CTTTCCTGCCAGACCAGATG	GGTTTCTCGCCTGTGTGAGT
mCdkn1a (p21)	CCTGGTGATGTCCGACCTG	CCATGAGCGCATCGCAATC
mCdkn1b (p27)	TCAAACGTGAGAGTGTCTAACG	CCGGGCCGAAGAGATTTCTG
mCcne1 (Cyclin E1)	CTCCGACCTTTCAGTCCGC	CACAGTCTTGTCAATCTTGGCA
mCcnd1 (Cyclin D1)	GCGTACCCTGACACCAATCTC	ACTTGAAGTAAGATACGGAGGGC

Western blot analysis

SMCs were seeded in three separate 60mm petri dish in complete media. After 24 hours the media was changed with DMEM containing 0.4%FBS. The next day, cells were lysate using triton lysis buffer (25mM HEPES, 100mM NaCl, 1mM EDTA, 10% v/v glycerol, 1% v/v Triton X-100) completed with proteinase inhibitors (Thermo Fischer scientific, cat. n. A32961). Protein concentration was assessed by Pierce BCA assays, accordingly to manufacturer's instructions. 25µg total protein extract/sample were separated on 4-12% sodium dodecylsulfate-polyacrylamide gel (SDS-PAGE; Novex® NuPAGE® 4-12% Bis-Tris Mini Gels, InvitrogenTM; Life Technologies) under denaturing and reducing conditions. Proteins are then transfered onto a nitrocellulose membrane by using the iBlotTM Gel Transfer Device (InvitrogenTM; Life Technologies), 5% non-fat dried milk in tris-buffered saline containing 0.2% of tween was used as blocking buffer. All the antibodies were diluted in 5% non-fat dried milk in tris-buffered saline with 0.2% of tween and incubate overnight at 4°C. Detection of primary antibodies was performed with secondary fluorescently labelled antibody and acquired with the Odissey FC system (LI-COR, Nebraska, USA). Quantitative densitometric analysis was performed with Image Studio software (LI-COR).

Antibody Abcam	Dilution	Antibody Millipore	Dilution
PCSK9	1:500	p21	1:200
LDLR	1:500	p27	1:200
LRP1	1:1000	Cyclin E	1:200
CD36	1:500	Cyclin D1	1:200
VLDLR	1:200	FLAG	1:1000
PDGFR	1:200		

Cell proliferation assay through cell counting

SMCs were seeded in triplicate in 35mm petri dish in DMEM supplemented with 0.4%FCS for 48 hours. Media was then replaced with DMEM 10%FCS and cells were collected at selected time point. Cell proliferation was determined by cell counting using the Coulter Counter model ZM. Doubling time was computed according to Elmore and Swift's formula [149].

Real-time monitoring of cell morphology and cell proliferation using the iCELLigence system

To assess SMCs morphology, 40,000 cells/well were plated into the E-Plate L8, and the extent of cell spreading was monitored every 10 min for 6 h with iCELLigence (ACEA Biosciences Inc, San Diego CA, USA). SMCs proliferation was measured by plating 10,000 cells/well and by monitoring the cell index every 15 min for 5 days. Cells were synchronized for 48 hours in DMEM 0.4% FBS before proliferation and morphology studies.

Cell cycle analysis

SMCs were seeded at 200.000cells/well in triplicate in 35mm petri dish in DMEM supplemented with 0.4%FCS for 48 hours. Media was then replaced with fresh DMEM 0.4%FCS with or without 20ng/mL of recombinant PDGF-BB (Sigma-Aldrich) and incubated for 24 hours. Cell were collected after trypsinization and permeabilized for 15 min using permeabilizing buffer (100mM Tris pH 7.4, 150mM NaCl, 1mM CaCl2, 0.5mM MgCl2, 0.1% NP-40) containing 40µg/mL of RNAse and 5µM of propidium iodide, protected from light. The DNA nuclear content was analysed with FACScan™ flow cytometer and BD CellQuest™ (both from BD Biosciences, San Jose, CA, USA).

Cell migration: Boyden's chamber assay.

The Boyden chamber and the polycarbonate membrane were purchased from Biomap (Agrate Brianza, Milan, Italy). The membranes were coated with 0.1 mg/mL of type I collagen solution (PureCol®, Nutacon BV, Leimuiden, The Netherlands) in 0.1 M acetic acid at 37°C. The lower compartments of the wells of a modified Boyden chamber were filled (in triplicate) with DMEM containing 0.4% FCS in the absence or presence of prorenin or PDGF-BB, whereas the upper compartments were filled with aliquots of the SMC suspensions containing 10^6 cells/mL. The chamber was incubated at 37°C for 6 h. The membrane was then carefully removed. Adherent SMCs on the top were eliminated, and the membrane was stained with a

Diff-Quik staining set (Biomap, Agrate Brianza, Milan, Italy). The number of transmigrated cells was counted in four random high-power fields under high magnification (×20 objective lens).

Cytoskeleton staining

Cover slips were coated over night with 0.1 mg/mL of type I collagen solution (PureCol®, Nutacon BV, Leimuiden, The Netherlands) in 0.1 M acetic acid at 37°C. Cells were then seeded in DMEM 0.4%FCS for 48h. Media was then replaced using DMEM 0.4%FCS with or without PDGF-BB and incubated for 15min at 37°C. Cells were then fixed in 4% paraformaldehyde and stained with rhodamine-phalloidin (Sigma Aldrich, Milan, ITALY) and analysed with Axiovert M220 fluorescent microscope (Zeiss Instruments).

G-LISA assay for Rac1-GTP and RhoA-GTP detections.

The intracellular amount of Rac1-GTP and RhoA-GTP was determined by G-LISA assay (Cytoskeleton, Inc Denver, CO, USA) from total cell lysates snap frozen in liquid nitrogen. Experiment was performed in triplicate accordingly to manufacturer's instruction.

BrdU incorporation assay

Seed 10.000cells/well in a 96-well plate in medium with 0.4%FCS (200µL/well). Every condition is done in triplicate, 2 extra wells were used to determining for protein concentration for every condition. Leave in the incubator for 48h. 100µL of media was then aspirate with a pipette and replace with fresh DMEM 0.4%FCS containing 20 ng/mL PDGF-BB and/or simvastatin 40µM (Sigma-Aldrich). BrdU assay following the manufacturer's instructions (Roche, Cat. N. 11 647 229 001).

Intracellular cholesterol content measure with HPLC.

Cells were seeded in duplicate in 60mm petri dish with DMEM 0.4%FCS and incubated at 37°C for 48h. Media was then replaced with fresh DMEM 0.4%FBS in the presence or absence of PDGF-BB and incubated for 24h. Cell were harvested, lipids were extracted in hexane/isopropyl alcohol (3:2) containing BHT 0.01%. Free- and esterified cholesterol were separated by HPTLC plates and quantified on a DANI 1000 gas liquid chromatographer.

Observational study

The Brisighella Heart study has been active since 1972 and is carried out in agreement with the Declaration of Helsinki [150]. The protocol was approved by the institutional ethics board of the University Hospital of Bologna. All participants gave written informed consent to participate.

Participants

For the present analysis, we selected from the general database of the Brisighella Heart Study 227 premenopausal women and 193 age-matched men and 460 postmenopausal women and 416 age-matched men, excluding participants who were active smokers, who were known to have carotid atherosclerosis [151] or who were in secondary prevention for CVD or in treatment with statins or vasodilating agents. Menopause was self-defined by the interviewed patients as the moment when menstruation definitively stopped and was confirmed with their general practitioners' clinical forms. All available routine clinical and laboratory parameters were sampled with standardized methods [152]. Estimated glomerular filtration rate (eGFR) was calculated using the CKD-EPI (Chronic Kidney Disease Epidemiology Collaboration) formula [153]. Conventional blood pressure was measured after 10 minutes of rest in the seated position within a half hour of obtaining blood samples and in the arm opposite that used for venesection. These measurements were obtained by a trained nurse using a mercury sphygmomanometer and an appropriately sized cuff according to the European Society of Hypertension guidelines [154].

Plasma PCSK9 evaluation

PCSK9 was blindly measured using a commercial ELISA kit (R&D Systems) with plasma aliquot collected after overnight fasting and stored at −80°C. The minimum detectable dose ranged from 0.030 to 0.219 ng/mL, with a mean concentration of 0.096 ng/mL.

Arterial Stiffness Evaluation

Arterial stiffness parameters were assessed using the Vicorder apparatus (Skidmore Medical Ltd), a validated cuff-based device that estimates central blood pressure using a brachial-to-aortic transfer function. Augmentation index is obtained through the blood pressure waveform analysis. It represents, as well as PWV, a measure of wave reflection and arterial stiffness and a marker of cardiovascular risk [155]. It is calculated as the ratio of the pressure

increment caused by the reflected wave (augmented pressure) to the pulse pressure [156]. Pulse wave analysis, from which the augmentation index is obtained, is recorded simply with a brachial cuff placed at the patient's right arm: The Vicorder apparatus registers the radial pressure and, with a specific algorithm, derives the central blood pressure curve. PWV is calculated with a simultaneous measurement of carotid and femoral blood pressure. A small neck pad containing a photoplethysmographic detector is placed around the neck, and a normal cuff is positioned around the thigh of the patient. The distance between the suprasternal notch and the thigh cuff is measured with a measuring tape. This length represents the distance covered by the pulse wave in its carotid–femoral path and is used by the Vicorder apparatus to establish the PWV value. The Vicorder system automatically adjusts the PWV measurement for heart rate and mean artery pressure, as they are simultaneously recorded.

Results

Effect of PCSK9 on neointima formation in Pcsk9$^{+/+}$ *and* Pcsk9$^{-/-}$ *mice after vascular injury.*

As described in **Extrahepatic effect of PCSK9**, PCSK9 is expressed in human atherosclerotic plaques and its expression seems to overlap with the presence of α-smooth muscle actin, a marker for smooth muscles cells (SMCs), suggesting that PCSK9 present in the plaque, derived indeed from the SMCs [82]. To define the role of PCSK9 in neointima formation we took advantage of the established collar model, which consists in a periadventitial carotid placement of a non-occlusive cuff. The placement of the collar induced a rapid macrophages and SMCs infiltration into the arterial sub-endothelium, associated with foam cell formation and extracellular lipid accumulation, without modifying the morphology of the endothelium. All of this features resemble the early human atherosclerotic plaque [157, 158]. Littermates sixteen-week-old *Pcsk9*$^{+/+}$ and *Pcsk9*$^{-/-}$ mice were subjected to collar placement around the right common carotid and they were fed a normal chow diet for 9 weeks. At the end of which, mice were sacrificed for morphometric and composition analysis of the right carotids; left carotids were used as sham-operated control.

Neointimal formation in *Pcsk9*$^{+/+}$ and *Pcsk9*$^{-/}$ *mice*$^{-}$.

The vascular manipulation of both *Pcsk9*$^{+/+}$ and *Pcsk9*$^{-/-}$ mice induced the formation of intimal lesion invading the luminal region, whereas no atherosclerotic lesions were observed in the sham-operated carotid arteries, as shown in the hematoxylin and eosin staining in **Figure 15**.

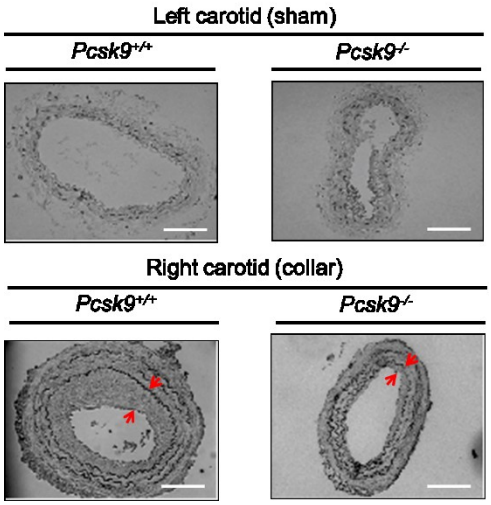

Figure 15. Representative hematoxylin and eosin staining of carotid cross-sections from Pcsk9$^{+/+}$ and Pcsk9$^{-/-}$ mice 9 weeks after perivascular manipulation. *The left carotid (sham-operated control) did not show neointima formation in both the strains, whereas there was a significant increase in neointimal lesion in the right carotid, as indicated by the red arrows. White bars = 100µM.*

The formation of neointima was evaluated by the assessment of morphological parameters: the intima area of *Pcsk9*$^{-/-}$ mice was 12.344 ± 1.668 µm^2 compared to 23.955 ± 1.832 µm^2 for *Pcsk9*$^{+/+}$ (p= 0.049); intima/media ratio in the *Pcsk9*$^{-/-}$ mice was 0.473 ± 0.090 compared to 1.380 ± 0.175 of the wild-type (p = 0.024). There was also a tendency to a higher lumen area in the *Pcsk9*$^{-/-}$ mice 30.194 ± 4.324 µm^2 vs. 18.283 ± 1.912 µm^2, although it did not reach a statistical significance **(Figure 16**). The serum cholesterol level measured as total and lipoprotein-fractions, was evaluated at sacrificed and, as expected, the *Pcsk9*-null mice displayed reduced serum cholesterol (13.6 ± 3.3 mg/dL vs. 47.1 ± 8.8 mg/dL; p < 0.001 for *Pcsk9*$^{-/-}$ and *Pcsk9*$^{+/+}$ respectively) and mainly associated with HDL particles (**Figure 17**).

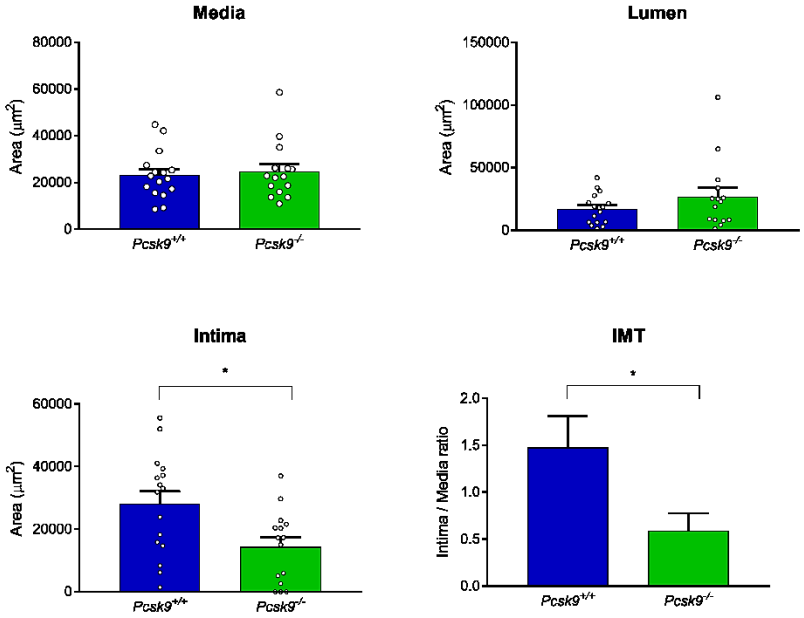

Figure 16. Morphometric analysis of right carotids of Pcsk9$^{+/+}$ and Pcsk9$^{-/-}$ mice 9 weeks after perivascular manipulation. *Intima/media ratio was determined dividing the intimal area by the media area. Differences between groups were assessed by Unpaired Student's t-test, *p < 0.05.*

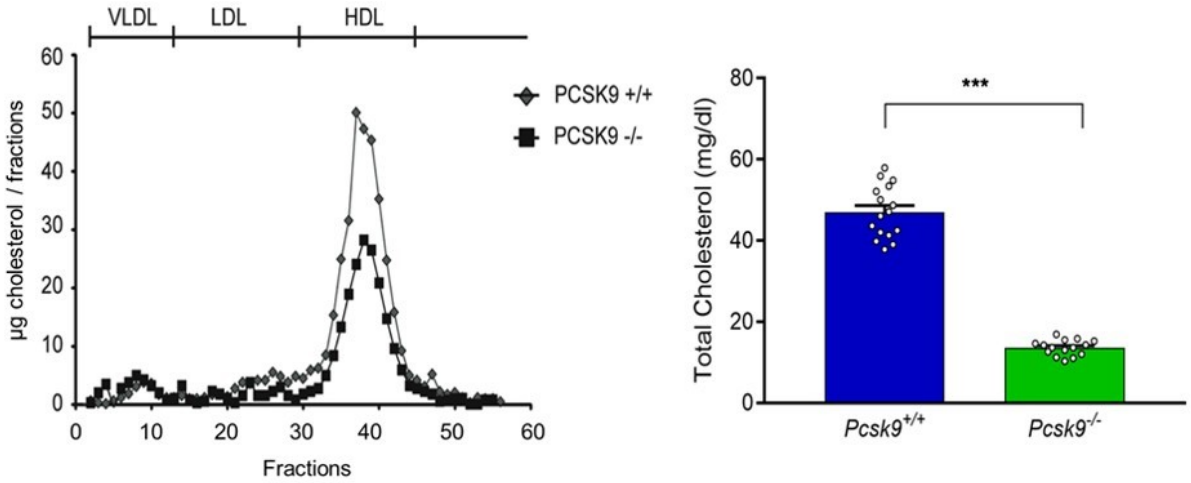

Figure 17. Analysis of serum cholesterol in Pcsk9$^{+/+}$ and Pcsk9$^{-/-}$ mice 9 weeks after perivascular manipulation. *Lipoprotein distribution measured by Fast Protein Liquid Chromatography (FPLC) analysis and represented as µg of cholesterol/lipoprotein fraction. Total serum cholesterol level is significantly reduced in Pcsk9-null mice (p<0.001 assessed by unpaired Student's t-test).*

Composition of *Pcsk9*$^{+/+}$ and *Pcsk9*$^{-/-}$ neointima after vascular manipulation.

Immunostaining for PCSK9 revealed an increased expression of PCSK9 in neointimal SMCs of right carotid arteries after collar placement, PCSK9 was also detectable in the sham-operated control SMCs (left carotid arteries), although at lower levels (Figure 18, left panel). The immunostaining for cell population and composition of the neointima, related to the right carotid arteries, displayed a decreased expression of α-smooth muscle actin (21.0 ± 7.6% and 10.7 ± 2.0 for *Pcsk9*$^{+/+}$ and *Pcsk9*$^{-/-}$ respectively, $p<0.001$) and a decreased content of collagen, analyzed under polarized light of Picrosirius red stained specimens (18.38 ± 7.9% vs. 10.45 ± 9.1% for *Pcsk9*$^{+/+}$ and *Pcsk9*$^{-/-}$ respectively; $p < 0.001$). Immunostaining with F4/80 antibody showed no difference in the macrophages content between the two groups (Figure 18, right panel).

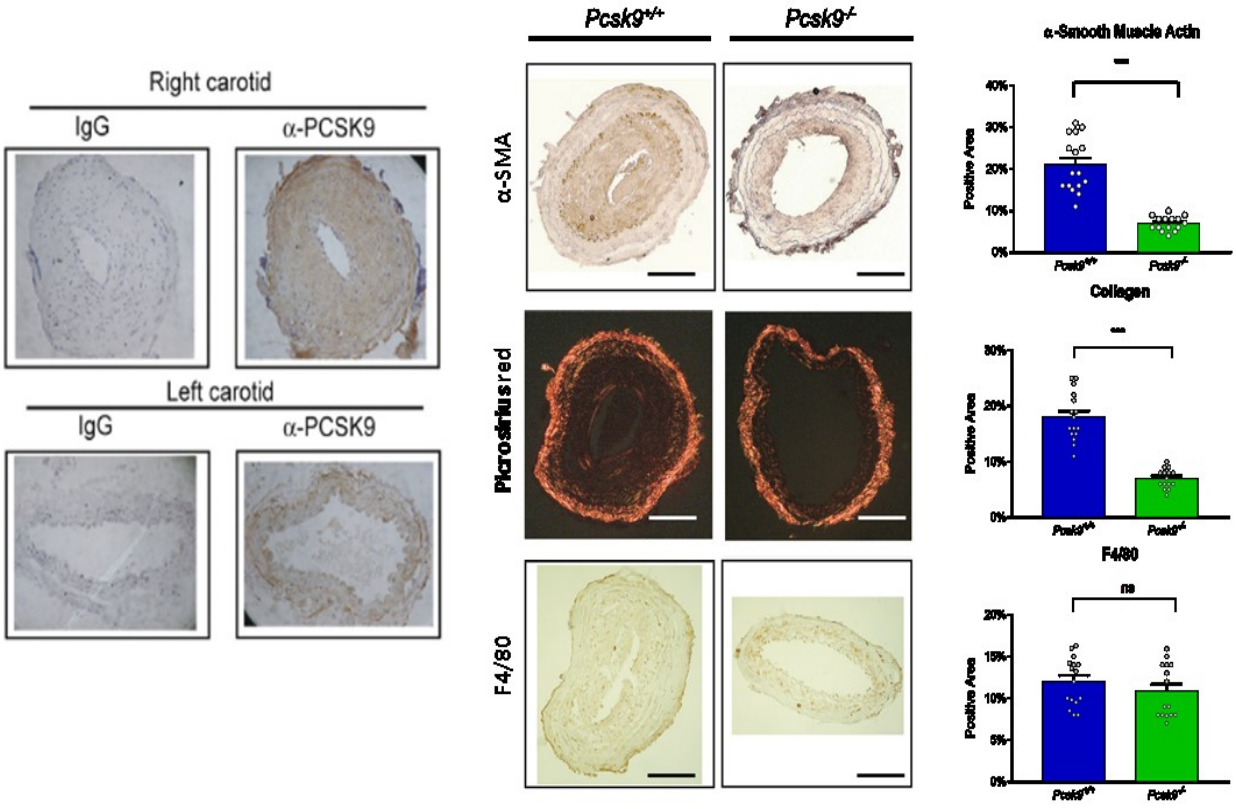

Figure 18. Composition of collar-induced neointimal lesions of Pcsk9$^{+/+}$ and Pcsk9$^{-/-}$ mice. *Left panel) PCSK9 immunostaining of left (control) and right (collared) carotid arteries of Pcsk9$^{+/+}$ mice. Immunostaining was performed using a rabbit polyclonal antibody to PCSK9 (provided by Dr. Philip. Costet), and normal IgG as control. Right panel) Neointima composition of right carotid arteries. Representative images of cross-sections and related quantification analysis are reported asides. Data are shown as percentage of positive area in the intima: first row, staining with α-SMA antibody; second row, positive area of Picrosirius red staining for collagen content; third row, F4/80 staining for evaluation of collagen content in the two groups. Data are expressed as mean ± SEM. Differences between groups were assessed by unpaired Student's t-test, ***p < 0.001.*

Effect of PCSK9 on SMCs isolated from Pcsk9$^{+/+}$ *and* Pcsk9$^{-/-}$ *mice.*

The immunostaining on atherosclerotic plaque, from both human and mice, revealed that PCSK9 expression is due to the presence of the SMCs, which are actively involved in the neointima formation (See **The role of smooth muscle cells during neointima hyperplasia**). To further investigate the role of PCSK9 in this process, we isolated SMCs from *Pcsk9*$^{+/+}$ and *Pcsk9*$^{-/-}$ aortas. From western blot analysis, as expected, *Pcsk9*$^{-/-}$ SMCs did not express PCSK9; the absence of PCSK9 was also associated with increased expression of LDLR, LRP1, VLDLR and CD36, biological target of PCSK9 (Figure 19, right panel). The mRNA of freshly isolated SMCs (Passage 1) was used to quantify the predominant phenotype of the *Pcsk9*$^{+/+}$ and *Pcsk9*$^{-/-}$ SMCs by real time qPCR, in the presence of low serum (FCS=0.4%): *Pcsk9*$^{-/-}$ SMCs expressed higher levels of *α-SMA* (2.24 ± 0.36fold), *Myosin heavy chain-II* (4.65 ± 1.55fold) and *Calponin* (3.25±1.20fold); as predicted the levels of *Pcsk9* were decreased in *Pcsk9*$^{-/-}$ SMCs (-68% ± 0.55%) (Figure 19).

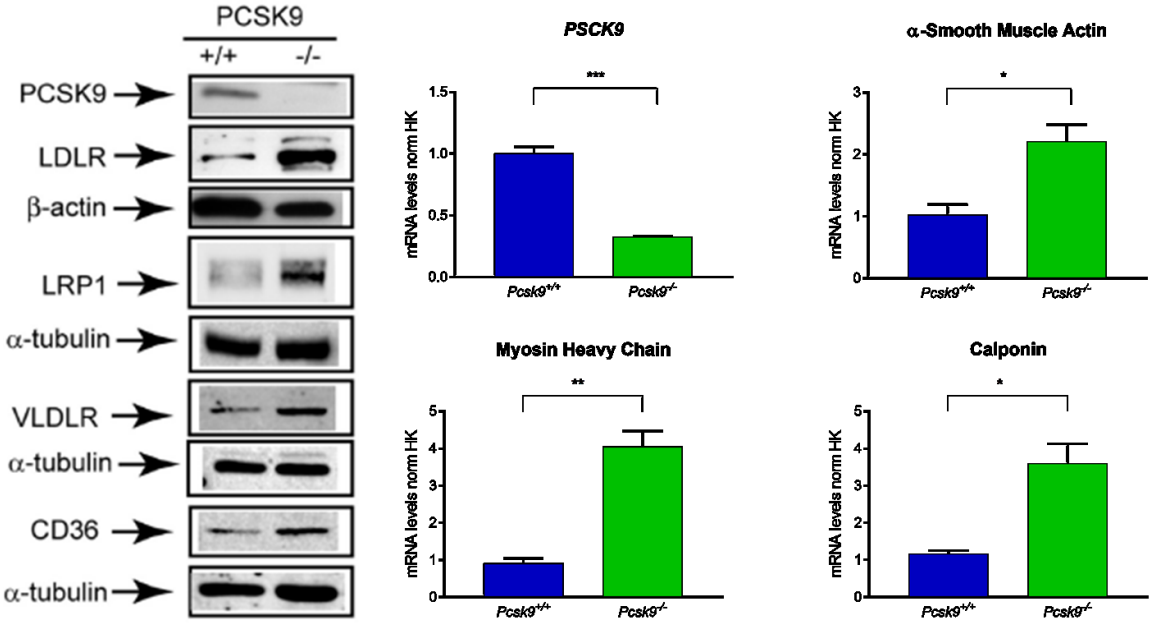

Figure 19. Characterization of cell phenotype on isolated Pcsk9$^{+/+}$ and Pcsk9$^{-/-}$ SMCs. *Right panel) Pcsk9$^{+/+}$ SMCs and Pcsk9$^{-/-}$ SMCs were seeded in DMEM containing 0.4% FCS. Cells were harvested after 24h and protein concentration evaluated with BCA kit. β-actin and α-tubulin were used as loading control. Left panel) Freshly isolated SMCs were cultured for 24 h with DMEM containing 0.4% FCS. Total RNA was than extracted and smooth muscle markers expression levels evaluated by real time PCR. RT-qPCR data are represented as mean value ±SEM form three separate experiments. Differences between groups were assessed by Student's t-test, *p < 0.05; **p < 0.01, ***p < 0.001.*

Effect of PCSK9 on cell proliferation rate of *Pcsk9*$^{+/+}$ and *Pcsk9*$^{-/-}$ SMCs

Pcsk9$^{+/+}$ and *Pcsk9*$^{-/-}$SMCs were seeded on i-Celligence plates in DMEM containing 0.4%FCS in order to synchronized them in G0/G1 phase, after 48h the media was changed with DMEM 10%FCS and cell proliferation was monitored in real-time for 120h. *Pcsk9*$^{-/-}$ SMCs appeared to slow down their proliferation rate after 60-70h from stimulation, while *Pcsk9*$^{+/+}$ SMCs continuously grow (Figure 20, left panel). The cell proliferation rate was also assessed by cell counting experiment at 6 days' time point. A similar difference in proliferation rate was observed also in this experiment with *Pcsk9*$^{-/-}$ SMCs doubling time of 106.3 ± 4.5 h, compared to 57.3 ± 2.1 h for *Pcsk9*$^{+/+}$ SMCs (Figure 20, right panel).

The doubling time (DT) was calculated with the following formula:

$DT = \frac{\mathrm{Log}(2)\times T}{\mathrm{Log}(C_P)-\mathrm{Log}(C_0)}$ where T = time point (h); C_p = cell number at time point; C_0 = cell number at time 0.

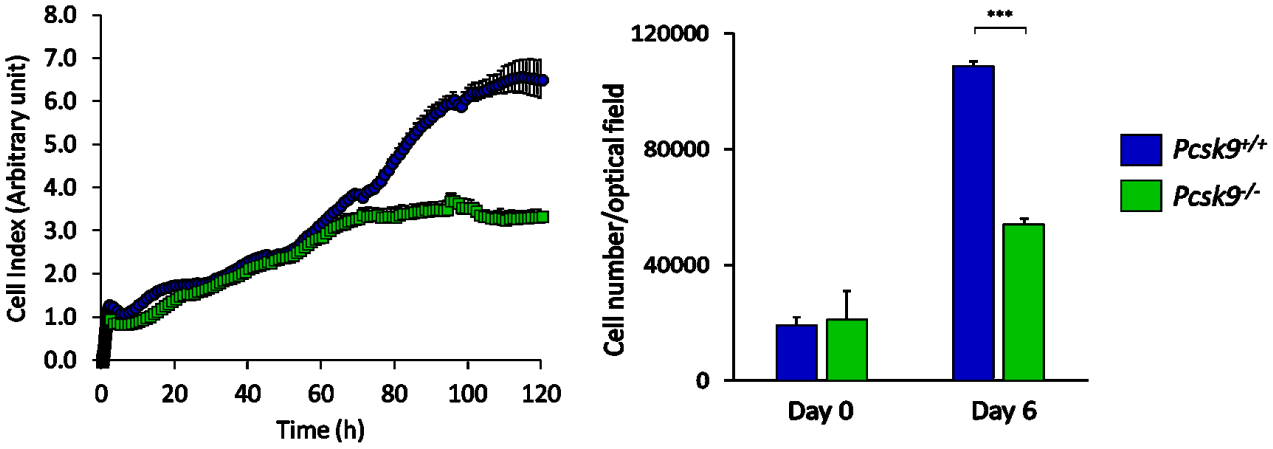

Figure 20. Cell proliferation rate of Pcsk9$^{+/+}$ and Pcsk9$^{-/-}$ SMCs. *Left panel) Pcsk9$^{+/+}$ and Pcsk9$^{-/-}$ SMCs were seeded on i-Celligence plates and proliferation was stimulated with DMEM 10%FCS and real time recorded for 120h, with time points each 15min. Data are represented as cell index which corresponds to the impedance between the electrodes in the well and the cell monolayer. Right panel) Pcsk9$^{+/+}$ and Pcsk9$^{-/-}$ SMCs were seeded in 35mm petri dishes and stimulated with DMEM 10%FCS after 48h synchronization, cell counting was assessed by coulter counter apparatus. Data shown as mean value ± SEM of triplicates from two separate experiments. Statistical analysis was estimated with unpaired Student's t test: ***p<0.001.*

The lower proliferative index of the *Pcsk9*$^{-/-}$ SMCs was observed also by the analysis of the cell cycle progression from a quiescent state (DMEM containing 0.4% FCS) to a proliferative state induced by the 24h incubation with 20ng/mL of recombinant PDGF-BB. In basal conditions (DMEM 0.4% FCS), as expected, most of the cells of both cell lines accumulated in G0/G1 phase; the amount of *Pcsk9*$^{-/-}$ SMCs was significantly higher in the G0/G1 phase, whereas was lower in the S and G2 phases compared to the wild-type (G0/G1 = 69.14% ± 0.89% vs 76.1% ± 0.54%, $p<0.001$; S = 9.8% ± 0.95% vs 5.54% ± 0.68%, $p<0.001$; G2 = 21.01% ± 1.2% vs 18.36% ± 0.45%, p<0.01 for *Pcsk9*$^{+/+}$ and *Pcsk9*$^{-/-}$ SMCs, respectively Figure 21, left panel).The stimulus with PDGF increased the number of cells in the S, that was significantly lower in the *Pcsk9*$^{-/-}$ SMCs compared to the wild-type phase (14.81% ± 0.87% vs 7.52% ± 0.46%, $p<0.001$ for *Pcsk9*$^{+/+}$ and *Pcsk9*$^{-/-}$ SMCs, respectively Figure 21, right panel).

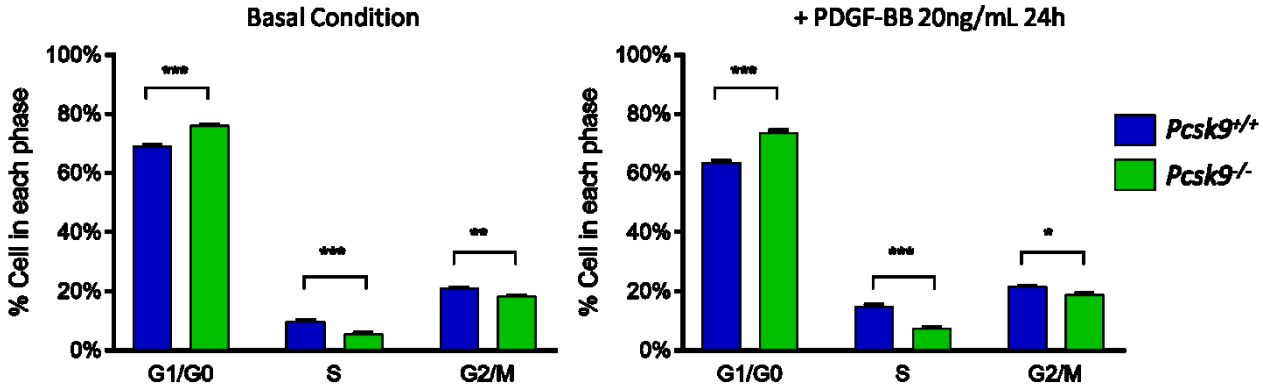

Figure 21. Cell cycle analysis of Pcsk9$^{+/+}$ and Pcsk9$^{-/-}$ SMCs. *SMCs were seeded in triplicate in 35mm petri dish in DMEM 0.4%FCS, after 48h media was changed with DMEM 0.4%FCS only (left panel) or with the addition of 20ng/mL of PDGF-BB (right panel) and incubated for 24h. Cells were permeabilized and treated with Propidium Iodide for 15min before analysis with flow-cytometry. Data shown as mean value ± SEM (n=3, N=2). Statistical analysis was estimated with two-way ANOVA test: ***p<0.01, ***p<0.001.*

Effect of PCSK9 on *Pcsk9*$^{+/+}$ and *Pcsk9*$^{-/-}$ SMCs migration and phenotype.

The other important feature that characterized neointima formation is the migration of SMCs, to evaluate the role of PCSK9 in this process we assessed migration capability of *Pcsk9*$^{+/+}$ and *Pcsk9*$^{-/-}$ SMCs in response of recombinant PDGF-BB. After 48h synchronization in DMEM 0.4%FCS, cells were seeded in the upper component of the Boyden's chamber whereas the chemotactic agent (PDGF-BB) was added in the lower component. After 6 hours the number of migrated cells was significantly lower in the *Pcsk9*$^{-/-}$ SMCs, with the highest difference in the 20ng/mL conditions (Figure 22).

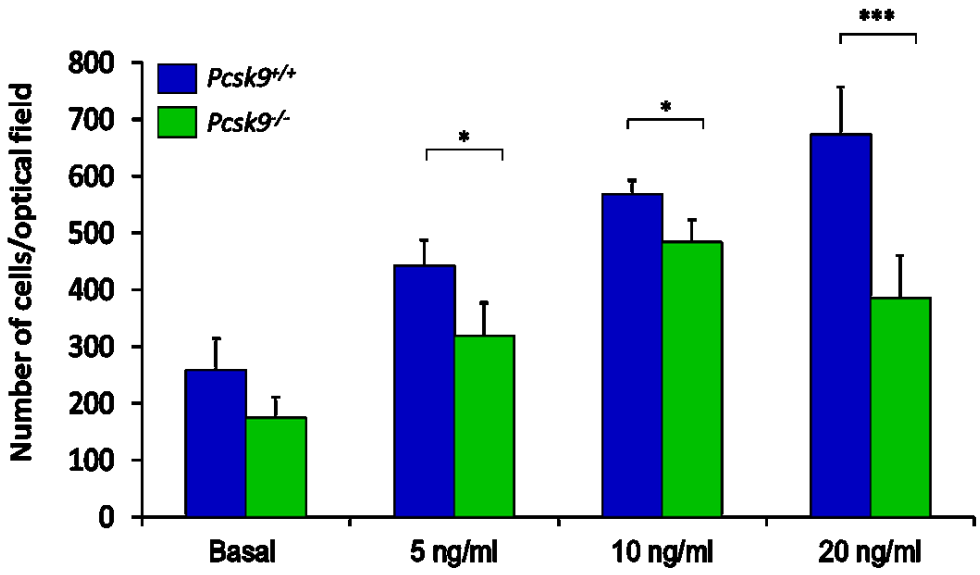

Figure 22. Cell migration capability assessed with Boyden's chamber assay. *Transmigrated cells were counted in six random high-power fields (HPFs) under high magnification (objective lens 20×). Basal indicates cells incubated in DMEM 0.4% FCS without PDGF-BB; differences between groups (n=6, N=2) were assessed by Student's t-test, *p < 0.05; **p < 0.01. n= number of replicates, N= number of experiments.*

The staining with rhodamine-phalloidin, that binds with high-affinity to filamentous actin, revealed a significant difference in the morphology of two cell lines after the incubation with PDGF-BB. The PDGF-treated cells responded to the chemotactic agent with the formation of protrusive structures termed lamellipodia, that were detectable only in the wild-type cell line. The real-time monitoring of morphology displayed also in this experiment an increasing response to PDGF-BB only in the wild-type SMCs (maximal induction after approximately 1.5

h and 2.5 h) compared to the knock-out cells (maximal pick after approximately 1.5 h of stimulation); no significant differences were observed at basal conditions (Figure 23).

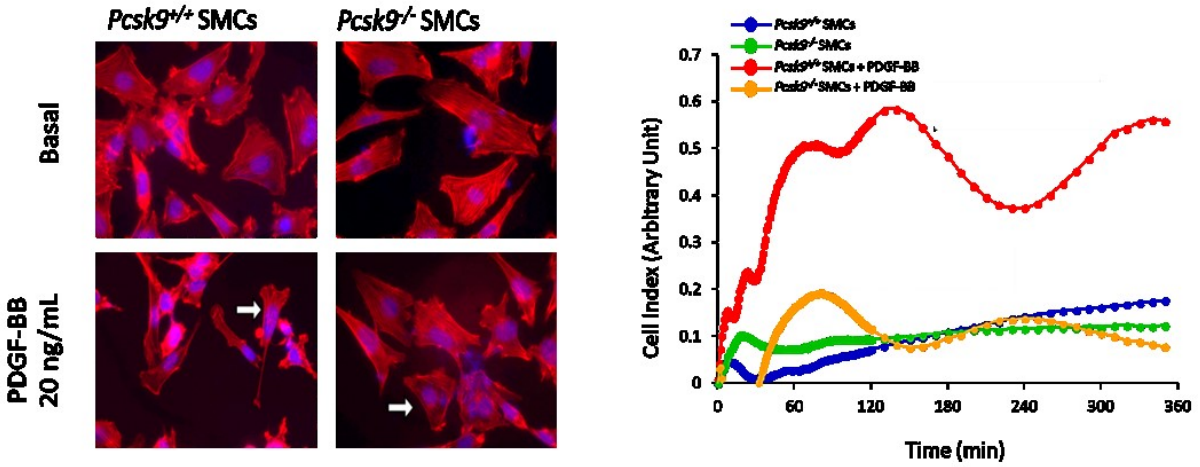

Figure 23. Morphological changes after the incubation with 20ng/mL of recombinant PDGF-BB. *Left panel) Cytoskeletal organization of SMCs was analyzed under basal condition (DMEM/0.4% FCS) or 15-min stimulation with PDGF-BB (20 ng/ml). F-actin is stained red with rhodamine-phalloidin while nuclei are stained blue with DAPI. Right panel) Morphological changes in PCSK9$^{-/-}$ SMCs and PCSK9$^{+/+}$ SMCs were recorded by i-Celligence system under basal condition (DMEM/0.4% FCS) and after stimulation with PDGF-BB for 6 h.*

The formation of lamellipodia is usually related to the activation of proteins, such as the small G proteins Rac1 and RhoA, which regulate the organization of cytoskeletal actin. The activation of those proteins is mediated by the binding to GTP, whereas the inactive proteins are bond to GDP. We measured the levels of Rac-1-GTP and RhoA-GTP in both basal and after the incubation with PDGF-BB in the two cell lines with the G-LISA kit; as shown in Figure 24 the absence of PCSK9 determined a decreased in the activation of both Rac1 and RhoA, significantly during incubation with PDGF-BB.

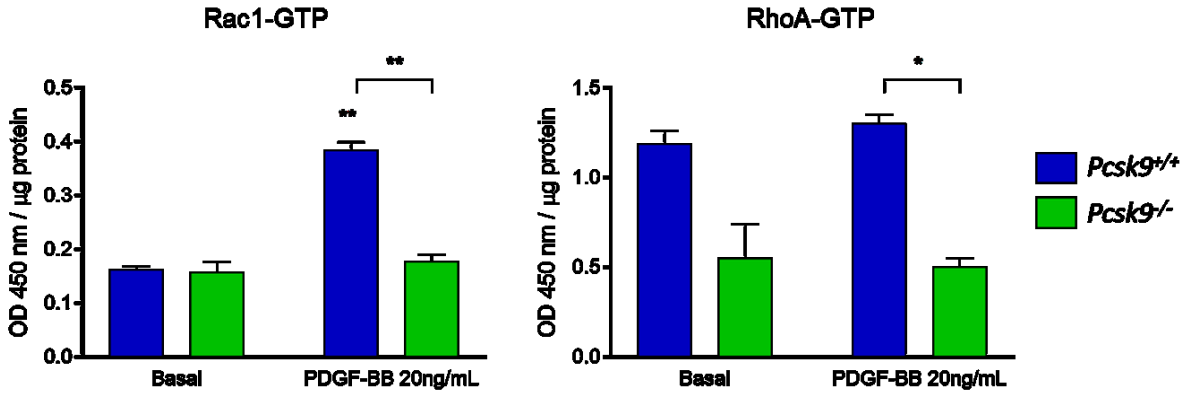

Figure 24. Small G-proteins activations in Psck9$^{+/+}$ and Pcsk9$^{-/-}$ SMCs. *Intracellular levels of Rac-1-GTP and RhoA-GTP were determined by G-LISA assay under basal condition (DMEM/0.4% FCS) and after stimulation for 5 min with 20 ng/mL of PDGF-BB. Data were normalized on protein content. Statistical analysis was estimated with two-way ANOVA test: *p<0.05, **p<0.01; unless otherwise indicated, statistics referred to basal conditions.*

Overall, those results indicate that the absence of PCSK9 appears to maintain the SMCs in a more contractile phenotype, associated with a decrease proliferation rate and migration capability and an impairment in the response to chemotactic agent (PDGF-BB).

Effect of reconstituted expression of PCSK9 in *Pcsk9*$^{-/-}$ SMCs.

To confirm the role of PCSK9 on SMCs, we stably reconstituted the expression of PCSK9 in the *Pcsk9*$^{-/-}$ SMCs by retroviral infection. The retroviral vectors encodes for human PCSK9 FLAG tag and exogenous PCSK9 FLAG tag was detected in *Pcsk9*$^{-/-}{}_{REC}$ cell line by using an antibody anti PCSK9 or anti FLAG, while it was not detectable in control cells transduced with empty retroviral vector; as expected, the reconstitution of PCSK9 was associated with a reduction on the levels of LDLR (Figure 25).

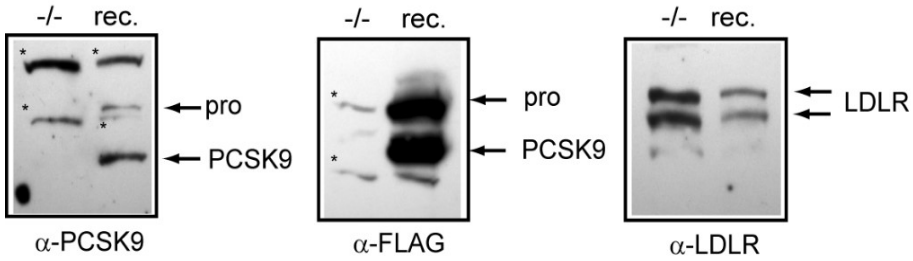

Figure 25. Western blot analysis on Pcsk9*$^{-/-}$ *SMCs and Pcsk9*$^{-/-}{}_{REC}$ *SMCs. *Pcsk9*$^{-/-}$ *SMCs were retrovirally transduced with empty retroviral vector or vector encoding for human PCSK9 FLAG-tag. After puromycin selection, expression of PCSK9 was evaluated by Western blot analysis from total cell lysates, using anti-PCSK9 antibody, anti-FLAG antibody; the expression of LDLR was evaluated by the incubation with anti-LDLR antibody.*

The effect of PCSK9 on the phenotype in the reconstituted cell line was evaluated by real-time qPCR (Figure 26), expression of contractile markers was decreased compared to the PCSK9-null cells with levels of α-smooth muscle actin reduced by 56% ± 2% (p<0.01), myosin heavy chain of -35% ± 0.8 (p<0.05) and a trend towards reduction of calponin was also observed (-25% ± 5.1; p=0.06). The markers associated with a synthetic phenotype were instead increased after the re-introduction of PCSK9 in the knock-out line (*Caldesmon*: 2.8 ± 0.9, p<0.05; KLF4: 4.5 ±1.1 p<0.05).

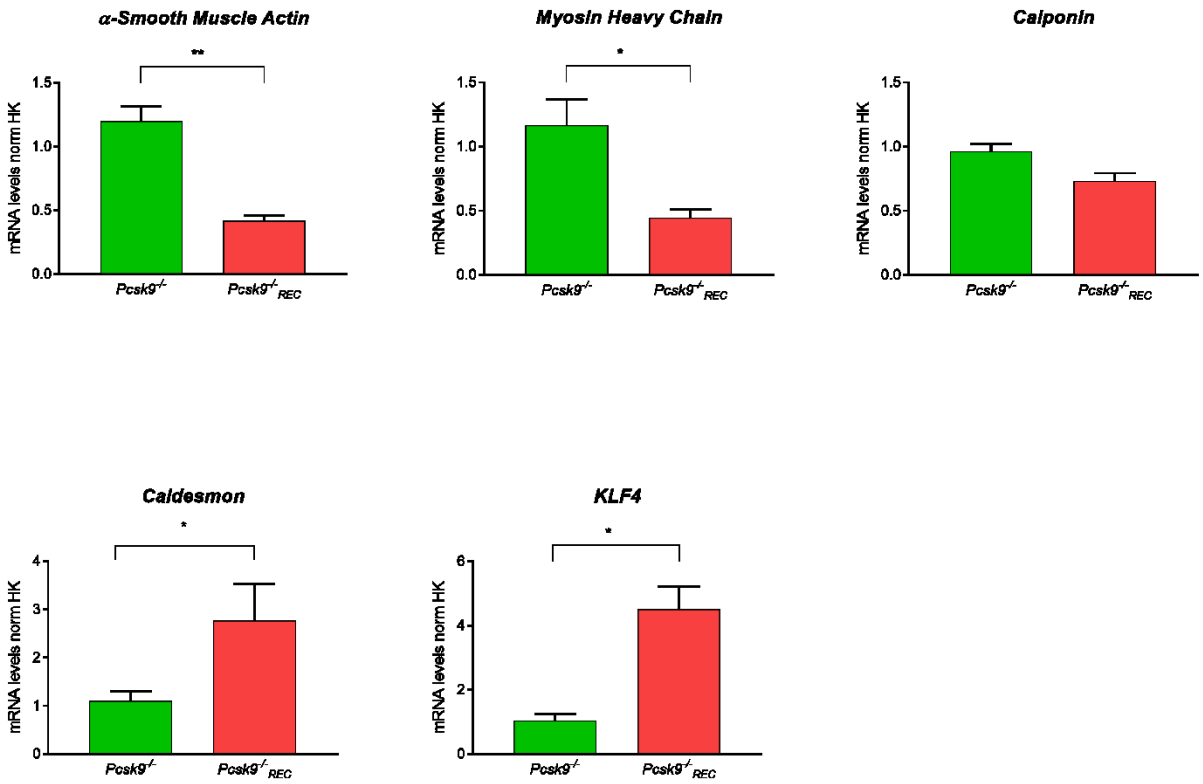

Figure 26. Real-time qPCR on SMCs phenotypic markers. *SMCs were cultured for 24 h with DMEM containing 0.4% FCS. Total RNA was than extracted and smooth muscle markers expression levels evaluated by real time PCR. Differences between groups were assessed by Student's t-test, *p < 0.05; **p < 0.01.*

The proliferation rate of those cells was assessed using the same protocol described before; the presence of PCSK9 restored the proliferation capability of the *Pcsk9*$^{-/-}$ SMCs as observed by the cell counting experiment and the real-time monitoring of the proliferation rate (Figure 27). The cell-cycle analysis confirms that the presence of PCSK9 induce a more proliferative state with a reduced number of cells in the G0/G1 phase and an increase of the percentage of cells in the S and G2 phases; those differences were observed both in basal (G0/G1 = 77.5% ± 0.89% vs 63.5% ± 0.54%, p<0.001; S = 6% ± 0.5% vs 14.5% ± 0.8%, p<0.001; G2 = 15.5% ± 1.2% vs 22.3% ± 0.45%, p<0.001) and after the incubation with 20ng/mL of PDGF-BB (G0/G1 = 66.5% ± 0.89% vs 53.13% ± 0.42%, p<0.001; G2 = 23.3% ± 0.89% vs 39.1% ± 0.74%, p<0.001) (Figure 28).

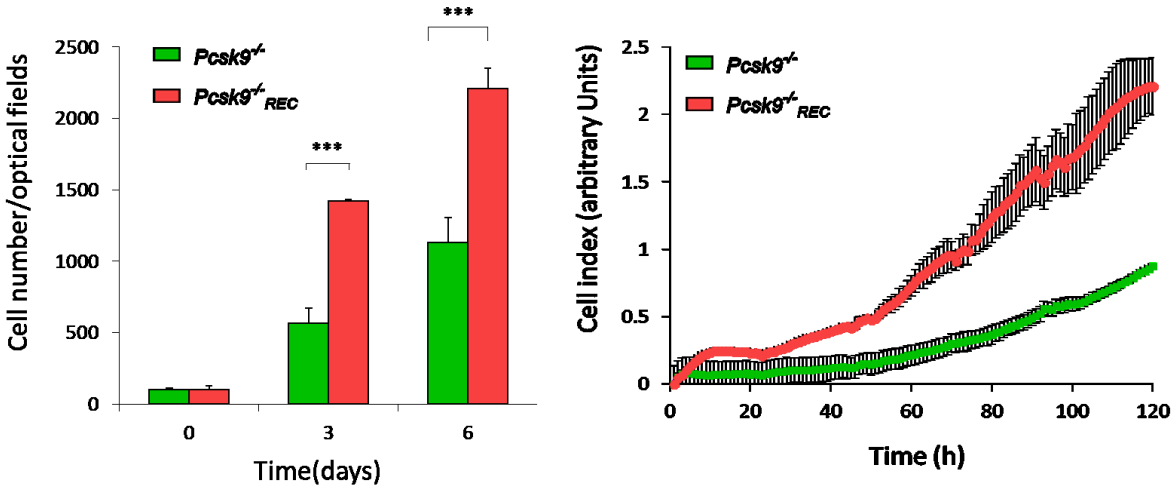

Figure 27. Proliferation capability of Pcsk9$^{-/-}$ SMCs and Pcsk9$^{-/-}$$_{REC}$ SMCs. *Left panel) For the cell counting experiment, SMCs were seeded in DMEM supplemented with 10% FCS after 48h of synchronization; cells were collected with trypsinization at different time points: day 0 (24h after seeding), day 3 and day 6. Culture media were replaced every 3 days to maintain a proper proliferation stimulus. Each bar represents mean ± SEM of triplicate dishes. For each time point, differences between groups were assessed by Student's t-test, ***p < 0.001. Right panel) Dynamic monitoring of cell proliferation was performed by i-Celligence system. SMCs were seeded in E-Plate L8 plates, in DMEM containing 10% FCS, then proliferation rate was monitored for 120 h (5 days) every 15 min.*

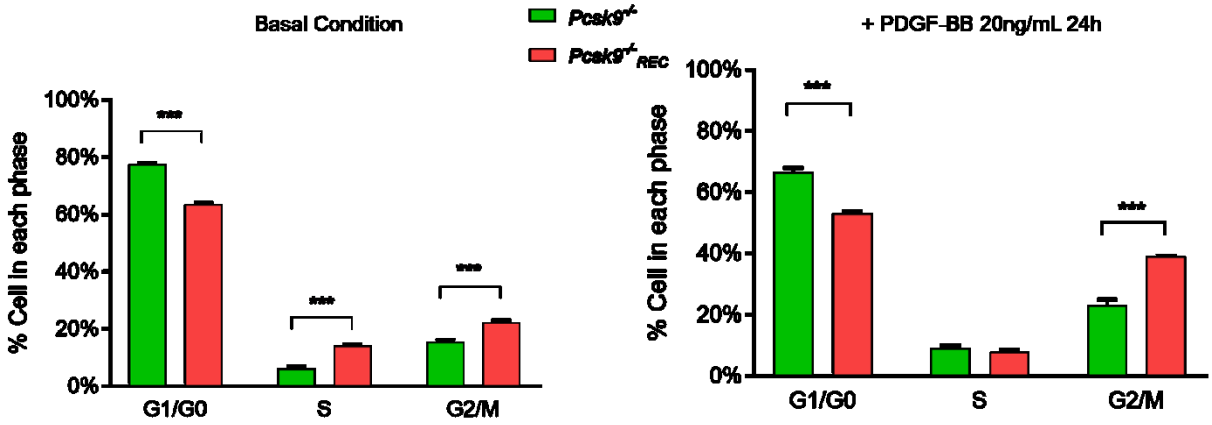

Figure 28. Cell cycle analysis of Pcsk9$^{-/-}$ SMCs and Pcsk9$^{-/-}$$_{REC}$ SMCs. *SMCs were seeded in triplicate in 35mm petri dish in DMEM 0.4%FCS, after 48h media was changed with DMEM 0.4%FCS only (left panel) or with the addition of 20ng/mL of PDGF-BB (right panel) and incubated for 24h. Cells were permeabilized and treated with Propidium Iodide for 15min before analysis with flow-cytometry. Data shown as mean value ± SEM (n=3, N=2). Statistical analysis was estimated with two-way ANOVA test: **p<0.01, ***p<0.001.*

The increase proliferative index was also evaluated by determining the levels of proteins involved in the cell cycle progression from G0/G1 to S phase. The level of p21, p27, cyclin E and cyclin D1 were measured after 6h and 24h incubation with PDGF-BB by both western blot and real-time qPCR. *Pcsk9*$^{-/-}_{REC}$ SMCs showed decreased level of inhibitory proteins (p21 and p27) compared to *Pcsk9*$^{-/-}$ SMCs with significant difference already at basal condition that grown more evident after the incubation with PDGF-BB. Vice versa, the levels of cell cycle-activating proteins (cyclin E and cyclin D1) were increased in the presence of PCSK9, both at the mRNA and the protein levels (Figure 29).

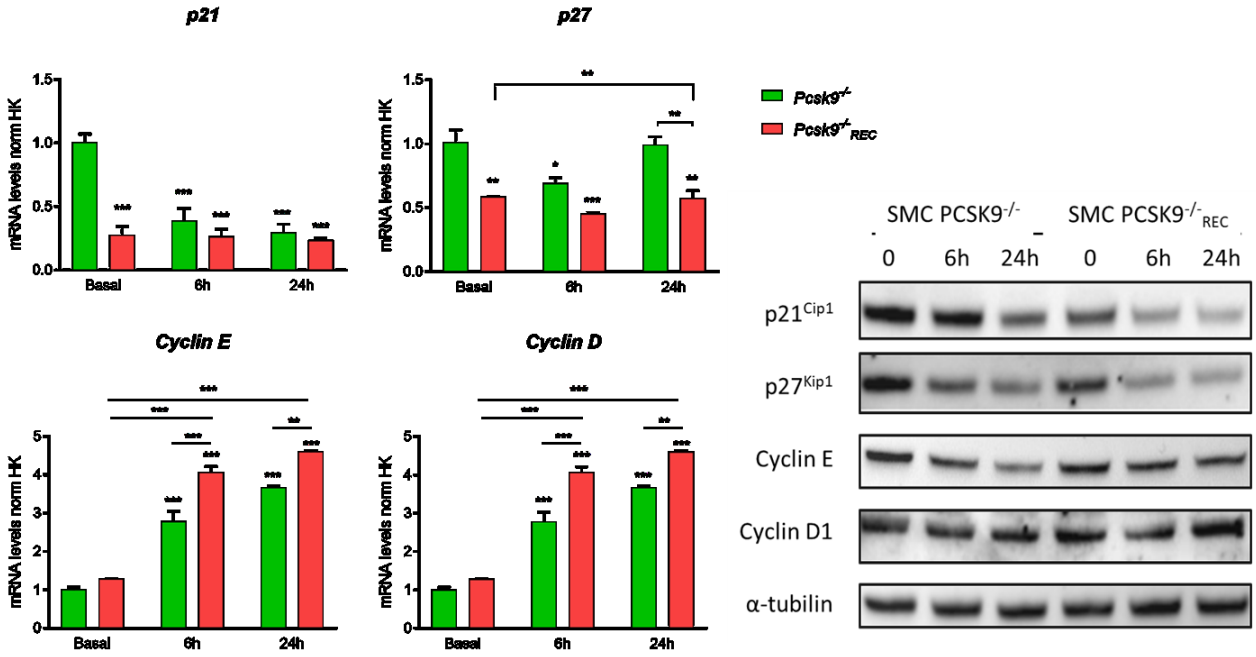

Figure 29. Cell cycle protein expression in Pcsk9$^{-/-}$ and Pcsk9$^{-/-}_{REC}$ SMCs. *SMCs were seeded in 60mm petri dish in DMEM 0.4%FCS; after 48h of synchronization, SMCs were incubated with 20ng/mL of PDGF-BB for 6h and 24h. For real time analysis, total RNA was extracted from one million cells per condition, the remaining cells were used for western blot analysis. Data are represented as mean ± SEM from three independent experiment. Statistical analysis was estimated with two-way ANOVA test: *p<0.05, **p<0.01, ***p<0.001. Protein expression was evaluated by western blot and anti-p21 antibody, anti-p27 antibody, anti-cyclin E antibody and anti-cyclin D1 antibody. Representative images were shown.*

The Bromo-deoxyuridine (BrdU) staining of *Pcsk9*$^{-/-}$ and *Pcsk9*$^{-/-}{}_{REC}$ SMCs, a thymidine analog that is incorporated into the DNA during DNA synthesis, confirmed a more proliferative state of the cells that expressed PCSK9, with increasing levels of incorporated BrdU after 12h incubation in DMEM 0.4%FCS containing 20ng/mL of PDGF-BB (Figure 30).

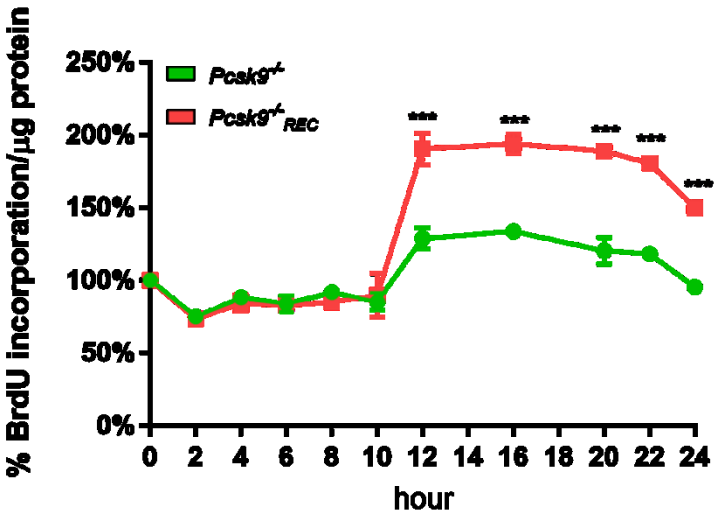

Figure 30. BrdU incorporation measured with BrdU ELISA kit. *Cells were seeded in quadruplicate in 48-wells plate in DMEM containing 0.4%FCS. After 48h, the media was replaced with DMEM 0.4%FCS containing 20ng/mL of PDGF-BB. Samples were collected every two hours for 24h. Data were normalized for protein content and expressed as percentage from baseline (0 time point). Statistical analysis was estimated with two-way ANOVA test: ***p<0.001*

A rescue in the migratory response was also observed in the presence of reconstituted PCSK9 after the incubation with 20ng/mL of PDGF-BB, with an increasing in the migration capability both at basal (DMEM 0.4%FCS) and after exposure to PDGF-BB (**Figure 31**).

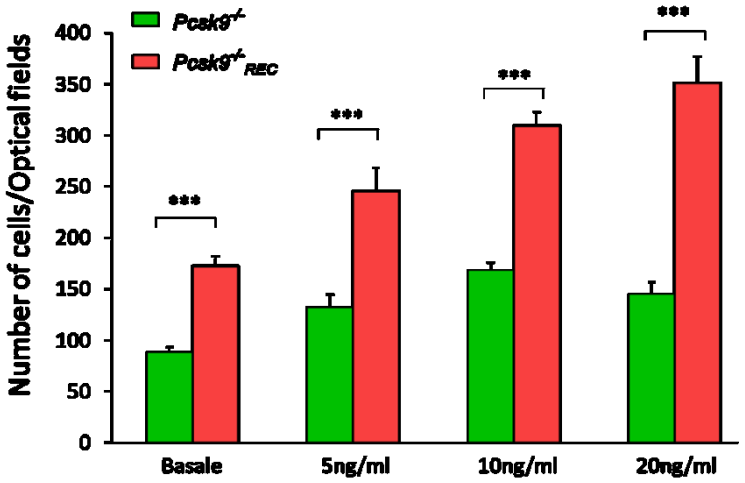

Figure 31. Cell migration capability of Pcsk9$^{-/-}$ SMCs and Pcsk9$^{-/-}{}_{REC}$ SMCs assessed with Boyden's chamber assay. *Transmigrated cells were counted in six random high-power fields (HPFs) under high magnification (objective lens 20×). Basal indicates cells incubated in DMEM 0.4% FCS without PDGF-BB; differences between groups (n=6, N=2) were assessed by Student's t-test, ***p < 0.001.*

In order to rule out that the pro-proliferative effect of PCSK9 was mediated by its effect on cholesterol homeostasis, we measured the intracellular content of cholesterol using High Performance Liquid Chromatography (HPLC) and the BrdU incorporation in the presence of simvastatin, which is known to inhibit SMCs proliferation by blocking cholesterol biosynthesis and the prenylation of proteins [159]. The assessment of intracellular levels of cholesterol measured by HPLC, after separation of triglycerides and phospholipids by thin liquid chromatography (TLC), showed no significant difference between *Pcsk9*$^{-/-}$ and *Pcsk9*$^{-/-}{}_{REC}$ either at basal and after 24h incubation with PDGF-BB; suggesting that the pro-proliferative effect of PCSK9 could be independent from cholesterol levels (Figure 32).

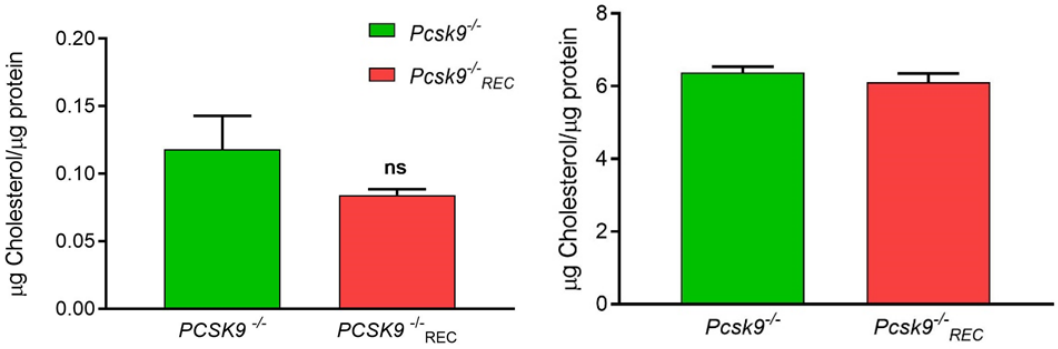

Figure 32. Evaluation of cholesterol content in Pcsk9$^{-/-}$ and Pcsk9$^{-/-}{}_{REC}$ SMCs. *Cell lipids were extracted in hexane/isopropyl alcohol (3:2) containing BHT 0.01%. Free- and esterified cholesterol were separated by HPLC plates and quantified on a DANI 1000 gas liquid chromatographer. Results were normalized by protein content. Left figure represents the basal condition, the right figures the incubation with PDGF-BB (20ng/mL).*

In the presence of simvastatin, the incorporation of BrdU is decreased in both the cell lines, compared to the untreated cells. Nonetheless, the presence of PCSK9 conferred a partial resistance to the antiproliferative effect of simvastatin compared to the PCSK9-null SMCs (**Figure 33**).

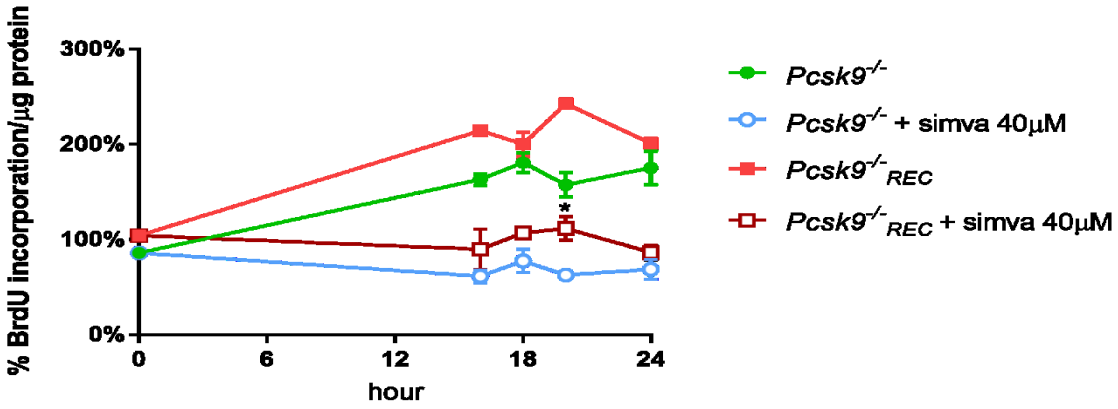

Figure 33. BrdU incorporation measured in the presence of simvastatin. Cells were seeded in quadruplicate in 48-wells plate in DMEM containing 0.4%FCS*. After 48h, the media was replaced with DMEM 0.4%FCS containing 20ng/mL of PDGF-BB ± simvastatin 40µM. Samples were collected every two hours starting from 16h to 24h time points. Data were normalized for protein content and expressed as percentage from baseline (0 time point). Statistical analysis was estimated with two-way ANOVA test: *p<0.05 related to the simvastatin-treated groups.*

To investigate the potential mechanism behind the pro-proliferative capacity of *Pcsk9*$^{-/-}_{REC}$ SMCs, we measured LRP1 and PDGFR expression by western blot after the incubation with 20ng/mL of PDGF-BB for 6 and 24 hours (Figure 34). The presence of PCSK9 was associated with decreased expression of LRP1 and increased expression of PDGFR.

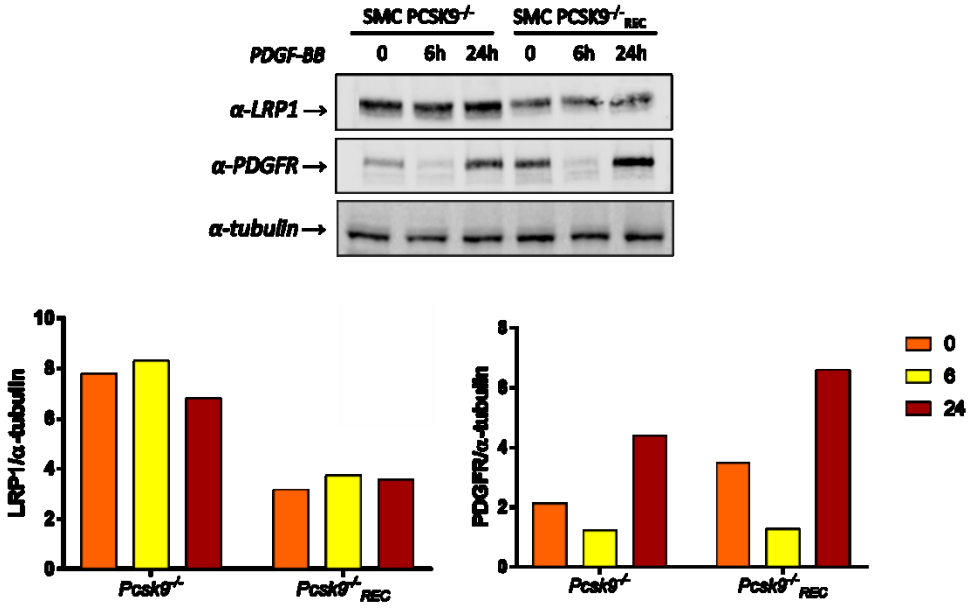

Figure 34. LRP1 and PDGFR expression after PDGF-BB treatment in Pcsk9$^{-/-}$ ***and Pcsk9***$^{-/-}_{REC}$ ***SMCs****. SMCs were seeded in 60mm petri dish in DMEM 0.4%FCS; after 48 hours, media was changed with DMEM 0.4%FCS containing 20ng/mL of PDGF-BB. Samples were collected after 6 and 24 hours of incubation. Data are shown as normalized abundance from western blot densitometry.*

Taken together, those results confirm the role of PCSK9 as an important modulator of SMCs proliferation and migration; moreover, the pro-proliferative role of PCSK9 seems to be

correlated with a different activation of PDGFR mediated by LRP1 but independent from intracellular cholesterol levels.

Relationship between circulating levels of PCSK9 and arterial stiffness.

To further investigate the role of PCSK9 on the artery wall, we took advantage of the historical cohort of the Brisighella Heart Study [151]. After exclusion of active smokers, participants in secondary prevention for cardiovascular disease, and patients in treatment with statins or vasodilating agents, we selected 227 premenopausal women and 193 age-matched men and 460 postmenopausal women and 416 age-matched men. Anagraphic, anthropometric, hemodynamic and laboratory characteristics were assessed for each group of participants (Figure 35). As expected, the older participants showed an increase in waist circumference, blood pressure, triglycerides, fasting plasma glucose, and serum uric acid (SUA) as well as pulse pressure and decreased glomerular filtration rate (GFR). LDL-C was significantly higher in postmenopausal versus premenopausal women, whereas similar concentrations were observed between younger and older men. High-density lipoprotein cholesterol was significantly lower in men than in women, independent of age.

	Premenopausal Women (n=227)	Younger Men (n=193)	Postmenopausal Women (n=460)	Older Men (n=416)
Age, y	41.0±8.4	40.3±7.7	66.8±10.6*	67.25±9.8*
WC, cm	80.9±15.9	92.5±11.1	90.3±15.4*	98.5±14.5*†
Heart rate, bpm	67.3±12.2†‡	61.6±11.5†‡	65.8±11.9†‡	61.5±11.4†‡
SBP, mm Hg	127.4±14.5	131.3±13.1†	148.0±13.5*	145.7±11.9*
DBP, mm Hg	68.8±8.6	72.4±9.5†	73.4±10.1*	76.9±9.5*
Pulse pressure, mm Hg	58.5±10.9	58.9±9.8	74.6±10.4*	68.7±10.8*†
MAP, mm Hg	94.3±10.9	95.9±11.2	104.7±13.9*	104.9±11.9*
TC, mg/dL	208.1±36.8	209.2±36.3	227.3±40.2	215.8±40.2
Triglycerides, mg/dL	95.9±62.4	118.2±76.8†	119.5±57.9*	131.0±78.7*
HDL-C, mg/dL	55.4±5.4	48.4±4.5†	54.3±5.5	48.0±4.7†
LDL-C, mg/dL	132.9±25.8	136.4±24.4	148.6±28.8*	135.6±30.5
Lipoprotein(a), mg/dL	17.4±15.6	19.3±17.6	26.3±22.0*	20.4±18.1†
FPG, mg/dL	87.2±17.1	90.5±9.8	95.1±16.7*	101.9±15.9*†
SUA, mg/dL	4.3±1.0	5.7±1.1†	4.9±1.2*	6.0±1.2†
eGFR, mL/min	79.1±13.5	85.9±12.8†	63.5±14.1*	68.7±13.4*†

Figure 35. Main characteristics of the selected participants divided by age and sex. *DBP indicated diastolic blood pressure; eGFR, estimate glomerular filtration rate (calculated using Chronic Kidney Disease Epidemiology Collaboration equation); FPG, fasting plasma glucose; HDL-C, high-density lipoprotein cholesterol; LDL-C, low-density lipoprotein cholesterol; MAP, mean arterial pressure; SBP, systolic blood pressure; SUA, serum uric acid; TC, total cholesterol; WC, waist circumference. *p<0.05 vs sex, younger category; †p<0.05 vs same age class, other sex; ‡p<0.001 vs other age class, other sex.*

The circulating PCSK9 was evaluated by ELISA assay from plasma samples from the participants (Figure 36). The postmenopausal women showed higher levels of PCSK9 compared to the premenopausal women (309.9 ± 84.0 ng/mL and 269.4±78.8 ng/mL, respectively p<0.001) and to the other groups of participants (p<0.001). As for the women, the older man showed significantly higher PCSK9 levels compared to the sex-matched group (283.2±75.8 and 260.9±80.4 ng/mL, respectively p=0.008).

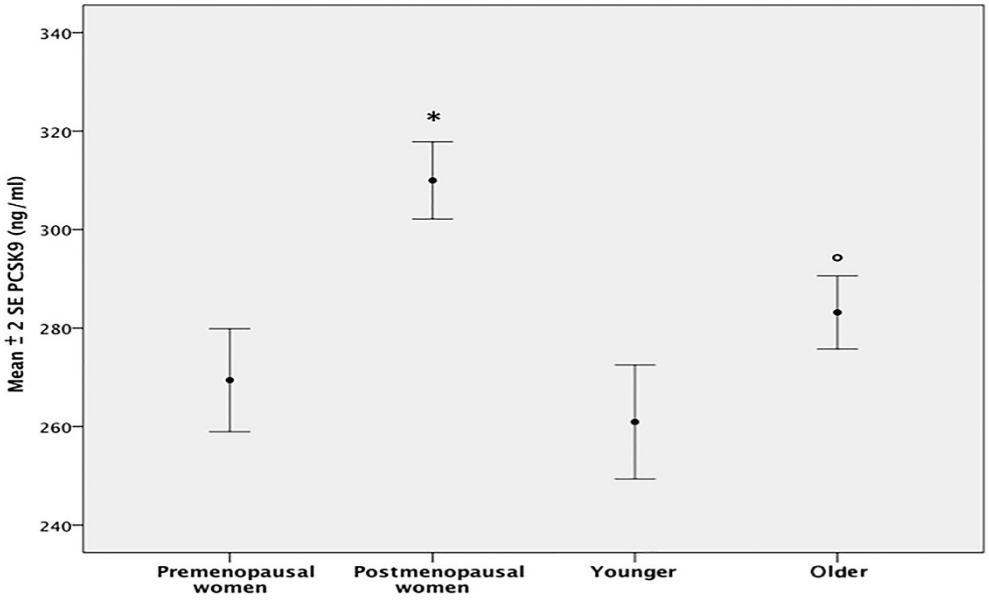

Figure 36. Serum levels of PCSK9 evaluated by ELISA assay. *Serum PCSK9 level are expressed as mean ± SEM in ng/mL (95% CI) in the study population. *p <0.001 vs all other groups; °p=0.008 for older men vs younger men.*

In the univariate model, circulating PCSK9 levels were related to age (r=0.180, P<0.001), systolic blood pressure (r=0.138, P<0.001), pulse pressure (r=0.143, P<0.001), mean arterial pressure (r=0.116, P<0.001), total cholesterol (r=0.159, P<0.001), triglycerides (r=0.178, P<0.001), LDL-C (r=0.089, P=0.001), SUA (r=−0.060, P=0.030), fasting plasma glucose (r=0.107, P<0.001), lipoprotein(a) (r=0.100, P<0.001), eGFR (r=−0.101, P<0.001), and carotid–femoral PWV (r=0.302, P<0.002).

The multiple linear regression model carried out on the whole population sample showed that PWV was predicted mainly by age (B=0.114, 95% CI 0.92–0.129, P<0.001), PCSK9 (B=0.027, 95% CI 0.021–0.033, P<0.001), and SUA (B=0.301 95% CI 0.022–0.388, P=0.029). Physical activity, LDL-C, high-density lipoprotein cholesterol, and eGFR were not significantly associated with PWV (P>0.05).

The significant predictors of PWV in the different subgroups were reported in Figure 37. Age and PCSK9 were the main factors associated with PWV, which also correlated with SUA but only in postmenopausal women.

	Premenopausal Women				Postmenopausal Women			
		95% CI				95% CI		
Predictor	B	Lower Limit	Upper Limit	*P* Value	B	Lower Limit	Upper Limit	*P* Value
Age	0.144	0.98	0.213	<0.001	0.225	0.135	0.316	0.003
PCSK9	0.021	0.008	0.031	0.002	0.036	0.026	0.045	<0.001
SUA				>0.05	0.496	0.088	0.901	0.017
	Younger Men				Older Men			
		95% CI				95% CI		
Predictor	B	Lower Limit	Upper Limit	*P* Value	B	Lower Limit	Upper Limit	*P* Value
Age	0.162	0.084	0.290	0.002	0.258	0.165	0.342	<0.001
PCSK9	0.029	0.018	0.046	<0.001	0.028	0.015	0.039	<0.001
SUA				>0.05				>0.05

Independent variables: age, physical activity, low-density lipoprotein cholesterol, high-density lipoprotein cholesterol, PCSK9, SUA, and estimated glomerular filtration rate (CKD-EPI [Chronic Kidney Disease Epidemiology Collaboration] equation). PCSK9 indicates proprotein convertase subtilisin/kexin type 9; SUA, serum uric acid.

Figure 37. Significant predictors of pulse wave velocity. *Multiple linear regression model on the whole population samples. B = regression coefficient calculated with 95%CI.*

These data indicate that increased levels of PCSK9 are correlated with increased arterial stiffness, which is an indirect parameter for atherosclerosis. Taken together these results further confirm the direct role of PCSK9 in the vascular remodeling.

Discussion

The discovery of PCSK9 and its role on cholesterol homeostasis represented a breakthrough in the cardiovascular field, especially in understanding the mechanism that leads to atherosclerotic lesions. The presence of PCSK9 in extrahepatic tissues, such as the brain, the kidneys, the pancreas and the cells that compose the artery wall suggested that PCSK9 could exert paracrine effects, besides its action of the LDLR. In the present study, we have investigated a possible paracrine role of PCSK9 on the arterial wall through experimental and clinical approaches. The main rational in performing this study is based on the previous observation from our research laboratory that PCSK9 was expressed and secreted by the SMCs; immunostaining with anti PCSK9 antibody revealed the presence of PCSK9 in human atherosclerotic plaques, in regions occupied by α-SMA positive cells [82]. One of the fundamental signs of atherosclerosis is the accumulation of SMCs, macrophages and lipids in the sub-endothelial space, leading to the formation of the so-called "neointima". To evaluate the effect of PCSK9 during neointima hyperplasia, we compared vascular response in C57BL/6 *Pcsk9*$^{+/+}$ and *Pcsk9*$^{-/-}$ mice in a consolidated model of vascular injury. The major finding of this in vivo experiment was that *Pcsk9*$^{-/-}$ mice were protected from neointima formation, as shown in **Figure 15** and **Figure 16**. The absence of PCSK9 impaired only the neointima formation, whereas the morphology of the vessel, assessed by measuring the areas of lumen and media, remained unchanged, mainly due to the mechanism through which the non-occlusive collar mediates the atherosclerotic lesion formation (**Figure 16**) [158]. The neointima formed at the end of nine weeks was composed mostly of SMCs and of collagen as shown by the staining with α-smooth muscle actin antibody and Picrosirius red respectively; these were reduced in the lesion of *Pcsk9*$^{-/-}$ mice. The macrophages content was minimal and without significant differences between the groups. This could be related to diet that those mice ate for nine weeks; in fact, the number of monocytes normally present in the wild type mice fed with chow diet were significantly lower compared to the ones found in wild-type mice fed with western diet, pointing to a less recruitment of these cells in sub-endothelial region. Moreover, the type of lesion induced by the collar resemble the early human atherosclerotic plaque, in which the recruitment of monocytes from the circulation is little [160]. The reduced cholesterolemia of *Pcsk9*$^{-/-}$ mice compared to the wild type littermates represented the major bias in this in vivo study (**Figure 17**). However, in our model we can exclude that hypercholesterolemia is the

driving force in neointima formation. The influence of hypercholesterolemia on neointima hyperplasia induced by the collar model was previously tested in our laboratory on *apoE*$^{-/-}$ mice or on wild type mice fed with western diet. As expected, the cholesterol levels were extremely higher in the hypercholesterolemic mice (78 ± 14 mg/dL up to 1380 mg/dL) but those levels did not impact the size of neointima, but rather its composition, consisting of mostly inflammatory cells and lipids [157]. Moreover, in our model, the cholesterol fraction is mainly HDL particles, whereas in *apoE*$^{-/-}$ or *Ldlr*$^{-/-}$ mice there was a significant increase in LDL particles that spontaneously induce atherosclerotic lesions formation [161]. The direct effect of PCSK9 on atherosclerotic plaques were demonstrated also by Denis et al. in a study conducted with *Psck9* transgenic and knock-out mice in a *Ldlr*$^{-/-}$ or *apoE*$^{-/-}$ background. The results from this study revealed that the proatherogenic effect of PCSK9 was mediated by the LDLR and in *apoE*$^{-/-}$/*Pcsk9*[Tg], the overexpression of PCSK9 significantly modify plaque composition, without altering cholesterol levels [161]. Recently, Giunzoni et al. demonstrated that PCSK9 overexpression in macrophages directly altered the lesion composition by recruiting more pro-inflammatory monocytes, despite no changes in lipid levels or lesion size [83]. All together, these results suggest a direct role of PCSK9 on the artery wall, independently from cholesterol levels.

The neointima formation consists of migration and proliferation of the SMCs from the media to the lumen of the vessel. We have further investigated the effect of PCSK9 on the SMCs isolated from Pcsk9+/+ and Pcsk9-/- mice. The direct comparison between the cell lines revealed that the absence of PCSK9 shifted the SMCs phenotype towards a more contractile one. As shown in Figure 19, the absence of PCSK9 was associated with higher expression of α-smooth muscle actin, myosin heavy chain and calponin (**Figure 19**). The contractile SMCs phenotype was also associated with a lower proliferative index, assessed by cell counting, i-Celligence and by measuring the cell cycle progression with flow-cytometry (**Figure 20**). The difference in proliferation capability could be seen already at basal condition (**Figure 21**), with higher percentage of cells in the G0/G1 phase. Moreover, the more contractile phenotype is also associated with reduced migratory capability, especially after incubation with 20 ng/mL of PDGF-BB (**Figure 22** and **Figure 23**). Efficient cell migration requires a profound cytoskeleton re-organization and formation of protrusive structures termed lamellipodia, filopodia, invadopodia and podosomes; those structures were associated with a different activation of the small G proteins Rac1 and RhoA, especially after incubation with PDGF-BB

(**Figure 24**). The different activation of Rac1 and RhoA after PDGF-BB stimulation could be explained by the effect of PCSK9 on membrane cholesterol handling or by a direct effect on the PDGF pathway. It is known that the expression and activation of the small G proteins are modulated by cholesterol membrane content and their localization in plasma membrane subdomains [162, 163]. Integrin recycling, focal adhesion formation, and lamellipodia protrusion as well as the formation the assembly of specialized cholesterol-containing microdomains called caveolae require cholesterol [164-166]. On this matter, it is tempting to speculate that the higher expression levels of LDLR, LRP1, CD36, and VLDLR found in *Pcsk9*$^{-/-}$ SMCs (Figure 19) could have been sufficient to alter the cholesterol membrane homeostasis and thus the cytoskeletal reorganization leading to decrease migration. Moreover, Hawkins et al. demonstrated PDGF could directly promote the activation of small G proteins by increased guanine nucleotide exchange and by inhibition of a Rac GTPase activity; those mechanisms are dependent on PDGF-stimulated synthesis of phosphatidylinositol (3,4,5)-trisphosphate [167]. Thus, hypothetically PCSK9 could promote small G protein activation also via a direct modulation of the PDGF pathway.

To establish the role of PCSK9 in SMCs phenotype, proliferation and migration we stably reconstituted the expression of PCSK9 in the *Pcsk9*$^{-/-}$ SMCs by retroviral infection. Western blot analysis clearly demonstrated the successfully re-introduction of the protein in the knock-out cell line (Figure 25). The RT-qPCR analysis showed that the reintroduction of PCSK9 promoted a synthetic phenotype with a reduced expression of *α-SMA*, *MyHC* and *Calponin* associated with increased expression of synthetic markers like *Caldesom* and *KLF4* (Figure 26). This synthetic phenotype was related to increasing proliferative index of the *Pcsk9*$^{-/-}{}_{REC}$ SMCs compared to the knock-out line as demonstrated by cell counting experiment, real-time monitoring (Figure 27) and cell cycle progression (Figure 28). Furthermore, the expression of the cell cycle protein was significantly different between the cell lines, as assessed by RT-qPCR and western blot (Figure 29). Notably, the expression of inhibitory protein (p21 and p27), significantly lower at basal condition, decreased upon PDGF stimulation, whereas the expression of cyclin E and cyclin D1 seemed to be constitutively active in the *Psck9*$^{-/-}{}_{REC}$ cell line, indicating that the presence of PCSK9 improved the transition to phase S. The increased proliferative index was also demonstrated by increased BrdU accumulation in the S phase of the cell cycle, whereas there were no differences in the time of entering the S phase (Figure 30), indicating that the presence of PCSK9 improved the DNA synthesis as well as the entering

in the phase G2/M (Figure 28, panel B). The re-expression of PCSK9 restored also the migratory capability, at basal condition and after incubation with PDGF-BB (Figure 31), undoubtedly proving the direct involvement of PCSK9 on SMCs phenotype, proliferation and migration.

Cholesterol biosynthesis has been shown to be necessary for growth and division of mammalian cells [168], in particular Singh et al demonstrated that cholesterol content increases in S phase and inhibition of cholesterol biosynthesis resulted in cell cycle arrest in G1 phase [169]. The increased proliferative capability seen in the presence of PCSK9 could be therefore related to a different intracellular content of cholesterol. Thus, we first measured the intracellular cholesterol content by HPLC at basal condition and after 24 hours incubation with PDGF-BB. The content of free cholesterol seemed to increase after incubation with the growth factor, but there were no significant differences between Pcsk9$^{-/-}$ and Pcsk9$^{-/-}{}_{REC}$, both at basal and after PDGF-BB treatment (**Figure 32**). We then measured the BrdU incorporation in the presence of simvastatin 40µM, which is known to inhibit SMCs proliferation by the block of cell cycle progression to G0/G1 phase [170, 171]. As expected, the incubation with simvastatin reduced the amount of BrdU positive cells in both groups; however, the BrdU accumulation was significantly higher in the Pcsk9$^{-/-}{}_{REC}$ cells compared to the knock-out line, even after incubation with simvastatin (**Figure 33**). Even though the mechanism by which simvastatin is able to block the cell cycle is not fully elucidated, it could be ascribed to the so-called pleiotropic effects of statins. Those effects are driven potentially by the reduction of isoprenoids synthesis resulting from the inhibition of mevalonate pathway. Isoprenoids are in fact substrate of prenyl-transferase enzymes, responsible for post-translational modification of proteins, such as Rac1 and RhoA, implicated in numerous cell processes. The concentration of simvastatin used in this experiment indeed not only is able to inhibit efficiently cholesterol biosynthesis but also the isoprenoids synthesis [172]. The increased proliferation seen in *Pcsk9$^{-/-}{}_{REC}$* SMCs in the presence of simvastatin could be therefore related to a direct increased activation of small G-proteins mediated by PCSK9, potentially via modulation of the PDGF pathway. Although those results are far from been fully exhaustive, mainly because simvastatin induces PCSK9 expression via Rac1 [173], it is tempting to speculate that the pro-proliferative effect driven by PCSK9 is independent from its action on cholesterol homeostasis. Moreover, the reduced expression of LRP1 in the *Pcsk9$^{-/-}{}_{REC}$* cell line seemed to be associated with higher expression of PDGF receptor (Figure 34). LRP-1, per se, is known to play a pivotal

role in vascular integrity [174]. Boucher et al. demonstrated that inactivation of LRP1 in vascular SMCs of mice causes PDGFR overexpression and abnormal activation of PDGFR signaling, resulting in disruption of the elastic layer, SMC proliferation, aneurysm formation, and marked susceptibility to cholesterol-induced atherosclerosis [175]. Thus, PCSK9 by mediating the degradation LRP1 intensifies the PDGF receptor pathway, this results in an increase activation of Rac1 and RhoA and therefore an enhanced proliferation and migration capability.

Taken together, those results demonstrate that PCSK9 directly impacts SMCs phenotype, proliferation and migration, potentially by promoting PDGF signaling through LRP1 degradation more than by influencing cholesterol homeostasis, furthermore, reinforce the idea of a local, direct effect of PCSK9 on the vasculature.

The observational study conducted in the cohort of Brisighella Heart Study finally established the role of PCSK9 on vascular remodeling. In the population described in Figure 35, we found that circulating PCSK9 was significantly higher in the older groups of patients compared to the sex-matched groups, with the highest concentration in the post-menopausal group Figure 36. The increased levels of PCSK9 with aging could be partially due to different levels of circulating growth hormones as described by Persson et al [176]. In the univariate model, as reported previously, PCSK9 correlated with other important cardiovascular risks like age, systolic blood pressure, LDL-C and fasting glucose levels. Our results from the multiple linear regression showed that PCSK9 was significantly associated with arterial stiffness (estimated in term of carotid–femoral PWV) regardless of sex and, in women, menopausal condition (Figure 37). In line with this evidence, a significant association between serum PCSK9 levels and intima–media thickening was reported in hypertensive patients and persisted after adjustment for blood lipids [177]. Furthermore, Werner et al demonstrated in a prospective cohort study that elevated PCSK9 serum concentrations were associated with cardiovascular events in patients with stable coronary artery disease, despite a well-controlled LDL-C concentration [51]. The results from the ATHEROREMO-IVUS study, clearly showed that the size of the necrotic core, assessed by intravascular ultrasound virtual histology (IVUS-VH), was positively associated with circulating levels of PCSK9, independently form LDL-C plasma levels [178]. Moreover, the inhibition of PCSK9 achieved with evolocumab in the Global Assessment of Plaque Regression With a PCSK9 Antibody as Measured by Intravascular Ultrasound (GLAGOV) trial

demonstrated a reduction of atheroma volume of about 1% (p<0.001), and an induced regression in a greater percentage of patients, compared with statin-only treated group [64].

In conclusion, this study demonstrates that PCSK9 directly influences the artery wall remodeling by promoting a SMCs synthetic phenotype, proliferation and migration. This effect is potentially related to the increasing activation of the PDGF pathway mediated by the degradation of LRP1. The clinical observation on the cohort of Brisighella Heart study furthermore confirmed the role of PCSK9 as an important factor involved in arterial stiffness by demonstrating the involvement of this protein in the morphology of the vessel. This study further confirms the beneficial effect on the inhibition of PCSK9 in the treatment of atherosclerotic cardiovascular diseases, not only by reducing the LDL particles in the circulation but also by a direct modulation of arterial wall remodeling. This aspect is extremely important during the process restenosis, which is one of the major adverse events after percutaneous coronary intervention (PCI). The inhibition of PCSK9, especially with the new small molecules, which can act on both intracellular and extracellular sides, could therefore prevent the migration and proliferation of SMCs and reduce both the formation of atheroma, at the beginning, and the re-occlusion of the vessel, after PCI.

Future studies are although required to confirm the mechanism of action by which PCSK9 promotes a pro-atherogenic phenotype in the SMCs. On this matter, it would be interesting to assess this in the presence of a dominant negative form of the PDGFR and evaluate the activation of downstream proteins, like Akt and Erk, which are known to modulate cell cycle progression but also phosphoinositide 3-kinase, required for the activation of Rac1.

Bibliography

1. Feingold, K.R. and C. Grunfeld, *Introduction to Lipids and Lipoproteins*, in *Endotext*, L.J. De Groot, et al., Editors. 2000: South Dartmouth (MA).
2. Diffenderfer, M.R. and E.J. Schaefer, *The composition and metabolism of large and small LDL.* Curr Opin Lipidol, 2014. **25**(3): p. 221-6.
3. Dawber, T.R., G.F. Meadors, and F.E. Moore, Jr., *Epidemiological approaches to heart disease: the Framingham Study.* Am J Public Health Nations Health, 1951. **41**(3): p. 279-81.
4. Dawber, T.R., F.E. Moore, and G.V. Mann, *Coronary heart disease in the Framingham study.* Am J Public Health Nations Health, 1957. **47**(4 Pt 2): p. 4-24.
5. Anderson, K.M., W.P. Castelli, and D. Levy, *Cholesterol and mortality. 30 years of follow-up from the Framingham study.* JAMA, 1987. **257**(16): p. 2176-80.
6. Keys, A., J.T. Anderson, and F. Grande, *Prediction of serum-cholesterol responses of man to changes in fats in the diet.* Lancet, 1957. **273**(7003): p. 959-66.
7. Neaton, J.D., et al., *Serum cholesterol level and mortality findings for men screened in the Multiple Risk Factor Intervention Trial. Multiple Risk Factor Intervention Trial Research Group.* Arch Intern Med, 1992. **152**(7): p. 1490-500.
8. Ross, R., *Atherosclerosis--an inflammatory disease.* N Engl J Med, 1999. **340**(2): p. 115-26.
9. Stary, H.C., et al., *A definition of initial, fatty streak, and intermediate lesions of atherosclerosis. A report from the Committee on Vascular Lesions of the Council on Arteriosclerosis, American Heart Association.* Circulation, 1994. **89**(5): p. 2462-78.
10. Napoli, C., et al., *Fatty streak formation occurs in human fetal aortas and is greatly enhanced by maternal hypercholesterolemia. Intimal accumulation of low density lipoprotein and its oxidation precede monocyte recruitment into early atherosclerotic lesions.* J Clin Invest, 1997. **100**(11): p. 2680-90.
11. van Diepen, J.A., et al., *Interactions between inflammation and lipid metabolism: relevance for efficacy of anti-inflammatory drugs in the treatment of atherosclerosis.* Atherosclerosis, 2013. **228**(2): p. 306-15.
12. Nakajima, K. and A. Tanaka, *Atherogenic postprandial remnant lipoproteins; VLDL remnants as a causal factor in atherosclerosis.* Clin Chim Acta, 2018. **478**: p. 200-215.
13. Ginsberg, H.N., *New perspectives on atherogenesis: role of abnormal triglyceride-rich lipoprotein metabolism.* Circulation, 2002. **106**(16): p. 2137-42.
14. Dietschy, J.M., *Dietary fatty acids and the regulation of plasma low density lipoprotein cholesterol concentrations.* J Nutr, 1998. **128**(2 Suppl): p. 444S-448S.
15. Shearer, M.J., X. Fu, and S.L. Booth, *Vitamin K nutrition, metabolism, and requirements: current concepts and future research.* Adv Nutr, 2012. **3**(2): p. 182-95.
16. Cooper, A.D., *Hepatic uptake of chylomicron remnants.* J Lipid Res, 1997. **38**(11): p. 2173-92.
17. Imaizumi, K., M. Fainaru, and R.J. Havel, *Composition of proteins of mesenteric lymph chylomicrons in the rat and alterations produced upon exposure of chylomicrons to blood serum and serum proteins.* J Lipid Res, 1978. **19**(6): p. 712-22.
18. Hussain, M.M., *A proposed model for the assembly of chylomicrons.* Atherosclerosis, 2000. **148**(1): p. 1-15.
19. Tiwari, S. and S.A. Siddiqi, *Intracellular trafficking and secretion of VLDL.* Arterioscler Thromb Vasc Biol, 2012. **32**(5): p. 1079-86.

20. Kesaniemi, Y.A. and T.A. Miettinen, *Cholesterol absorption efficiency regulates plasma cholesterol level in the Finnish population.* Eur J Clin Invest, 1987. **17**(5): p. 391-5.
21. Roy, C.C.A.S.E., *Lipoprotein Analysis: A practical approach*, ed. R. D. 1992.
22. Masuda, D. and S. Yamashita, *Postprandial Hyperlipidemia and Remnant Lipoproteins.* J Atheroscler Thromb, 2017. **24**(2): p. 95-109.
23. Langsted, A., J.J. Freiberg, and B.G. Nordestgaard, *Fasting and nonfasting lipid levels: influence of normal food intake on lipids, lipoproteins, apolipoproteins, and cardiovascular risk prediction.* Circulation, 2008. **118**(20): p. 2047-56.
24. Scow, R.O., E.J. Blanchette-Mackie, and L.C. Smith, *Role of capillary endothelium in the clearance of chylomicrons. A model for lipid transport from blood by lateral diffusion in cell membranes.* Circ Res, 1976. **39**(2): p. 149-62.
25. Chapman, M.J., *Animal lipoproteins: chemistry, structure, and comparative aspects.* J Lipid Res, 1980. **21**(7): p. 789-853.
26. Skalen, K., et al., *Subendothelial retention of atherogenic lipoproteins in early atherosclerosis.* Nature, 2002. **417**(6890): p. 750-4.
27. Goldstein, J.L. and M.S. Brown, *A century of cholesterol and coronaries: from plaques to genes to statins.* Cell, 2015. **161**(1): p. 161-172.
28. Goldstein, J.L. and M.S. Brown, *The LDL receptor.* Arterioscler Thromb Vasc Biol, 2009. **29**(4): p. 431-8.
29. Heinecke, J.W., *Mechanisms of oxidative damage of low density lipoprotein in human atherosclerosis.* Curr Opin Lipidol, 1997. **8**(5): p. 268-74.
30. Yoshida, H. and R. Kisugi, *Mechanisms of LDL oxidation.* Clin Chim Acta, 2010. **411**(23-24): p. 1875-82.
31. Emerging Risk Factors, C., et al., *Major lipids, apolipoproteins, and risk of vascular disease.* JAMA, 2009. **302**(18): p. 1993-2000.
32. Tall, A.R., *Plasma high density lipoproteins: Therapeutic targeting and links to atherogenic inflammation.* Atherosclerosis, 2018. **276**: p. 39-43.
33. Grundy, S.M., et al., *Implications of recent clinical trials for the National Cholesterol Education Program Adult Treatment Panel III Guidelines.* J Am Coll Cardiol, 2004. **44**(3): p. 720-32.
34. Conroy, R.M., et al., *Estimation of ten-year risk of fatal cardiovascular disease in Europe: the SCORE project.* Eur Heart J, 2003. **24**(11): p. 987-1003.
35. Versteylen, M.O., et al., *Comparison of Framingham, PROCAM, SCORE, and Diamond Forrester to predict coronary atherosclerosis and cardiovascular events.* J Nucl Cardiol, 2011. **18**(5): p. 904-11.
36. Piepoli, M.F., et al., *2016 European Guidelines on cardiovascular disease prevention in clinical practice: The Sixth Joint Task Force of the European Society of Cardiology and Other Societies on Cardiovascular Disease Prevention in Clinical Practice (constituted by representatives of 10 societies and by invited experts)Developed with the special contribution of the European Association for Cardiovascular Prevention & Rehabilitation (EACPR).* Eur Heart J, 2016. **37**(29): p. 2315-2381.
37. European Association for Cardiovascular, P., et al., *ESC/EAS Guidelines for the management of dyslipidaemias: the Task Force for the management of dyslipidaemias of the European Society of Cardiology (ESC) and the European Atherosclerosis Society (EAS).* Eur Heart J, 2011. **32**(14): p. 1769-818.
38. Perk, J., et al., *European Guidelines on cardiovascular disease prevention in clinical practice (version 2012). The Fifth Joint Task Force of the European Society of Cardiology and Other Societies on Cardiovascular Disease Prevention in Clinical Practice*

(constituted by representatives of nine societies and by invited experts). Eur Heart J, 2012. **33**(13): p. 1635-701.

39. Klose, G., et al., *New AHA and ACC guidelines on the treatment of blood cholesterol to reduce atherosclerotic cardiovascular risk.* Wien Klin Wochenschr, 2014. **126**(5-6): p. 169-75.
40. Emerging Risk Factors, C., et al., *Lipoprotein(a) concentration and the risk of coronary heart disease, stroke, and nonvascular mortality.* JAMA, 2009. **302**(4): p. 412-23.
41. Nordestgaard, B.G., et al., *Lipoprotein(a) as a cardiovascular risk factor: current status.* Eur Heart J, 2010. **31**(23): p. 2844-53.
42. Ference, B.A., et al., *Low-density lipoproteins cause atherosclerotic cardiovascular disease. 1. Evidence from genetic, epidemiologic, and clinical studies. A consensus statement from the European Atherosclerosis Society Consensus Panel.* Eur Heart J, 2017. **38**(32): p. 2459-2472.
43. Ference, B.A., et al., *Effect of naturally random allocation to lower low-density lipoprotein cholesterol on the risk of coronary heart disease mediated by polymorphisms in NPC1L1, HMGCR, or both: a 2 x 2 factorial Mendelian randomization study.* J Am Coll Cardiol, 2015. **65**(15): p. 1552-61.
44. Defesche, J.C., et al., *Familial hypercholesterolaemia.* Nat Rev Dis Primers, 2017. **3**: p. 17093.
45. Soutar, A.K. and R.P. Naoumova, *Mechanisms of disease: genetic causes of familial hypercholesterolemia.* Nat Clin Pract Cardiovasc Med, 2007. **4**(4): p. 214-25.
46. Abifadel, M., et al., *Mutations in PCSK9 cause autosomal dominant hypercholesterolemia.* Nat Genet, 2003. **34**(2): p. 154-6.
47. Seidah, N.G., et al., *The secretory proprotein convertase neural apoptosis-regulated convertase 1 (NARC-1): liver regeneration and neuronal differentiation.* Proc Natl Acad Sci U S A, 2003. **100**(3): p. 928-33.
48. Seidah, N.G. and A. Prat, *The biology and therapeutic targeting of the proprotein convertases.* Nat Rev Drug Discov, 2012. **11**(5): p. 367-83.
49. Costet, P., M. Krempf, and B. Cariou, *PCSK9 and LDL cholesterol: unravelling the target to design the bullet.* Trends Biochem Sci, 2008. **33**(9): p. 426-34.
50. Naoumova, R.P., et al., *Severe hypercholesterolemia in four British families with the D374Y mutation in the PCSK9 gene: long-term follow-up and treatment response.* Arterioscler Thromb Vasc Biol, 2005. **25**(12): p. 2654-60.
51. Werner, C., et al., *Risk prediction with proprotein convertase subtilisin/kexin type 9 (PCSK9) in patients with stable coronary disease on statin treatment.* Vascul Pharmacol, 2014. **62**(2): p. 94-102.
52. Horton, J.D., J.L. Goldstein, and M.S. Brown, *SREBPs: activators of the complete program of cholesterol and fatty acid synthesis in the liver.* J Clin Invest, 2002. **109**(9): p. 1125-31.
53. Reihner, E., et al., *Influence of pravastatin, a specific inhibitor of HMG-CoA reductase, on hepatic metabolism of cholesterol.* N Engl J Med, 1990. **323**(4): p. 224-8.
54. Scott, R., *Lipid modifying agents: mechanisms of action and reduction of cardiovascular disease.* Clin Exp Pharmacol Physiol, 1997. **24**(5): p. A26-8.
55. Cholesterol Treatment Trialists, C., et al., *Efficacy and safety of more intensive lowering of LDL cholesterol: a meta-analysis of data from 170,000 participants in 26 randomised trials.* Lancet, 2010. **376**(9753): p. 1670-81.

56. Jones, P.H., R. Nair, and K.M. Thakker, *Prevalence of dyslipidemia and lipid goal attainment in statin-treated subjects from 3 data sources: a retrospective analysis.* J Am Heart Assoc, 2012. **1**(6): p. e001800.
57. Hamilton-Craig, I., *Statin-associated myopathy.* Med J Aust, 2001. **175**(9): p. 486-9.
58. Cannon, C.P., et al., *Ezetimibe Added to Statin Therapy after Acute Coronary Syndromes.* N Engl J Med, 2015. **372**(25): p. 2387-97.
59. Olsson, A.G., et al., *Can LDL cholesterol be too low? Possible risks of extremely low levels.* J Intern Med, 2017. **281**(6): p. 534-553.
60. Stein, E.A. and G.D. Swergold, *Potential of proprotein convertase subtilisin/kexin type 9 based therapeutics.* Curr Atheroscler Rep, 2013. **15**(3): p. 310.
61. Bittner, V.A., et al., *PCSK9 inhibitors for prevention of atherosclerotic cardiovascular disease.* J Clin Lipidol, 2018. **12**(4): p. 835-843.
62. Kampangkaew, J., S. Pickett, and V. Nambi, *Advances in the management of dyslipidemia.* Curr Opin Cardiol, 2017. **32**(4): p. 348-355.
63. Nicholls, S.J., et al., *Effect of Evolocumab on Progression of Coronary Disease in Statin-Treated Patients: The GLAGOV Randomized Clinical Trial.* JAMA, 2016. **316**(22): p. 2373-2384.
64. Nissen, S.E. and S.J. Nicholls, *Results of the GLAGOV trial.* Cleve Clin J Med, 2017. **84**(12 Suppl 4): p. e1-e5.
65. Bergeron, N., et al., *Proprotein convertase subtilisin/kexin type 9 inhibition: a new therapeutic mechanism for reducing cardiovascular disease risk.* Circulation, 2015. **132**(17): p. 1648-66.
66. Ray, K.K., et al., *Inclisiran in Patients at High Cardiovascular Risk with Elevated LDL Cholesterol.* N Engl J Med, 2017. **376**(15): p. 1430-1440.
67. Khvorova, A., *Oligonucleotide Therapeutics - A New Class of Cholesterol-Lowering Drugs.* N Engl J Med, 2017. **376**(1): p. 4-7.
68. Norata, G.D., et al., *Biology of proprotein convertase subtilisin kexin 9: beyond low-density lipoprotein cholesterol lowering.* Cardiovasc Res, 2016. **112**(1): p. 429-42.
69. Tavori, H., et al., *Human PCSK9 promotes hepatic lipogenesis and atherosclerosis development via apoE- and LDLR-mediated mechanisms.* Cardiovasc Res, 2016. **110**(2): p. 268-78.
70. Nishikido, T. and K.K. Ray, *Inclisiran for the treatment of dyslipidemia.* Expert Opin Investig Drugs, 2018. **27**(3): p. 287-294.
71. Fujita, H., et al., *Low-density lipoprotein profile changes during the neonatal period.* J Perinatol, 2008. **28**(5): p. 335-40.
72. Hegele, R.A., et al., *Nonstatin Low-Density Lipoprotein-Lowering Therapy and Cardiovascular Risk Reduction-Statement From ATVB Council.* Arterioscler Thromb Vasc Biol, 2015. **35**(11): p. 2269-80.
73. Koren, M.J., et al., *Long-term Low-Density Lipoprotein Cholesterol-Lowering Efficacy, Persistence, and Safety of Evolocumab in Treatment of Hypercholesterolemia: Results Up to 4 Years From the Open-Label OSLER-1 Extension Study.* JAMA Cardiol, 2017. **2**(6): p. 598-607.
74. Robinson, J.G., et al., *Efficacy and safety of alirocumab in reducing lipids and cardiovascular events.* N Engl J Med, 2015. **372**(16): p. 1489-99.
75. Zaid, A., et al., *Proprotein convertase subtilisin/kexin type 9 (PCSK9): hepatocyte-specific low-density lipoprotein receptor degradation and critical role in mouse liver regeneration.* Hepatology, 2008. **48**(2): p. 646-54.

76. Ouguerram, K., et al., *Apolipoprotein B100 metabolism in autosomal-dominant hypercholesterolemia related to mutations in PCSK9.* Arterioscler Thromb Vasc Biol, 2004. **24**(8): p. 1448-53.
77. Dijk, W., C. Le May, and B. Cariou, *Beyond LDL: What Role for PCSK9 in Triglyceride-Rich Lipoprotein Metabolism?* Trends Endocrinol Metab, 2018. **29**(6): p. 420-434.
78. Poirier, S., et al., *Implication of the proprotein convertase NARC-1/PCSK9 in the development of the nervous system.* J Neurochem, 2006. **98**(3): p. 838-50.
79. Jonas, M.C., C. Costantini, and L. Puglielli, *PCSK9 is required for the disposal of non-acetylated intermediates of the nascent membrane protein BACE1.* EMBO Rep, 2008. **9**(9): p. 916-22.
80. Liu, M., et al., *PCSK9 is not involved in the degradation of LDL receptors and BACE1 in the adult mouse brain.* J Lipid Res, 2010. **51**(9): p. 2611-8.
81. Zimetti, F., et al., *Increased PCSK9 Cerebrospinal Fluid Concentrations in Alzheimer's Disease.* J Alzheimers Dis, 2017. **55**(1): p. 315-320.
82. Ferri, N., et al., *Proprotein convertase subtilisin kexin type 9 (PCSK9) secreted by cultured smooth muscle cells reduces macrophages LDLR levels.* Atherosclerosis, 2012. **220**(2): p. 381-6.
83. Giunzioni, I., et al., *Local effects of human PCSK9 on the atherosclerotic lesion.* J Pathol, 2016. **238**(1): p. 52-62.
84. Davies, P.F., et al., *The atherosusceptible endothelium: endothelial phenotypes in complex haemodynamic shear stress regions in vivo.* Cardiovasc Res, 2013. **99**(2): p. 315-27.
85. Ding, Z., et al., *Hemodynamic shear stress via ROS modulates PCSK9 expression in human vascular endothelial and smooth muscle cells and along the mouse aorta.* Antioxid Redox Signal, 2015. **22**(9): p. 760-71.
86. Ricci, C., et al., *PCSK9 induces a pro-inflammatory response in macrophages.* Sci Rep, 2018. **8**(1): p. 2267.
87. Geovanini, G.R. and P. Libby, *Atherosclerosis and inflammation: overview and updates.* Clin Sci (Lond), 2018. **132**(12): p. 1243-1252.
88. Geng, Y.J. and P. Libby, *Progression of atheroma: a struggle between death and procreation.* Arterioscler Thromb Vasc Biol, 2002. **22**(9): p. 1370-80.
89. *Compensatory enlargement of human atherosclerotic coronary arteries.* N Engl J Med, 1987. **317**(25): p. 1604.
90. Arnett, E.N., et al., *Coronary artery narrowing in coronary heart disease: comparison of cineangiographic and necropsy findings.* Ann Intern Med, 1979. **91**(3): p. 350-6.
91. Grundy, S.M., et al., *Implications of recent clinical trials for the National Cholesterol Education Program Adult Treatment Panel III guidelines.* Circulation, 2004. **110**(2): p. 227-39.
92. Crea, F. and P. Libby, *Acute Coronary Syndromes: The Way Forward From Mechanisms to Precision Treatment.* Circulation, 2017. **136**(12): p. 1155-1166.
93. Stone, G.W., et al., *A prospective natural-history study of coronary atherosclerosis.* N Engl J Med, 2011. **364**(3): p. 226-35.
94. Cristell, N., et al., *High-sensitivity C-reactive protein is within normal levels at the very onset of first ST-segment elevation acute myocardial infarction in 41% of cases: a multiethnic case-control study.* J Am Coll Cardiol, 2011. **58**(25): p. 2654-61.
95. Schonbeck, U., et al., *Regulation of matrix metalloproteinase expression in human vascular smooth muscle cells by T lymphocytes: a role for CD40 signaling in plaque rupture?* Circ Res, 1997. **81**(3): p. 448-54.

96. Liuzzo, G., et al., *Monoclonal T-cell proliferation and plaque instability in acute coronary syndromes.* Circulation, 2000. **101**(25): p. 2883-8.
97. Liuzzo, G., et al., *Identification of unique adaptive immune system signature in acute coronary syndromes.* Int J Cardiol, 2013. **168**(1): p. 564-7.
98. Ridker, P.M., et al., *Interleukin-1beta inhibition and the prevention of recurrent cardiovascular events: rationale and design of the Canakinumab Anti-inflammatory Thrombosis Outcomes Study (CANTOS).* Am Heart J, 2011. **162**(4): p. 597-605.
99. Ridker, P.M., et al., *Antiinflammatory Therapy with Canakinumab for Atherosclerotic Disease.* N Engl J Med, 2017. **377**(12): p. 1119-1131.
100. Shiomi, M., et al., *Vasospasm of atherosclerotic coronary arteries precipitates acute ischemic myocardial damage in myocardial infarction-prone strain of the Watanabe heritable hyperlipidemic rabbits.* Arterioscler Thromb Vasc Biol, 2013. **33**(11): p. 2518-23.
101. Duewell, P., et al., *NLRP3 inflammasomes are required for atherogenesis and activated by cholesterol crystals.* Nature, 2010. **464**(7293): p. 1357-61.
102. Day, A.J., *The structure and regulation of hyaluronan-binding proteins.* Biochem Soc Trans, 1999. **27**(2): p. 115-21.
103. Jia, H., et al., *Effective anti-thrombotic therapy without stenting: intravascular optical coherence tomography-based management in plaque erosion (the EROSION study).* Eur Heart J, 2017. **38**(11): p. 792-800.
104. Shimokawa, H., et al., *Rho-kinase-mediated pathway induces enhanced myosin light chain phosphorylations in a swine model of coronary artery spasm.* Cardiovasc Res, 1999. **43**(4): p. 1029-39.
105. Shimokawa, H., *2014 Williams Harvey Lecture: importance of coronary vasomotion abnormalities-from bench to bedside.* Eur Heart J, 2014. **35**(45): p. 3180-93.
106. Masumoto, A., et al., *Suppression of coronary artery spasm by the Rho-kinase inhibitor fasudil in patients with vasospastic angina.* Circulation, 2002. **105**(13): p. 1545-7.
107. Lanza, G.A., G. Careri, and F. Crea, *Mechanisms of coronary artery spasm.* Circulation, 2011. **124**(16): p. 1774-82.
108. Timmis, A., et al., *European Society of Cardiology: Cardiovascular Disease Statistics 2017.* Eur Heart J, 2018. **39**(7): p. 508-579.
109. Yusuf, S., et al., *Effect of potentially modifiable risk factors associated with myocardial infarction in 52 countries (the INTERHEART study): case-control study.* Lancet, 2004. **364**(9438): p. 937-52.
110. Kocemba, J., et al., *Isolated systolic hypertension: pathophysiology, consequences and therapeutic benefits.* J Hum Hypertens, 1998. **12**(9): p. 621-6.
111. Lee, Y.H. and R.E. Pratley, *The evolving role of inflammation in obesity and the metabolic syndrome.* Curr Diab Rep, 2005. **5**(1): p. 70-5.
112. Chu, N.F., et al., *Plasma insulin, leptin, and soluble TNF receptors levels in relation to obesity-related atherogenic and thrombogenic cardiovascular disease risk factors among men.* Atherosclerosis, 2001. **157**(2): p. 495-503.
113. Ran, J., et al., *Angiotensin II infusion decreases plasma adiponectin level via its type 1 receptor in rats: an implication for hypertension-related insulin resistance.* Metabolism, 2006. **55**(4): p. 478-88.
114. Leshan, R.L., et al., *Leptin receptor signaling and action in the central nervous system.* Obesity (Silver Spring), 2006. **14 Suppl 5**: p. 208S-212S.
115. Laakso, M. and S. Lehto, *Epidemiology of risk factors for cardiovascular disease in diabetes and impaired glucose tolerance.* Atherosclerosis, 1998. **137 Suppl**: p. S65-73.

116. Veiraiah, A., *Hyperglycemia, lipoprotein glycation, and vascular disease.* Angiology, 2005. **56**(4): p. 431-8.
117. Packard, C.J., W.S. Weintraub, and U. Laufs, *New metrics needed to visualize the long-term impact of early LDL-C lowering on the cardiovascular disease trajectory.* Vascul Pharmacol, 2015. **71**: p. 37-9.
118. Duckers H. J., N.G.E., Serruys P. W. , *Essential of restenosis: for the interventional cardiologist*. 1 ed. 2007: Humana Press.
119. Farooq, V., B.D. Gogas, and P.W. Serruys, *Restenosis: delineating the numerous causes of drug-eluting stent restenosis.* Circ Cardiovasc Interv, 2011. **4**(2): p. 195-205.
120. Vaez, M., et al., *Regional differences in coronary revascularization procedures and outcomes: a nationwide 11-year observational study.* Eur Heart J Qual Care Clin Outcomes, 2017. **3**(3): p. 243-248.
121. National Heart, L. *Stent*. Available from: https://www.nhlbi.nih.gov/health-topics/stents.
122. Owens, G.K., M.S. Kumar, and B.R. Wamhoff, *Molecular regulation of vascular smooth muscle cell differentiation in development and disease.* Physiol Rev, 2004. **84**(3): p. 767-801.
123. Campbell, J.H. and G.R. Campbell, *The role of smooth muscle cells in atherosclerosis.* Curr Opin Lipidol, 1994. **5**(5): p. 323-30.
124. Rensen, S.S., P.A. Doevendans, and G.J. van Eys, *Regulation and characteristics of vascular smooth muscle cell phenotypic diversity.* Neth Heart J, 2007. **15**(3): p. 100-8.
125. Wasteson, P., et al., *Developmental origin of smooth muscle cells in the descending aorta in mice.* Development, 2008. **135**(10): p. 1823-32.
126. Jiang, X., et al., *Fate of the mammalian cardiac neural crest.* Development, 2000. **127**(8): p. 1607-16.
127. Frid, M.G., et al., *Smooth muscle cells isolated from discrete compartments of the mature vascular media exhibit unique phenotypes and distinct growth capabilities.* Circ Res, 1997. **81**(6): p. 940-52.
128. Nguyen, A.T., et al., *Smooth muscle cell plasticity: fact or fiction?* Circ Res, 2013. **112**(1): p. 17-22.
129. Bochaton-Piallat, M.L., et al., *Cultured arterial smooth muscle cells maintain distinct phenotypes when implanted into carotid artery.* Arterioscler Thromb Vasc Biol, 2001. **21**(6): p. 949-54.
130. Hellstrom, M., et al., *Role of PDGF-B and PDGFR-beta in recruitment of vascular smooth muscle cells and pericytes during embryonic blood vessel formation in the mouse.* Development, 1999. **126**(14): p. 3047-55.
131. Li, X., et al., *Suppression of smooth-muscle alpha-actin expression by platelet-derived growth factor in vascular smooth-muscle cells involves Ras and cytosolic phospholipase A2.* Biochem J, 1997. **327 (Pt 3)**: p. 709-16.
132. Hao, H., et al., *Heterogeneity of smooth muscle cell populations cultured from pig coronary artery.* Arterioscler Thromb Vasc Biol, 2002. **22**(7): p. 1093-9.
133. Kotani, M., et al., *Chimeric DNA-RNA hammerhead ribozyme targeting PDGF A-chain mRNA specifically inhibits neointima formation in rat carotid artery after balloon injury.* Cardiovasc Res, 2003. **57**(1): p. 265-76.
134. Shah, N.M., A.K. Groves, and D.J. Anderson, *Alternative neural crest cell fates are instructively promoted by TGFbeta superfamily members.* Cell, 1996. **85**(3): p. 331-43.

135. Sinha, S., et al., *Transforming growth factor-beta1 signaling contributes to development of smooth muscle cells from embryonic stem cells.* Am J Physiol Cell Physiol, 2004. **287**(6): p. C1560-8.
136. Hautmann, M.B., C.S. Madsen, and G.K. Owens, *A transforming growth factor beta (TGFbeta) control element drives TGFbeta-induced stimulation of smooth muscle alpha-actin gene expression in concert with two CArG elements.* J Biol Chem, 1997. **272**(16): p. 10948-56.
137. Moustakas, A., et al., *Mechanisms of TGF-beta signaling in regulation of cell growth and differentiation.* Immunol Lett, 2002. **82**(1-2): p. 85-91.
138. Ichii, T., et al., *Fibrillar collagen specifically regulates human vascular smooth muscle cell genes involved in cellular responses and the pericellular matrix environment.* Circ Res, 2001. **88**(5): p. 460-7.
139. Tsai, M.C., et al., *Shear stress induces synthetic-to-contractile phenotypic modulation in smooth muscle cells via peroxisome proliferator-activated receptor alpha/delta activations by prostacyclin released by sheared endothelial cells.* Circ Res, 2009. **105**(5): p. 471-80.
140. Boesen, M.E., et al., *A systematic literature review of the effect of carotid atherosclerosis on local vessel stiffness and elasticity.* Atherosclerosis, 2015. **243**(1): p. 211-22.
141. Arroyo, L.H. and R.T. Lee, *Mechanisms of plaque rupture: mechanical and biologic interactions.* Cardiovasc Res, 1999. **41**(2): p. 369-75.
142. Richardson, P.D., M.J. Davies, and G.V. Born, *Influence of plaque configuration and stress distribution on fissuring of coronary atherosclerotic plaques.* Lancet, 1989. **2**(8669): p. 941-4.
143. Simon, A., et al., *Intima-media thickness: a new tool for diagnosis and treatment of cardiovascular risk.* J Hypertens, 2002. **20**(2): p. 159-69.
144. Suceava, I., et al., *The association between arterial stiffness and carotid intima-media thickness in patients with known cardiovascular risk factors.* Clujul Med, 2013. **86**(3): p. 222-6.
145. Zaid, M., et al., *Coronary Artery Calcium and Carotid Artery Intima Media Thickness and Plaque: Clinical Use in Need of Clarification.* J Atheroscler Thromb, 2017. **24**(3): p. 227-239.
146. Hirata, K., M. Kawakami, and M.F. O'Rourke, *Pulse wave analysis and pulse wave velocity: a review of blood pressure interpretation 100 years after Korotkov.* Circ J, 2006. **70**(10): p. 1231-9.
147. Naka, K.K., et al., *Flow-mediated changes in pulse wave velocity: a new clinical measure of endothelial function.* Eur Heart J, 2006. **27**(3): p. 302-9.
148. Le May, C., et al., *Proprotein convertase subtilisin kexin type 9 null mice are protected from postprandial triglyceridemia.* Arterioscler Thromb Vasc Biol, 2009. **29**(5): p. 684-90.
149. Elmore, E. and M. Swift, *Growth of cultured cells from patients with ataxia-telangiectasia.* J Cell Physiol, 1976. **89**(3): p. 429-31.
150. Cicero, A.F., et al., *Serum uric acid change and modification of blood pressure and fasting plasma glucose in an overall healthy population sample: data from the Brisighella heart study.* Ann Med, 2017. **49**(4): p. 275-282.
151. Cicero, A.F., et al., *Association between serum uric acid, hypertension, vascular stiffness and subclinical atherosclerosis: data from the Brisighella Heart Study.* J Hypertens, 2014. **32**(1): p. 57-64.

152. Cicero, A.F., et al., *High serum uric acid is associated to poorly controlled blood pressure and higher arterial stiffness in hypertensive subjects.* Eur J Intern Med, 2017. **37**: p. 38-42.
153. Stevens, P.E., A. Levin, and M. Kidney Disease: Improving Global Outcomes Chronic Kidney Disease Guideline Development Work Group, *Evaluation and management of chronic kidney disease: synopsis of the kidney disease: improving global outcomes 2012 clinical practice guideline.* Ann Intern Med, 2013. **158**(11): p. 825-30.
154. O'Brien, E., et al., *European Society of Hypertension recommendations for conventional, ambulatory and home blood pressure measurement.* J Hypertens, 2003. **21**(5): p. 821-48.
155. Van Bortel, L.M., et al., *Expert consensus document on the measurement of aortic stiffness in daily practice using carotid-femoral pulse wave velocity.* J Hypertens, 2012. **30**(3): p. 445-8.
156. Ageenkova, O.A. and M.A. Purygina, *Central aortic blood pressure, augmentation index, and reflected wave transit time: reproducibility and repeatability of data obtained by oscillometry.* Vasc Health Risk Manag, 2011. **7**: p. 649-56.
157. Baetta, R., et al., *Perivascular carotid collar placement induces neointima formation and outward arterial remodeling in mice independent of apolipoprotein E deficiency or Western-type diet feeding.* Atherosclerosis, 2007. **195**(1): p. e112-24.
158. Booth, R.F., et al., *Rapid development of atherosclerotic lesions in the rabbit carotid artery induced by perivascular manipulation.* Atherosclerosis, 1989. **76**(2-3): p. 257-68.
159. Raiteri, M., et al., *Pharmacological control of the mevalonate pathway: effect on arterial smooth muscle cell proliferation.* J Pharmacol Exp Ther, 1997. **281**(3): p. 1144-53.
160. Moore, K.J., F.J. Sheedy, and E.A. Fisher, *Macrophages in atherosclerosis: a dynamic balance.* Nat Rev Immunol, 2013. **13**(10): p. 709-21.
161. Denis, M., et al., *Gene inactivation of proprotein convertase subtilisin/kexin type 9 reduces atherosclerosis in mice.* Circulation, 2012. **125**(7): p. 894-901.
162. Navarro-Lerida, I., et al., *A palmitoylation switch mechanism regulates Rac1 function and membrane organization.* EMBO J, 2012. **31**(3): p. 534-51.
163. Adorni, M.P., et al., *Free cholesterol alters macrophage morphology and mobility by an ABCA1 dependent mechanism.* Atherosclerosis, 2011. **215**(1): p. 70-6.
164. Ramprasad, O.G., et al., *Changes in cholesterol levels in the plasma membrane modulate cell signaling and regulate cell adhesion and migration on fibronectin.* Cell Motil Cytoskeleton, 2007. **64**(3): p. 199-216.
165. Garcia-Melero, A., et al., *Annexin A6 and Late Endosomal Cholesterol Modulate Integrin Recycling and Cell Migration.* J Biol Chem, 2016. **291**(3): p. 1320-35.
166. Echarri, A. and M.A. Del Pozo, *Caveolae internalization regulates integrin-dependent signaling pathways.* Cell Cycle, 2006. **5**(19): p. 2179-82.
167. Hawkins, P.T., et al., *PDGF stimulates an increase in GTP-Rac via activation of phosphoinositide 3-kinase.* Curr Biol, 1995. **5**(4): p. 393-403.
168. Chen, H.W., A.A. Kandutsch, and C. Waymouth, *Inhibition of cell growth by oxygenated derivatives of cholesterol.* Nature, 1974. **251**(5474): p. 419-21.
169. Singh, P., et al., *Cholesterol biosynthesis and homeostasis in regulation of the cell cycle.* PLoS One, 2013. **8**(3): p. e58833.
170. Wang, S.T., et al., *Simvastatin-induced cell cycle arrest through inhibition of STAT3/SKP2 axis and activation of AMPK to promote p27 and p21 accumulation in hepatocellular carcinoma cells.* Cell Death Dis, 2017. **8**(2): p. e2626.

171. Corsini, A., et al., *Non-lipid-related effects of 3-hydroxy-3-methylglutaryl coenzyme A reductase inhibitors.* Cardiology, 1996. **87**(6): p. 458-68.
172. Ferri, N., R. Paoletti, and A. Corsini, *Lipid-modified proteins as biomarkers for cardiovascular disease: a review.* Biomarkers, 2005. **10**(4): p. 219-37.
173. Ferri, N., et al., *Geranylgeraniol prevents the simvastatin-induced PCSK9 expression: Role of the small G protein Rac1.* Pharmacol Res, 2017. **122**: p. 96-104.
174. Au, D.T., et al., *Role of the LDL Receptor-Related Protein 1 in Regulating Protease Activity and Signaling Pathways in the Vasculature.* Curr Drug Targets, 2018. **19**(11): p. 1276-1288.
175. Boucher, P., et al., *LRP: role in vascular wall integrity and protection from atherosclerosis.* Science, 2003. **300**(5617): p. 329-32.
176. Persson, L., et al., *Circulating proprotein convertase subtilisin kexin type 9 has a diurnal rhythm synchronous with cholesterol synthesis and is reduced by fasting in humans.* Arterioscler Thromb Vasc Biol, 2010. **30**(12): p. 2666-72.
177. Lee, C.J., et al., *Association of serum proprotein convertase subtilisin/kexin type 9 with carotid intima media thickness in hypertensive subjects.* Metabolism, 2013. **62**(6): p. 845-50.
178. Cheng, J.M., et al., *PCSK9 in relation to coronary plaque inflammation: Results of the ATHEROREMO-IVUS study.* Atherosclerosis, 2016. **248**: p. 117-22.
179. Dubuc, G., et al., *Statins upregulate PCSK9, the gene encoding the proprotein convertase neural apoptosis-regulated convertase-1 implicated in familial hypercholesterolemia.* Arterioscler Thromb Vasc Biol, 2004. **24**(8): p. 1454-9.
180. Guo, Y.L., et al., *Short-term impact of low-dose atorvastatin on serum proprotein convertase subtilisin/kexin type 9.* Clin Drug Investig, 2013. **33**(12): p. 877-83.
181. Chong, J.J., et al., *Human embryonic-stem-cell-derived cardiomyocytes regenerate non-human primate hearts.* Nature, 2014. **510**(7504): p. 273-7.
182. Liu, Y.W., et al., *Human embryonic stem cell-derived cardiomyocytes restore function in infarcted hearts of non-human primates.* Nat Biotechnol, 2018. **36**(7): p. 597-605.